NISTIR 6266

Materials and Fracture Mechanics Assessments of Railroad Tank Cars

Prepared by:
Akram Zahoor
Zenith Corporation
P.O. Box 8231
Gaithersburg, MD 20898
Purchase Order Number:
43NANB813069

Prepared for:
U.S. DEPARTMENT OF COMMERCE
Technology Administration
Materials Performance Group
Metallurgy Division
National Institute of Standards
and Technology
Gaithersburg, MD 20899

NIST

NISTIR 6266

Materials and Fracture Mechanics Assessments of Railroad Tank Cars

Prepared by:
Akram Zahoor
Zenith Corporation
P.O. Box 8231
Gaithersburg, MD 20898
Purchase Order Number:
43NANB813069

Prepared for:
U.S. DEPARTMENT OF COMMERCE
Technology Administration
Materials Performance Group
Metallurgy Division
National Institute of Standards
and Technology
Gaithersburg, MD 20899

September 1998

U.S. DEPARTMENT OF COMMERCE
William M. Daley, Secretary

TECHNOLOGY ADMINISTRATION
Gary R. Bachula, Acting Under Secretary
for Technology

NATIONAL INSTITUTE OF STANDARDS
AND TECHNOLOGY
Raymond G. Kammer, Director

U.S. DEPARTMENT OF ENERGY
Washington, D.C. 20858

CONTENTS

ABSTRACT

This report presents a review of fracture mechanics assessments and the mechanical and fracture toughness data for four steels used in the manufacture of railroad tank cars that carry hazardous materials. Thirteen reports developed between 1975 and 1995 by National Institute of Standards and Technology (NIST, formerly NBS) and Association of American Railroads (AAR) were reviewed. The report reviews data for the A212 steel, AAR TC 128 grade B, A515 grade 70, and an experimental steel A 8XX, a control-rolled steel. The materials data reviewed were the tensile strength and stress rupture data, CVN, DT, NDT, DWTT, FATT, J_{Ic}, CTOD, K_{Ic}, and K_{Ia} at tank car operating and accident temperatures. Where possible, the mechanical and fracture toughness data are organized in a tabular or graphical format to allow a quick comparison of properties for the four steels. The review covered primarily the tank car shell structure. Where appropriate, assumptions used or implied are noted and their applicability is discussed. Critical crack size analysis results and service experience crack propagation data are presented. Areas where slide graph method should be enhanced or replaced by latest fracture mechanics methods are identified and discussed.

NOTE: The data presented in this report are not fully in compliance with the NIST policy regarding the use of SI units as defined in NIST SP 811. This is a summary report that includes data tables and figures taken directly from NBS and NIST reports that were written before the policy on the use of SI units was implemented and data from non-NIST publications.

Section 1

INTRODUCTION

This report presents a review of fracture mechanics assessments and the mechanical and fracture toughness data for four steels used in the manufacture of railroad tank cars that carry hazardous materials. Thirteen reports developed between 1975 and 1995 by National Institute of Standards and Technology (NIST, formerly NBS), Association of American Railroads (AAR) and Railroad Progress Institute (RPI)-AAR were reviewed and these are listed as References 1 through 13. These reports cover accidents and their investigations and analyses going back to the 1960's. Specifically, this report covers the review for the A212 steel, AAR TC 128 grade B, A515 grade 70, and an experimental steel A 8XX, a control-rolled steel. The materials data reviewed were the tensile strength and stress rupture data, CVN, DT, NDT, DWTT, FATT, J_{Ic}, CTOD, K_{Ic}, and K_{Ia} at tank car operating and accident temperatures. Where possible, the mechanical and fracture toughness data are organized in a tabular or graphical format to allow a quick comparison of properties for the four steels. This format can be useful in the development of materials data guidelines for use by the FRA staff.

This report is organized primarily from a fracture mechanics evaluation perspective. A fracture mechanics evaluation involves calculation, estimation and availability of two major elements: the crack driving potential of the structure and the crack resisting properties of the material. When the former exceeds the latter, the initiation of crack extension occurs. The crack will continue to extend if the crack driving potential is maintained above the material's resistance to crack extension. In some structures, the crack driving potential cannot be maintained due to inherent design features or some other flaw growth mechanism such as leak-before-break. Consequently, the structure would not fail in a catastrophic manner. The type of failure, brittle or ductile, depends on the material characteristics at the temperature, loading rate and other service conditions of the structure.

The crack driving potential of the structure is a calculated quantity and is expressed in the form of K, J or some other fracture parameter. The most commonly used fracture parameters are discussed in Section 7. The crack driving potential is calculated from solutions that require the knowledge of operating loads or stresses, structural geometry, flaw size and shape, and the material stress-strain curve or in its simplest form the yield and ultimate tensile strengths. The material's resistance to crack initiation and extension is a material property which depends on temperature, loading rate, and the microstructure of the material. It is measured by several fracture toughness parameters such as K_{Ic}, K_{Id}, K_{Ia}, CVN, J and CTOD. Any one or a combination of these fracture toughness data is used in a fracture assessment. The service history of the structure is an essential element in defining the location and type of cracks/flaws when assessing structural integrity. All these elements are used in a fracture mechanics evaluation directed toward determining whether the structure is prone to failure under certain conditions. Fracture mechanics evaluations also can provide insight into future improvements in design, fabrication quality and material replacement decisions.

The sections of this report are organized to provide first a review of various elements needed in fracture mechanics evaluation of railroad tank cars. The review was limited to materials data and

information contained in reports listed in Section 9 (References 1 through 13) and covered primarily the tank car shell structure. Where appropriate, assumptions used or implied are noted and their applicability is discussed. Following these, an overview of fracture mechanics methods used in the evaluation of tank car failures are presented. First, the basic elements of AAR slide graph method which is based on transition temperature concept is presented. Areas where this method should be enhanced or replaced by newer J-based methods are identified and discussed. Critical crack size analysis results are extracted from reports. Service experience crack length data are also included. Tables and figures are provided at the end of each section. Some tables and figures taken from old reports contain data that are not in SI units.

Section 2

GENERAL OVERVIEW OF REPORTS ON PRESSURE TANK CARS

The National Institute of Standards and Technology's, NIST, formerly NBS, involvement with tank car research for the Federal Railroad Administration (FRA) began in 1970 with the metallurgical study of a tank car that ruptured upon impact in Belle, West Virginia. In that same year, the Association of American Railroads (AAR) in cooperation with the Railway Progress Institute (RPI) initiated a large research program on the structural integrity of tank cars involved in railroad accidents. The program included detailed review of service history, material properties data and fracture mechanics evaluations with the objective of developing a comprehensive understanding of tank cars failure in accidents [1-3, 14-16]. As a result of these studies, remedial measures for structural protection were developed, which included shelf couplers, head shields, and thermal insulation.

By 1983 guidelines for fracture-safe and fatigue-reliable design were developed [4, 5, 15-18] and applied to explain the reasons for relatively small number of tank car failure by brittle fracture. Nineteen cases of accident-related brittle fracture were analyzed in Reference [4], of which sixteen cases were for pressure tank cars in accidents during the period 1965 to 1980. The other three fractures were: Austin, Manitoba case (1/10/82) and two cases (1/11/48) and (6/ 26/61) involving carbon dioxide cars. By 1983 several reports [19-24] were developed, which addressed fabrication quality, structural integrity following derailment, and the feasibility of using new microalloyed and control-rolled steels for tank cars.

Subsequent work particularly at NIST involved the development of metallurgical and fracture toughness data base for the steels involved in accidents and the "future" steel. New test methods for metallurgical and fracture evaluations evolved in the 1980s. Consequently, crack-tip opening displacement (CTOD), elastic-plastic fracture mechanics (J), Nil ductility transition temperature, NDTT, and Charpy V-notch impact tests were also conducted for the present and future steels at both high and very low temperatures representing tank car fires and coldest regions of the North American continent [6-11]. These Reports (1990-92) generated data for normalized, inclusion shape controlled, and normalized and stress relieved conditions of AAR TC 128 grade B Steel, and microalloyed, control-rolled, and inclusion shape controlled A 8XX grade B Steel. The weld and heat affected zone crack arrest properties were investigated in Reference [10]. In addition to large data base development, a fracture mechanics analysis using the latest fracture mechanics method was conducted in 1992 [12]. This report determined the critical crack size of a circumferential crack in the tank car shell. The residual stress concern for skip welds was addressed in Reference [13]. Recently, NIST prepared a historical metallurgical review of tank car accident investigations [26].

Section 3

DESIGN LOADINGS FOR PRESSURE TANK CARS

Pressure tank cars are designed to carry a wide range of liquefied gas ladings. Table 3-1 lists the tank car types by rating and their design hydrostatic and burst pressures. The hydrostatic test pressure was defined using a factor of safety of 2.5 on the burst pressure. The structure was assumed to be free of any defect or flaw.

Table 3-2 lists liquified gas ladings that are used primarily in certain type of tank cars. A large number of tank cars transport the propane (LPG) and anhydrous ammonia (AA) and it is for this reason Type 112A340W tank cars were selected for fracture assessments in previous studies [4, 5].

The largest stress in the tank car shell from internal pressure of lading is the hoop stress. This stress would act to open a flaw or crack oriented in the axial (longitudinal) direction of the tank car. By design, the design hoop stresses for welded pressure vessels are typically limited to a maximum of 0.4 to 0.5 of the yield stress.

The hoop stress is calculated from $S = Pr/(1000t)$, where S is the hoop stress (ksi), r and t are radius and minimum shell wall thickness (inches), and P is the internal pressure (psig). The minimum wall thickness for TC-128 grade B steel and A212B steel tank cars are approximately 0.6 in. (15 mm) and 0.7 in. (18 mm), respectively. Table 3-3 summarizes the hoop stresses for four pressure events in a Type 112A340W tank car [5]. This car has a shell radius of 59 in. (1.5 M).

The hoop stress due to lading vapor pressure should be a small fraction of these design event stresses. Figure 3-1 shows the vapor pressure versus temperature curves for eight liquefied gasses [4, 5]. The stresses calculated from these pressures are shown in Figure 3-2. The largest hoop stress for LPG and AA is about 10 ksi which is a factor 2.3 below the safety relief valve discharge event and a factor of seven below the burst event. This comparison demonstrates conservative design stress levels used in tank car design. However, these calculations assume no defect/flaw in the tank welds. If a defect/flaw develops, then the level of conservatism is reduced. An estimation of the reduction in safety margin due to a flaw involves fracture mechanics evaluation.

Table 3-1

Design Pressures for Pressure Tank Cars

Tank Car Rating	Hydrostatic Test Pressure (psig)	Calculated Burst Test Pressure (psig)
300W	300	750
340W	340	850
400W	400	1000
500W	500	1250
600W	600	1500

Table 3-2

Liquified Gas Lading By Tank Car Type

Liquified Gas Lading	Tank Car Type
Propane, ammonia, vinyl chloride	112A340W, 105A300W
Carbon dioxide, sulfur dioxide, chlorine	105A500W
Hydrogen sulfide, hydrogen chloride	105A600W

Table 3-3

Hoop Stress in A212B and TC-128B Steel Tank Cars

Event	Pressure psig	Hoop Stress, ksi (Mpa) for A212B	Hoop Stress, ksi (Mpa) for TC-128B
Burst	850	70 (483)	81 (558)
Hydrostatic Test	340	28 (193)	33 (224)
Valve Flow Rating	308	26 (179)	30 (207)
Safety Relief Valve Discharge	280	23 (158)	27 (186)

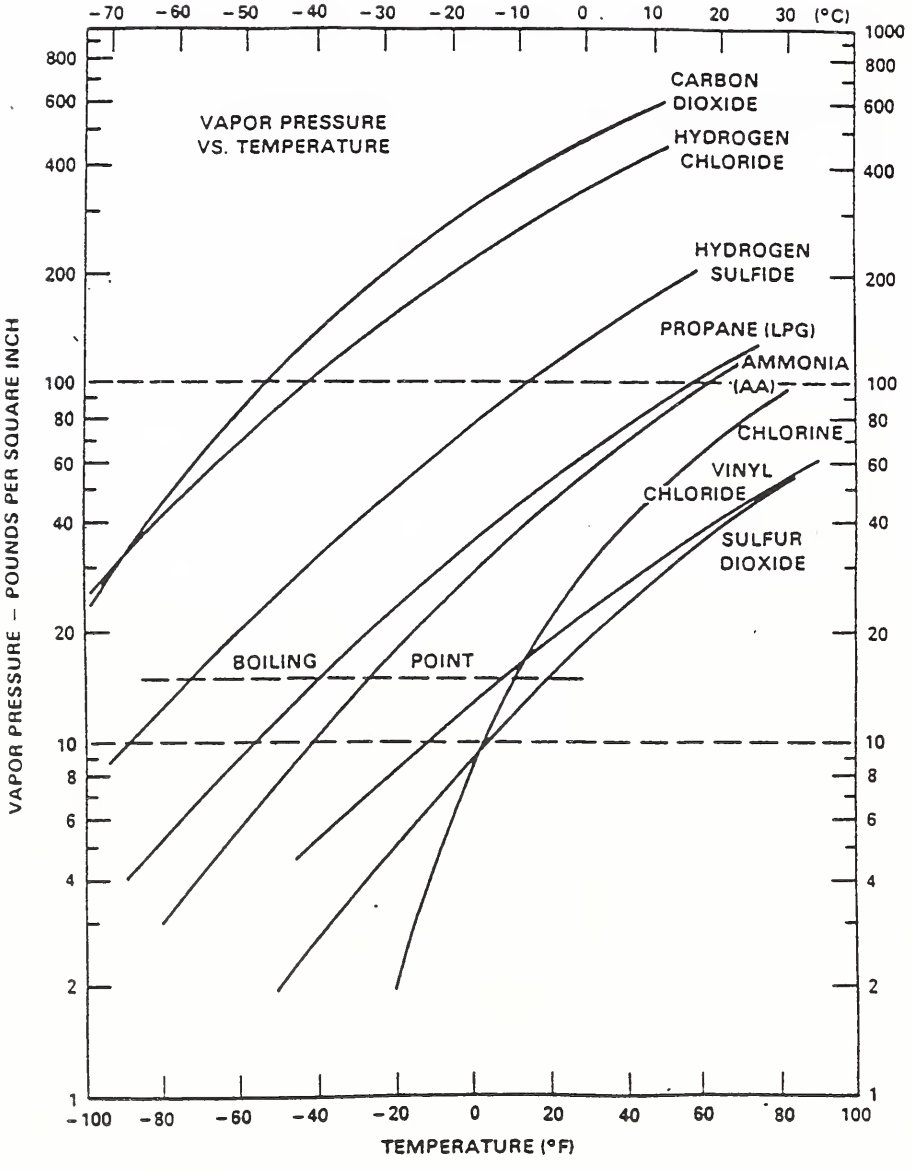

Figure 3-1 Vapor Pressure Curves for Several Ladings.

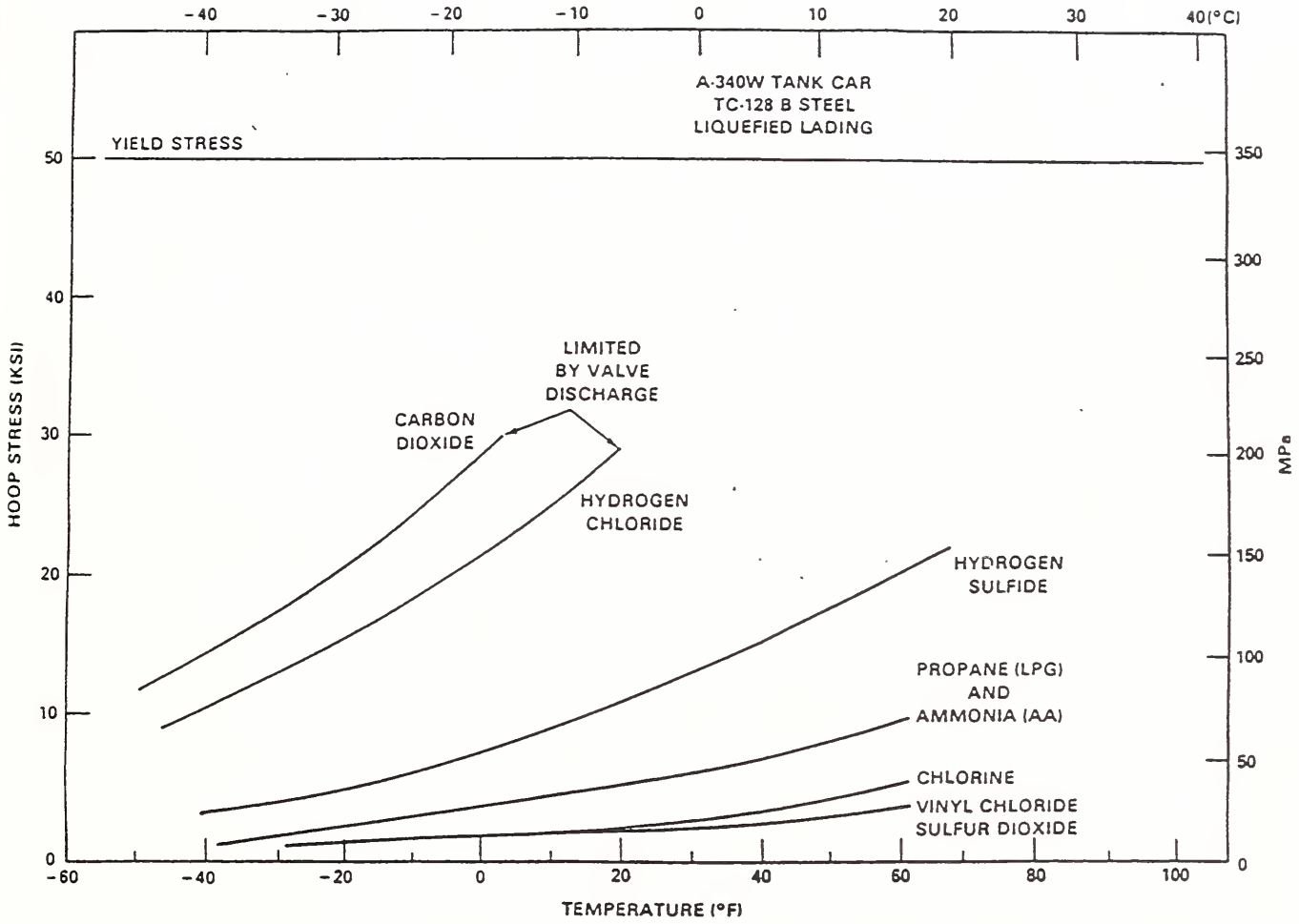

Figure 3-2 Hoop Stress For Different Lading Cases, TC128B A340W Tank Car.

Section 4

MATERIALS DATA FOR PRESSURE TANK CARS

The materials data summarized in this section are the tensile strength, stress-rupture, K_{Ic}, K_{Id}, K_{Ia}, CVN, NDTT, DT, FATT, J_{Ic} and CTOD. The J_{Ic} and CTOD standards were developed in the 1980's. In the AAR research programs, these data were developed for the whole range of operating and accident temperatures. Reference [3] contains the largest data base generated for tank car steels. Additional materials data were developed by NIST for the FRA and are contained in References [6-11]. This section presents a summary of the data for the A212 steel, AAR TC 128 grade B, A515 grade 70, and an experimental A 8XX control-rolled steel. Where possible, the mechanical and fracture toughness data are organized in a tabular or graphical format to allow for a quick comparison of properties for the four steels. This format can be useful in the development of materials data guidelines for use by the FRA staff.

Several steels have been used in the fabrication of pressure tank cars. Prior to 1965 most pressure tank cars were built of A212-B steel. The A212B Specification was superceded in 1966 by ASTM A515-70. During the mid-1960's a majority of tank cars were built of as-rolled TC-128B steel, while some were built of TC-128A steel. All pressure tank cars built thereafter employed TC-128B steel. As of 1989, the normalized and stress relieved TC-128 grade B steel is used as per FRA requirements.

The AAR TC128 steels are produced according to an American Association of Railroads specification M128.00: Specification for high strength carbon manganese steel plates for tank cars, AAR TC128-70. This specification covers both grade A and grade B of this steel. Both are classified as flange quality and are made to fine-grain practice. Grade A requires a minimum of 0.02 weight percent vanadium, whereas Grade B has no minimum vanadium content requirement. The Grade B steel specification has maximum limits for nickel, chromium, molybdenum, copper and vanadium contents. Maximum limits are not specified for the Grade A steel.

The ASTM A515 grade 70 Steel is classified by the American Society for Testing and Materials (ASTM) as a carbon-silicon steel used for intermediate and higher-temperature service in welded boilers and other pressure vessels. The designation "grade 70 " refers to the minimum allowed tensile strength, which is 485 MPa (70 ksi). Plates less than 50.8 mm (2 inches) in thickness would normally be supplied in the as rolled condition. The maximum content permitted for manganese is the least for the A515 steel, intermediate for the A516 steel, and is greater for the TC128 steels. In addition, the specification for A515 permits slightly higher carbon content than for the other grades.

Fracture toughness properties are not a part of the material specifications for tank cars except for certain low temperature applications.

A large materials data base was generated under Phase 03 of the RPI-AAR Tank Car Safety Research and Test Project and is documented in Reference [3]. This program examined three categories of

materials: (1) steels currently specified and used in tank car tank construction (current steels), (2) steels from tank car tanks involved in accidents (accident steels), and (3) steels formerly used in the construction of tank car tanks which are now obsolete or no longer used in pressure tank car tanks (old steels).

The current steel samples were obtained from several of the tank car companies sponsoring the RPI-AAR Project. These samples included AAR TC128-B, ASTM A515-70, and ASTM A516-70 shell and head plate steels and represent the steels most commonly used in the manufacture of both pressure and non-pressure tank car tanks. The shell and head plate samples were between 0.6 to 0.8 inch in thickness. The samples reflected various conditions of heat treatment and types of forming operations (for head samples).

Samples removed from tank car tanks involved in accidents represented (l) mechanical damage due to impact, (2) tensile failure due to reduced strength of a locally overheated area and (3) sudden over pressure resulting from overheated product. Samples from twelve tank cars involved in eight accidents were used. Samples of steels formerly used in tank car construction were obtained from vintage tank cars removed from service. These samples represented A285, A212B and M115 in thickness between 0.52 and 1.125 inches. The A212B Specification was superceded in 1966 by ASTM A515-70.

In all, samples of twelve shell plate steels and eight formed head plate steels from current production, head and shell plate samples from twelve tank cars involved in eight accidents, and six shell plate samples from old tank cars were included in the test program [3]. The tests included tensile strength, chemical analyses, Charpy V-notch (CVN), dynamic tear (DT), drop weight (DW-NDT), and drop weight tear tests (DWTT). The reason for conducting these tests as described in Ref. [3] is as follows. The CVN test was conducted primarily to provide familiar reference data since historically the CVN test is the only fracture toughness test that has been employed. The drop weight (DW) test defines the NDT temperature above which a material exhibits increasing ductility under full-scale fracture conditions. The drop weight tear test (DWTT) defines the temperature at which the full-scale fracture mode changes from brittle to ductile fracture propagation. The dynamic tear (DT) test is a new test that offers the promise of providing information on the full-scale ductile to brittle fracture propagation transition temperature and also on the toughness of the material. These data are summarized in the sections that follow.

In conjunction with the RPI-AAR research program, NIST began a series of mechanical property and fracture toughness tests in 1988 for the FRA [6-8]. The objective of these programs was to develop an extensive data base for a newly developed, control-rolled, micro-alloyed Cb-V steel, A 8XX grade B. The need for a similar data base for normalized AAR TC128 grade B steel was also recognized for comparison and evaluation purposes. The NIST data are reported in References [6-8]. These two steels tested by NIST were similar to, but not the same as, the steels intended for use because both steels had been made using inclusion shape control (ISC) practice. The background to these test programs is summarized in Section 4.1 along with the tensile data, and other materials property data are summarized in subsequent sections.

As of January 1989, the FRA requires new tank cars that carry hazardous commodity be constructed of normalized AAR TC128 grade B steel and that the tank car be stress relieved after fabrication. The added feature of inclusion shape control (ISC) practice is not a part of the AAR requirement. Therefore, additional tests were conducted by NIST [9] to develop a comprehensive mechanical property and fracture toughness database for TC128 grade B steel in both normalized and stress relieved condition. These tests followed the same procedures as those used in previous test programs [6-8] and are summarized in appropriate sections. Because a crack may initiate from a weld or heat-affected zone, a test program [10] was conducted to determine the crack arrest fracture toughness from welded plates of normalized AAR TC128 grade B steel currently used in appropriate tank cars.

These test programs [6-10] focused on the steel's mechanical and fracture toughness properties from room temperature to the lowest temperature the steel could possibly encounter while in use in North America. Two major conclusions reached as a result of these test programs were: (1) the normalized material showed better impact properties at low test temperatures than the as-rolled AAR TC128 grade B steel and (2) the normalized and stress relieved steel showed more resistance to crack initiation and better crack arrest toughness than as-rolled or normalized AAR TC128 grade B steel. Test data at accident temperatures (case where a tank car is exposed to fire) were needed to fully understand the performance of the normalized and stress relieved steel. To this end, the elevated temperature test program was conducted to develop mechanical and fracture toughness data, and the results are reported in Reference [11].

4.1 TENSILE STRENGTH PROPERTIES

This section summarizes the ambient and elevated temperature tensile properties including the stress-rupture data. Table 4-1 lists the specified tensile properties for tank car steels.

In the Phase 03 study **[3]**, tensile properties were determined in accordance with ASTM Specification A370, "Mechanical Testing of Steel Products." On the old steels both longitudinal and transverse tests were conducted. Tests on current and accident steels were conducted in a direction transverse to the principal rolling direction on two-inch gauge length (0.500-inch diameter) tensile specimens. The rolling direction of the shell plate is in the circumferential direction of the tank shell. For the current steel head plate samples the rolling direction was either indicated by the tank car manufacturer or determined by metallurgical check. Additional details are given in [3]. Tables 4-2 through 4-5 lists the tensile properties for current, accident, and old materials [3]. The data in these tables cover all the samples discussed in the introduction to Section 4.

The knowledge of the elevated-temperature mechanical properties of tank car steels is essential to an understanding of the fracture of tank cars carrying compressed gases when subjected to fire environments. To this end and as part of the FRA sponsored research program, two full-scale rail tank cars (RAX 201 and RAX 202) filled with liquified petroleum gas (LPG) were subjected to fire engulfment tests. Both tank cars were fabricated from 5/8 inch-thick, fine-grained steel plate in the as-rolled condition, produced to specification AAR M128-69, Grade B, Flange quality. Following these tests, the elevated-temperature mechanical and fracture properties of AAR M128-B steel were determined by NBS **[2]** from tests on selected steel plates taken from insulated tank car RAX 202.

The ambient-temperature mechanical properties tests were also conducted to determine if the requirements of specification AAR M128-69-8 were satisfied.

The NBS test program [2] involved three plate samples representing the highest temperature, least temperature and the unfailed shell regions of the RAX 202 tank car. Plate sample TC2-(1) was taken from the top of the failed shell course in the region experiencing the highest temperature during the fire test and contained a portion of the stress-rupture crack believed to have been the site of the initial rupture of the tank car. Plate sample TC2-(3) was removed from the bottom of the failed shell course in the region heated the least during the fire test. Plate sample TC2-(11B) was taken from the bottom of the tank car in an unfailed shell course and was selected because of its location in an undeformed and relatively unheated region of the tank car.

Forty-five specimens from three plate samples were tested. Of these, eight specimens were tested for determining ambient temperature properties. The specimens for ambient-temperature and hot-tensile tests and the stress-rupture tests were prepared in accordance with ASTM E8-69, Tension Testing of Metallic Materials. Four ASTM Recommended Practices are applicable to these three tests. Ambient temperature tension tests were conducted as per ASTM E8, Tension testing of Metallic Materials. The hot-tensile tests were conducted as per ASTM E21, Elevated temperature Tension Tests of Metallic Materials. The stress-rupture testing is covered by either ASTM E139, Conducting Creep, Creep-Rupture, and Stress-Rupture Tests of Metallic Materials or ASTM E150, Conducting Creep and Creep-Rupture Tension Tests of Metallic materials under Conditions of Rapid Heating and Short Times. The elevated-temperature tests were conducted at temperatures of 1100°F, 1150°F, 1200°F, and 1250°F.

The results of ambient-temperature tensile tests showed that all three plate samples met the ultimate tensile strength, yield strength, and percent elongation requirements of specification AAR M128-69B. The results of hot-tensile tests showed a continuous decrease in ultimate tensile strength and yield strength, and an increase in tensile ductility with the increase in temperature. These results indicated that dynamic strain ageing was not significant in the temperature range and the testing speeds investigated.

Figures 4-1 and 4-2 show a comparison of the elevated temperature tensile strength properties with RAX 201 data and other published data [2]. This comparison shows that the variation in the ambient-temperature ultimate tensile strength allowed by specification AAR M128-B and the effect of the rate of testing can result in significant variations in the elevated-temperature strength properties. Reference [2] concludes that the lack of substantial elevated-temperature mechanical property data in the literature appears to preclude the development of a design or trend curve for the variation of burst pressure with temperature for AAR M128-B steel. The knowledge of the lower bound to the burst pressure-temperature curve for AAR M128-B would be useful in the evaluation of existing relief-valve design.

Figure 4-3 shows the stress-rupture data developed in Reference [2] and compares it with other relevant data. The data indicate that a decrease in the initial stress of approximately 20 to 30 percent results in a twelve-fold increase in the rupture life from fifteen minutes to three hours.

The comparisons in Figures 4-1 through 4-3 indicated that there is substantial disagreement between the data for the uninsulated tank car RAX 201 and the insulated tank car RAX 202 [2]. The steel plates used to fabricate both tank cars were produced from the same heat of steel. It is highly probable that the differences in stress-rupture strength values are not a result of compositional variations. It is possible that significant variations in properties are the result of differences in the rupture environment seen by the plate samples tested. Apart from this speculation, however, the reason for the large difference in elevated-temperature properties could not be explained [2]. Reference [2] concludes that the rupture life of AAR M128-B steel is a strong function of both temperature and applied stress. Therefore, modifications of tank car technology which would either reduce the temperature dependence of the properties of the steel or reduce the maximum stresses and/or time at maximum stress experienced by the pressurized tank cars could be important in efforts to reduce the possibility of a tank car failing catastrophically when subjected to a fire environment.

As part of the data base development work in Reference **[6]**, NIST received four plates (9/16 inch thick) each of the micro-alloyed, control-rolled A 8XX grade B steel and the normalized AAR TC128 grade B steel. The latter material was supposed to be similar to that used for tank car construction as of January 1989. However, it was later determined that both steels were made using inclusion shape control (ISC) practice. The test program involved microscopic examinations, nil-ductility transition temperature test, Charpy V-notch impact (CVN), J-integral and crack-tip opening displacement (CTOD) tests. The control-rolled A 8XX grade B steel plate specimens were labeled A, B, C, and D, whereas the normalized AAR TC128 grade B steel plate specimens were labeled E, F, G, and H. All tests were conducted at temperatures from -80°F to +73°F, at 20°F intervals for temperatures below 0°F.

The test specimen matrix involved both the ASTM L-T and T-L orientations. Figure 4-4 illustrates the ASTM definition for test specimen orientation. The ASTM LT specimen is defined as one in which the loading axis of the specimen is parallel to the rolling (L) direction and the crack is in the direction normal to the rolling direction (T). This specimen is sometimes referred to as "longitudinal" specimen. Similarly, in the TL specimen the loading axis of the specimen is perpendicular to the rolling direction and the crack is oriented in the rolling direction (L).

Microscopic examinations of the grain size of the A 8XX steel showed that it was not as fine as-expected in a normal controlled-rolled steel. The AAR TC128 grade B steel tested was not typical of the conventional normalized AAR TC128 grade B steel that is currently used in the manufacture of all new tank cars. In addition to a normalizing heat treatment, the steel had been made using inclusion shape control (ISC) practice. This practice is known to enhance the notch toughness properties of the steel by spheroidizing the inclusions.

Tensile specimens were prepared according to ASTM designation A370-88. Duplicate tensile tests, for both the LT and TL orientations, were conducted at temperatures from -60°F to room temperature. Figure 4-5 shows the ultimate tensile and the 0.2% offset yield strengths of both steels for both orientations. The data indicate that the yield strength of A 8XX steel was on the average 10 ksi higher than the AAR TC128 grade B steel.

The NDT temperature and Charpy V-notch test results [6] revealed that the new A 8XX grade B steel had lower impact properties at low test temperatures, and a higher NDT temperature than the AAR TC128 grade B steel. Both steels were found to have been made using inclusion shape control (ISC) practice. The primary reason for the difference in notch toughness properties was that the ferrite/pearlite grain size of the normalized and ISC AAR TC128 grade B steel was more uniform and finer than that of the control-rolled and ISC A 8XX steel. Because the CVN impact and NDT temperature test results were not in agreement with those obtained by the AAR-RPI Research Committee or those certified by the Bethlehem Steel Corporation in its Certificate of Analysis, retesting was requested by the Committee and conducted by NIST.

The retesting program involved determination and reconfirmation of the rolling direction, grain size, NDT and Charpy V-notch impact properties of both steels. The results of retesting are discussed in Reference [7] and summarized in sections that follow. Subsequent to these reconfirmation tests, crack arrest fracture toughness tests were conducted for both steels by NIST and are reported in Reference [8]. Because the added feature of inclusion shape control (ISC) practice is not part of the AAR requirement, additional tests on steels presently used in tank cars were conducted by NIST [9] to develop a comprehensive mechanical property and fracture toughness database. Tests were conducted on TC128 grade B steel in both normalized and stress relieved condition. These tests followed the same procedures as those used in previous test programs [6-8].

In the test program [9], the steel plates were acquired from the same supplier as that for test programs [6-8]. The number, size and thickness of the plates were the same, i.e., four plates each, 1.4 cm (9/16 inch) in thickness by 183 cm (72 inches) by 183 cm (72 inches). The plates were in the normalized condition and supplied to AAR specification TC128 grade B, flange quality steel. The four plates were identified as I, J, K, and L and plate I was used for all test specimens. The test program was designed to develop data for the ultimate and yield strengths, reduction-in-area, percent elongation, and fracture toughness properties J integral, CTOD, K_{Ic} and K_{Ia}. Data for both the normalized, and normalized and stress relieved conditions were developed. For preparing and testing specimens in stress-relieved condition, a section of plate I was stress relieved, according to the AAR Specification M-128, at 635°C (1175°F) for one hour.

The tensile specimens were tested at -51°C (-60°F), -40°C (-40°F), -29°C (-20°F), -18°C (0°F), and 22°C (+72°F) according to ASTM Method A 370-90. The ultimate tensile strength (UTS) results for both conditions are shown in Figure 4-6. The UTS for the as-received normalized condition in the L-T orientation was greater than those for any other combination of orientation and stress relief. The lowest UTS was found for the normalized and stress relieved T-L specimens. These values are representative of a typical TC128 grade B steel.

The 0.2% offset yield strength (YS) results are shown in Figure 4-7. The yield strength in the L-T orientation for normalized, and the normalized and stress relieved steels was found to be greater than those in the T-L orientation. Further, the YS in the T-L orientation was essentially the same from -18°C (0°F) to room temperature. The reduction-in-area (RA) results indicated that the ductility in the T-L orientation is enhanced by stress relieving at 635°C (1175°F) for one hour.

The weld and heat affected zone fracture properties were investigated in Reference [10]. The test program involved determination the crack arrest fracture toughness from welded plates of normalized and stress relieved AAR TC128 grade B steel, currently used in tank cars. Plates 1.4 cm (9/16 in.) in thickness, 28 cm (11 in.) in width, and 91 cm (36 in.) in length of normalized AAR TC128 grade B steel were welded by Union Tank Car Company (UTC). The plates were welded by submerged arc welding (SAW) and stress relieved. Tensile specimens were machined from the centerline of welded plates according to ASTM Method A 370-90. The specimens were tested at -51°C (-60°F), -40°C (-40°F), -29°C (-20°F), and -18°C (0°F). Figure 4-8 shows tensile test results for all weld specimens. It was found that the yield strength, 545 MPa (80 ksi), remained almost the same for the entire test temperatures. The reduction in area and elongation for all weld material was comparable to the base plate material. Vickers hardness measurements indicated that the weld metal, heat-affected zone, and base metal were within allowable limits. No hard, brittle zones were found.

The elevated temperature performance of the normalized and stress relieved TC128 grade B steel was investigated in Reference [11]. This test program was initiated to develop the needed data base for the case where the tank car is exposed to fire. Previous investigations concluded that fire temperatures at accident sites ranged from about 593°C (1100°F) to about 677°C (1250°F), and once a tank car was engulfed in fire it would probably rupture in about 90 minutes. These conclusions were derived from accidents before a thermal shield was required on tank cars. The NIST test program was designed to reflect these temperatures and exposure times. Tests were conducted at 593, 621, 649, and 677°C for 30, 60, 90, and 120 minutes, respectively, at crosshead speeds of 0.0127 cm/min (0.005 inch/min) and 0.127 cm/min (0.05 inch/min) to determine the effects of time, temperature, and strain rate. The two crosshead speeds were the same speeds investigated in the 1975 test program [2]. The steel plates used in this program were part of the same plates procured for a previous program [9]. The as-rolled and normalized plate "J" was stress relieved according to AAR specifications at 649°C (1200°F) for one hour. The hot tensile and stress rupture tests were conducted for both the L-T and T-L specimens.

The elevated temperature tensile test results can be described in two parts. The first is the effect of exposure time at the elevated temperature and the second is the effect of elevated temperature.

Figures 4-9 and 4-10 show the effects of exposure time, temperature and crosshead speed on the UTS. The UTS was not affected by the crosshead speed (rate of loading) except at the highest temperature of 677°C. Similar comparisons for the yield strength are shown in Figures 4-11 and 4-12. Increased rate of loading produced an increase in the YS regardless of test temperature or time at temperature. Other conclusions derived from the test data were: (1) increased rate of loading produced a decrease in the difference between the UTS and YS values, i.e., the YS increased while the UTS remained unchanged, (2) at the lower rate of loading, the difference between the UTS and YS was about 36 percent and (3) at the higher rate of loading this difference was only 15 percent.

Figures 4-13 through 4-16 show the effects of temperature on the UTS and YS values. Both UTS and YS decreased continuously with the increase in test temperature and time at temperature. The percent elongation was found to continuously increase with the increase in test temperature. The reduction-in-area was not as sensitive to temperature as the elongation. For both L-T and T-L orientations, the yield-to-ultimate strength ratio (Y/T) was unaffected by test temperature or time at

temperature. The Y/T ratio was 0.60 and 0.80 for crosshead speeds of 0.0127 and 0.127 cm/minute, respectively. The ductility increased as the test temperature was raised above 316°C (600°F). Dynamic strain ageing probably did not affect these strength properties over the test temperatures used in this investigation.

The results of the stress-rupture tests are shown in Figure 4-17. It is a log-log plot of the applied stress versus time to rupture. The rupture time could be increased by decreasing the 10-minute lifetime stress level. Table 4-6 predicts the increase in rupture life. At 593°C, the rupture life would increase to three hours if the 10-minute lifetime stress were decreased by 27%. At higher temperatures a larger decrease in the stress is required to attain the same rupture life (43% reduction at 677°C). These results suggest that the stress-rupture time of this steel could be enhanced by reducing the time during which the tank car experiences the maximum internal pressure or by reducing the maximum internal pressure. This could possibly be achieved by using additional relief valves, larger flow capacity relief valves, lower opening-pressure relief valves, or a combination of all three.

Figure 4-18 shows a log-log plot of the minimum creep rate as determined from the stress rupture tests versus rupture time. It shows a linear relationship on the log-log plot. Figure 4-19 shows the relationship between the minimum creep rate and applied stress for each test temperature. These figures can be used to predict the rupture life of the steel for the specified combination of applied stress and temperature.

4.2 REFERENCE NDT TEMPERATURE DATA

The statistical NDT temperature distributions for various types of steels are discussed in Reference [1, 5]. Table 4-7 summarizes the NDT temperature range for seven different classifications of steels. It covered pearlitic (low and intermediate strength, LIS) and martensitic and bainitic (high strength, HS) steels in as-rolled (AR), normalized (N), and quenched and tempered (Q&T) conditions. The table entries are in the ascending order of strength, with highest strength steel listed as the last in this table. Class 1 represents the upper limit of the total NDT population. Class 2 represents the design-reference based on a major fraction of the NDT population. The designer may select either Class 1 or Class 2, upper-limit NDT temperatures depending upon the degree of conservatism desired in fracture analyses [5]. Other notations used in the table are: CGP = coarse-grained pearlitic; FGP = Fine grain melting practice; FGP + N = very fine grain type steel; CR = Control-rolled; ICR = Intense cold rolling; and ICR+AC = ICR plus on-line accelerated (fast) cooling by water spray upon completion of rolling.

The NDT temperature range shown in Table 4-7 could be due to microstructural differences that are sometimes present in the large scale production of standard grade steels. It is not due to test scatter because NDT tests have demonstrated very little scatter. Statistical NDT testing of standard grade steels normally results in a Gaussian (bell-shaped) frequency distribution curve. Table 4-7 indicates that the temperature range of the NDT frequency distribution is between 50 and 70°F (10 and 21°C), averaging 60°F (33°C) wide.

4.3 NDT TEMPERATURE DATA FOR RAILROAD TANK CARS

Figure 4-20 shows five NDT distribution curves for steels used in tank car construction [1, 5]. The dashed curves represent the as-rolled condition, whereas the solid curves represent the normalized condition. This data is also presented in tabular form in Table 4-8. These include old, current practice as well as a hypothetical steel under consideration.

The highest temperature NDT band is labeled as "Typical C/Mn" steels which represents the as-rolled, M-115 and A-212B steels used in old tank cars. The band is cut off at 60°F (16°C) to represent steels rolled at conventional temperatures. However, the band may be increased to 100°F (38°C) for old steels that have been rolled at excessively high temperatures. The band next to the highest one is labeled as "Best C/Mn & Alloy" which represents the as-rolled TC-128B steel. The maximum NDT temperature is expected to be 40°F (4°C) for this steel. The next lower NDT band is for normalized "Typical C/Mn" steels that are produced by fine-grain practice. The generic band for this steel covers the maximum NDT temperature range of -40°F (-40°C) to 0°F (-18°C). The next band is for normalized TC-128B steel and is labeled as "Best C/Mn & Alloy." The maximum NDT temperature for this steel is expected to be -30°F (-34°C). The NDT data for all specimens tested are given in Tables 4-10 through 4-12.

The last of these is the curve for normalized "Cb" (Nb) steels with an expected maximum NDT temperature of approximately -50°F (-46°C). The new control-rolled Cb (Nb) steel under consideration in future tank cars is described in [19]. The most optimistic expectation for control-rolled "future" steels is a guaranteed maximum NDT temperature of -80°F (-62°C) [19]. It is being considered because its maximum NDT temperature is close to the lowest expected shell temperature for LPG lading, which would assure prevention of brittle fracture for the lowest anticipated service temperature (LAST).

The NDT distribution curves in Figure 4-20 were truncated to a 40°F (22°C) band width for slide-graph fracture mechanics analysis discussed in Section 7 [5].

The NDT data from several programs [6-11] conducted by NIST are summarized in Table 4-4. In the Reference [6] test program, the nil-ductility transition temperature test specimens were prepared according to ASTM designation E208-87. The Reference [7] retest program used the ASTM test method E 208-87a.

4.4 DYNAMIC TEAR (DT) DATA

The Dynamic Tear (DT) test is the newest of the four fracture toughness tests utilized in Phase 03 of the RPI-AAR steel evaluation program. It originated at the U. S. Naval Research Laboratory and employed either a falling weight or a pendulum machine to fracture the test specimen. It has been used for many years at the NRL and by some research laboratories. A standard ASTM test method for the DT test was under development at the time of Phase 03 studies. All of the DT specimens contained a 0.625 inch deep notch. Additional details are given in Reference [1, 3].

Reference [1] contains dynamic tear (DT) data for AAR TC128-B, ASTM A515 -70, A212-B, and old tank car steels. Test data for as rolled and stress relieved (AR-SR) AAR TC128-B steels indicated that there is approximately a 2 to 1 ratio of plastic fracture resistance (L to T orientation, strong to weak directions) in the shell plates. As expected, the low end of DT curves (brittle fracture region) is not sensitive to orientation. Reference [1] also contains DT data for TC128-B in the normalized and stress relieved (N-SR) condition and includes head steel in the normalized (N), cold formed (CF) and stress relieved (SR) condition (N+). Data for all these conditions from current production steels were plotted together to establish reference curves for TC128-B steels. Figure 4-21 shows the resulting two reference bands for the AR-SR and N-SR (or N +) conditions. These bands represent a statistical definition of the expected properties of the TC128-B steels for the specified heat treatment.

Reference [1] states that the separation of AR-SR and N-SR steels into two characteristic DT-transition bands is directly related to the differences in grain size. The normalized steels feature a much finer grain size compared to the as-rolled steels. The ASTM grain size is typically in the 8.3 to 9. 5 (13 to 20 μm) range for the as-rolled steels and typically in the 9. 6 to 10.2 (10 to 13 μm) range for the normalized steels. The finer the ferrite grain size (the higher the ASTM number), the lower the transition temperature of the DT curve.

The correspondence of grain size to the location of the steels in AR or N band is very significant [1]. It indicates that simple micrographic examination can be used to define whether the steels feature N-band or AR-band fracture properties. This observation is very useful for cases where fracture property information is required from relatively small samples or for any other condition that precludes obtaining fracture test data.

The DT data for all TC128-B head steels from tank cars involved in accidents are shown in Figure 4-22 [1]. With the exception of one case, the data represent N-type properties whether derived from normalizing or the high temperature hot forming, followed by air cooling. Similar comparison is made in Figure 4-23 for all shell steels of TC128-B type. Based upon these data, the AAR-RPI investigators concluded that the current production TC128-B materials were produced to good metallurgical control.

The DT data for A212-B steels and one A515-70 steel are shown in Figure 4-24. The data suggest that the AR-SR band for the A 212-B and A 515-70 materials is wider than the band for the TC128-B materials. The TC128-B materials appear to be either processed to tighter controls or the technology has advanced resulting in the improvement [1, 5].

4.5 CVN, DWTT and FATT Data

The minimum CVN energy absorption requirements for materials used in tank car construction is 15 ft-lb at the NDT temperature. When AAR TC128 grade B steel is specified for low temperature service it must be furnished normalized to meet the 15 ft-lb (20.3 J) minimum average of three specimens and 10 ft-lb (13.5 J) minimum for one specimen at -50°F in the longitudinal direction of rolling (ASTM L-T orientation, see Figure 4-4).

In the Phase 03 study [3], fracture toughness tests included Charpy V-notch impact (CVN), drop weight (NDT), drop weight tear (DWTT) and dynamic tear (DT) tests. The DT tests are summarized in Section 4.4. The Charpy V-notch impact tests were conducted in accordance with ASTM Specification E 23-72 "Notched Bar Impact Testing of Metallic Materials." Most of the specimens were full size 10 mm x 10 mm with the axis of the notch oriented through-the-thickness of the materials. An impact energy transition temperature curve was established for most samples in the transverse direction over the temperature range of -50°F to 212°F (-46 to 100°C). In addition, a sufficient number of samples were tested in the longitudinal direction to establish the upper shelf or plateau energy level.

The Drop Weight (NDT) tests were conducted in accordance with ASTM Specification E208-69 "Conducting Drop-Weight Test to Determine Nil-Ductility Transition (NDT) Temperature of Ferritic Steels." The Drop Weight Tear (DWTT) tests were conducted in accordance with ASTM Specification E436-71. "Drop Weight Tear Tests of Ferritic Steels." The DWTT provides information on the transition in fracture appearance. The test specimen thickness was equal to the plate thickness and specimens were oriented in the transverse direction. Wherever a sufficient plate sample was available, the DWTT tests were made on the same steels as were the NDT tests.

Tables 4-10 through 4-12 lists the fracture toughness properties for current, accident, and old steels, respectively [3]. The data in these tables cover all the samples discussed in the introduction to Section 4. The results for all the current steels and accident samples indicate the CVN 15 foot-pound (20.3 J) or 15 mil lateral expansion transition temperatures are within plus or minus 20°F of the NDT temperatures. The DT 50-percent SATT provides an indication of the full-scale ductile to brittle transition temperature when the DT specimen thickness is close to the actual tank thickness. The data show that the DT transition temperatures are 50 to 125 F above the respective CVN transition temperatures.

The CVN data from several programs [6-11] conducted by NIST are summarized below.

In the Reference [6] test program, the CVN specimens were tested according to ASTM designation E23-88. Duplicate CVN impact tests were conducted at temperatures from -73°F to +71°F.

Figure 4-25 shows a comparison of the energy absorbed as a function of test temperature for the micro-alloyed, control-rolled A 8XX grade B steel and the normalized AAR TC128 grade B steel [6]. In the temperature range of -70°F to +20°F (-57 to -7°C), the ASTM L-T specimens revealed that the A 8XX grade B steel had lower impact strength compared to the AAR TC128 grade B steel. Similar trends were also found for the lateral expansion measurements for these two steels. The minimum energy absorbed (lower shelf energy) for the ASTM L-T orientation AAR TC128 grade B test specimens was about 46 ft-lb, whereas the lower shelf energy for similarly oriented A 8XX test specimen was about 10 ft-lb.

The retest program, Reference [7], produced the following result. For the AAR TC128 grade B steel, the energy absorbed for L-T specimens was slightly greater than that for the T-L specimens over the entire range of test temperatures. For the A 8XX grade B steel a pronounced difference between the energy absorbed for L-T and T-L specimens was found. This difference was more pronounced at

higher test temperatures. Figure 4-26 shows the energy absorbed versus test temperature for L-T and T-L orientations for both steels. At -70°F the average energy absorbed for the L-T specimens of AAR TC128 grade B and the A 8XX grade B steels was 34 ft-lb and 9.5 ft-lb, respectively. At -50°F these values were 47 ft-lb and 17 ft-lb, respectively. At about -12°F, the A 8XX grade B steel shows higher energy absorbed value in the L-T orientation than that for the AAR TC128 grade B steel. In the initial investigation [6], this cross over was found at about +16°F. NIST concludes that this shift (from +16°F to -12°F) is due to the variability in the microstructure of the A 8XX grade B steel.

A comparison of the CVN impact values from NIST retest program and the industrial supplier (as reported in its certificate of analysis) is shown in Table 4-13. As shown, significantly higher CVN values are reported by the industrial supplier.

The major conclusions of the retest program were as follows. The retest program confirmed the Charpy V-notch impact, nil-ductility transition temperature, chemical, and inclusion analysis results of NIST test results reported in [6]. The normalized and inclusion shape controlled AAR TC128 grade B steel had a lower NDT temperature and better impact properties at low test temperatures than the new control-rolled and inclusion shape controlled A 8XX grade B steel.

In the Reference [9] test program, the Charpy V-notch impact tests were conducted at -51°C (-60°F), -40°C (-40°F), -29°C (-20°F), -18°C (0°F), and 22°C (+72°F). The CVN results for the normalized AAR TC128 grade B steel are shown in Figure 4-27. The CVN values for the L-T orientation were found to be greater than those for the T-L orientation. At the lowest test temperature, -51°C (-60°F), the average CVN values were 77 J (57 ft-lb) and 29 J (22 ft-lb) for the L-T and T-L orientations, respectively. The upper shelf CVN values were 169 J (125 ft-lb) and 68 J (50 ft-lb) for the L-T and T-L orientations, respectively.

The CVN impact test results for the normalized and stress relieved steel are shown in Figure 4-28 [9]. These results show that stress relieving had a dramatic effect on impact properties in the L-T orientation. Only a slight improvement in impact properties was found in the T-L orientation. At -51 C (-60 F), the average CVN values were 94 J (69 ft-lb) and 24 J (18 ft-lb) for the L-T and T-L orientations, respectively. For the L-T orientation, the upper shelf value was 203 J (150 ft-lb).

The FATT is the temperature at which the fracture appearance of the specimen contains 50% ductile fracture and 50% cleavage fracture. The FATT data from NIST [9] are summarized in Table 4-14. The FATT data developed in References [1, 3] are given in Tables 4-10 through 4-12.

4.6 K_{Ic}, K_{Id} and K_{Ia} data

Generally, the failure of tank cars involves three stages. First, a pre-existing flaw or crack begins to grow under static or dynamic loading conditions. The condition under which the flaw/crack begins to extend is known as the crack initiation and is defined by the static fracture toughness, K_{Ic}. Following the initiation the crack propagates under dynamic or impact loading. The crack continues to propagate if the crack driving force is greater than the dynamic fracture toughness, K_{Id}, of the steel. The crack driving force, expressed as the stress intensity factor K_I in predominantly elastic structures,

depends upon the loading rate, crack size, the structural configuration and the material tensile properties. Finally, if the crack driving force falls below a critical value, the crack arrests. Sometimes crack arrest is not possible and catastrophic failure occurs, e.g., the reported unstable fractures of tank cars into two or more sections. To understand the potential catastrophic nature of failures, it is essential to determine the crack arrest fracture properties of tank car steels at various temperatures.

The dynamic fracture toughness, K_{Id}, is determined from tests that use rapid loading rates. The crack arrest fracture toughness, K_{Ia}, is determined from tests that simulate conditions under which a fast propagating crack arrests. Both K_{Id} and K_{Ia} are dependent upon temperature and loading rate. In most cases, the K_{Id} and K_{Ia} fracture toughness values are known to be lower than K_{Ic}. All three fracture toughness values increase with the increase in temperature.

The K_{Ic}, K_{Id} and K_{Ia} data from several programs [6-11] conducted by NIST are summarized below.

The K_{Ic} data for A 8XX grade B and AAR TC128 grade B steels were developed in References [6, 7]. In these references, the K_{Ic} values were inferred from the J-integral or CTOD tests and these are described in Section 4.7.

In the Reference [8] test program, the crack arrest specimens were tested according to ASTM Designation E 1221-88, Standard Method for Determining Plane-Strain Crack-Arrest Fracture Toughness, K_{Ia}, for Ferritic Steels. This test method provides an estimate of the minimum value of the stress intensity factor, K, at which a fast running (i.e., unstable crack) will arrest. Thirty crack arrest specimens each were tested for the two steels. The test temperatures ranged from -46°C (-50°F) to -18°C (0°F). The tests involved both the T-L and L-T specimens were tested. The details of the testing procedure are given in Reference [8].

Tables 4-15 and 4-16 show comparisons of crack initiation and crack arrest fracture toughness values for both steels. For the N+ISC AAR TC128 grade B steel, the crack arrest toughness, K_{Ia}, was found to be essentially the same from -46°C (-50°F) to -26°C (-15°F) for both T-L and L-T orientations. The average crack arrest fracture toughness was 67 $\pm$ 11 MPa·m$^{1/2}$ (61 $\pm$ 10 Ksi·in$^{1/2}$) over this temperature range. The crack arrest fracture toughness for the CR+ISC A 8XX grade B steel over the same temperature range was 56 $\pm$ 9 MPa·m$^{1/2}$ (51 $\pm$ 8 Ksi·in$^{1/2}$). Further, over this temperature range the crack initiation toughness (K_{Ic}) for the AAR TC128 grade B steel was significantly higher than that for the A 8XX grade B steel. The average K_{Ic} for the AAR TC128 grade B steel, in both L-T and T-L orientations, was 303 MPa·m$^{1/2}$ (275 Ksi·in$^{1/2}$), whereas for the A 8XX grade B steel the average was 75 MPa·m$^{1/2}$ (68 Ksi·in$^{1/2}$). At temperatures above -18°C (0°F), the A 8XX steel showed K_{Ic} values comparable to those measured for the AAR TC128 grade B steel. The A 8XX steel was rejected by the industry because of its poor welding characteristics.

The crack arrest toughness data on AAR TC128 grade B steel in the normalized, and normalized and stress relieved conditions were reported in Reference [9]. Figure 4-29 shows the results for both the L-T and T-L orientation. As expected, the crack arrest value increased with temperature. The normalized and stress relieved material did not show a continuously increasing toughness with temperature. More data would be needed to clearly establish the trend. However, both the normalized, and normalized and stress relieved materials had crack arrest values that are characteristic

of other ferrite/pearlite steels. The differences between the crack initiation toughness value (Fig 4-30) and the arrest toughness value (Figure 4-29) were found to be greater for the normalized and stress relieved material than for the normalized material.

Because cracks have been known to initiate from welds or heat affected zones (HAZ), crack arrest fracture toughness tests [10] were also conducted for welded plates of normalized and stress relieved AAR TC128 grade B steel. Two types of specimens were prepared. For all weld metal specimen, the crack was entirely within the weld metal, whereas for the HAZ the crack was located along the heat-affected zone, the zone adjacent to the weld. These specimens were tested according to ASTM Method 1221-90. Tests were begun at -51°C (-60°F) which represented the lowest expected service test temperature to which this tank car steel would be exposed. It was not possible to initiate a crack in the all weld metal specimen. This observation led to the conclusion that the weld metal was very resistant to crack initiation and had a higher crack initiation toughness value than the base plate material. Further, it was concluded that if a crack initiated in the base plate, it probably would not propagate in the weld metal.

Crack arrest tests for the heat-affected zone were successfully conducted at -51°C and -18°C. The Crack arrest fracture toughness, K_a, values of 48 and 69 MPa·m$^{1/2}$ (44 and 63 Ksi·in$^{1/2}$) were obtained for tests at -51°C (-60°F). These values were found to be comparable to the K_a values for the base metal (Fig. 4-30). A higher crack arrest value of 156 MPa·m$^{1/2}$ (172 Ksi·in$^{1/2}$) was obtained for tests conducted at -18°C (0°F).

These crack arrest fracture toughness results indicated that both the weld metal and the HAZ for the welded normalized and stress relieved AAR TC128 grade B steel were highly resistant to crack initiation and possessed the ability to arrest a propagating crack.

The elevated temperature crack arrest behavior of the normalized and stress relieved steel was investigated in Reference [11]. This test program was initiated to develop the toughness data for the case where the tank car is exposed to fire. Fracture toughness tests were conducted on both the normalized, and normalized and stress relieved steel at 593, 621, 649, and 677°C. Fracture toughness in the L-T and T-L orientations was investigated. The specimens did not produce crack extension upon loading in any of the tests. This crack behavior suggests that the steel had sufficient toughness to prevent the initial fatigue crack from propagating.

Figure 4-31 shows that the fracture toughness decreases with the increase in test temperature. Both the normalized (N), and normalized and stress relieved (N+SR) materials show higher fracture toughness in the L-T orientation than in the T-L orientation due to inclusion orientation. However, the fracture toughness was greater for the normalized and stress relieved steel than for the normalized steel. At the highest temperature, the toughness was almost the same for the N and N+SR materials. These results indicate that the steel is highly resistant to crack extension in the L-T orientation even at 677°C (see Fig. 4-30 for comparison with service temperature).

4.7 J_{Ic} and CTOD Data

The ASTM E 813-88 test method was used in the determination of the plane-strain toughness, J_{Ic}. This test method can be used to determine the fracture toughness at the initiation of slow stable crack growth for metallic materials. This type of fracture usually occurs in the transition and upper shelf regions of the normal "S" type Charpy impact curve (e.g., see Fig. 4-28). The test method defines conditions that must be met for a valid J_{Ic} determination. The main requirements are: (1) a slow stable crack growth, i.e., no rapid cleavage fracture upon loading of the test specimen, and (2) the test specimen is of certain minimum thickness. The single specimen, compliance method was used to determine the J_{Ic} in all tests conducted by NIST [6-11].

The ASTM E 1290-89 test method was used for determining crack-tip opening displacement (CTOD). This test method may be used to characterize the fracture toughness of materials that are too ductile or for cases where the Compact Tension (CT) specimens do not meet the minimum thickness requirements for the plain-strain fracture toughness K_{Ic}, or test show a propensity for unstable crack extension that would prevent the determination of a valid J_{Ic}. This test method is appropriate for materials that exhibit a change from ductile to brittle behavior with decreasing temperature.

The J_{Ic} and CTOD data from several programs [6-11] conducted by NIST are summarized below.

In the Reference [6] test program, the J-integral test specimens were prepared according to ASTM designation E813-88 for both the AAR TC128B and A 8XX steels and tested at temperatures from -63°F to +73°F. All tests were conducted on compact tension (CT, see Figure 4-4) specimens that had 1T thickness (full plate thickness). The crack-tip opening displacement (CTOD) specimens were prepared according to ASTM designation E1290-89 and tested at temperatures from -80°F to +73°F. Most of the CTOD tests used CT specimens but some were also three-point bend specimens.

Both the CTOD and J-integral fracture toughness tests on the normalized and inclusion shape controlled AAR TC128 grade B steel revealed that it did not fail in an unstable manner, even at a test temperature of -80°F. In contrast, the A 8XX steel showed unstable fracture behavior over the entire test temperature range, -80°F to +20°F.

Post-test analysis of the J test data indicated that the minimum specimen thickness requirement was not met for any of the specimens and therefore a valid J_{Ic} (plane-strain J value) was not determined. Therefore, the equation applicable to plane-stress conditions was used to calculate the fracture toughness.

Table 4-17 compares the fracture toughness for the two steels determined from the CTOD test data. The results indicate that there is less variability among the fracture toughness test results for the AAR TC128 grade B steel than among similar results for the A 8XX steel. Tables 4-18 and 4-19 compare fracture toughness results from CT and CTOD test results for both steels. The values obtained from CTOD specimens were consistently higher than those from CT specimens. These results show less scatter in the fracture toughness values for the AAR TC128 steel than for the A 8XX steel. Further, the fracture toughness of the A 8XX steel was found to be much lower than that of the AAR TC128

grade B steel. The A 8XX steel was rejected by the industry because of its poor welding characteristics.

The fracture toughness test data on AAR TC128 grade B steel in the normalized, and normalized and stress relieved conditions was reported in reference [9]. J-integral and CTOD tests were conducted at -51°C (-60°F), -40°C (-40°F), -29°C (-20°F), and -18°C (0°F). The results of J tests are shown in Figure 4-30. These results show that the normalized and stress relieved steel was more resistant to crack initiation than the normalized steel. The two curves marked "S" represent cases where severe crack tip blunting was experienced by the specimen. Consequently, a high K value was obtained for these specimens. In the case of the normalized material, stable crack extension was possible only at temperature -18°C (0°F). Below this temperature, unstable crack extension occurred. The CTOD tests were performed only at -51°C (-60°F) because stable crack growth was not obtained even at this temperature. The CTOD and the corresponding fracture toughness values showed that the normalized and stress relieved steel was more resistant to crack initiation than the normalized steel.

4.8 RESIDUAL STRESS MEASUREMENTS

The high residual stresses in welds have been known to cause leaks and fracture of pressurized structures. In 1986 the FRA was informed of the presence of non-conforming welds on a group of several thousand older tank cars used to transport hazardous products. Continuous, external axial stiffeners had been added to these cars in 1976, which ran along the tank car underbelly between the existing stub sills. This modification was required to increase the tank shell buckling strength. Each stiffener was attached to narrow rectangular pads which were directly attached to the tank car shell. The welding procedure required continuous fillet welds from the stiffener to the pads and intermittent or "skip" welds from the pads to the tank shell. The pad corners and the gap between pads were to be free of weld metal.

Figure 4-32 shows three examples of non-conforming welds, i.e., two skip welds running together, welds continued to pad corner, and welds continued around corners and filled the gap between pads [13]. The pad-to-shell welds were thought to be the cause of reported leaks in some railroad tank cars. Consequently, these welds were considered to be possible sources of high residual stress which might promote crack formation and subsequent propagation.

Welding causes local plastic deformation which produces residual stresses that could be as high as the yield stress of the material. Theoretical analyses and experimental work indicated the residual stresses in skip welds to be the source of the crack initiation. As a result of these preliminary studies, a program to determine the through-thickness distribution of residual stresses in skip welds was conducted at NIST [13]. Eight steel plates of ASTM Specification A 515 grade 70 steel, 61 cm (24 in.) long by 15 cm (6 in.) wide and 1.3 cm (0.5 in.) thick were used in the investigation. The mechanical properties, according to the ASTM specification were: yield strength, 260 Mpa (38 ksi), tensile strength, 485 to 620 MPa (70-90 ksi), and a minimum elongation in 50 mm of 21 %. The weld type was one pass, skip, bead-on plate and the welding method used was shielded metal arc welding (SMAW). Four welded plate specimens representing different combinations of welding parameters (welding current, leading angle and travel speed) were tested. The plate specimens contained two

beads that represent the skip weld process.

Two nondestructive techniques, neutron diffraction and X-ray diffraction, were employed for the measurement of residual stresses. The Neutron diffraction technique is used to measure residual stresses below the surface of the weld. The investigation focused on weld residual stresses in the vicinity of the start and stop positions of welds.

A satisfactory description of residual stresses requires measurement of triaxial state of stress. The residual stress measurements for one of the four specimens (A1) are shown in Figure 4-33a and 4-33b. Here, the direction parallel to the weld is denoted as the longitudinal (L) direction. The direction perpendicular to the weld, in the plane of the plate, is denoted as the transverse (T) direction. Finally, the direction perpendicular to the plate is denoted as the normal (Z) direction.

The results are shown for four depth positions relative to the weld surface (0.25, 3, 6, and 9 mm). The 0.25 mm measurement is from the X-ray technique. As shown the longitudinal stresses were tensile and largest close to the surface at positions close to the weld tip positions. The maximum value of longitudinal stress was found to be as high as or even higher than the yield strength of the steel, 260 MPa (38 ksi). The longitudinal stress diminished in all three directions. A through-the-thickness stress gradient plot of residual stress vs. depth was not developed. The stress plots for three other specimens are reported in Reference [13].

The residual stresses in conjunction with the primary loading stresses can produce localized high stresses typically exceeding the yield stress. The high combined stresses can lead to crack initiation and propagation. The NIST study [13] speculated that the initial direction of crack propagation would be perpendicular to the weld direction. The crack initiation can take place anywhere along the weld bead region. However, with subsequent crack growth the longitudinal stresses are relaxed and the crack might enter a region where the transverse stress is high. This change could force the propagating crack to turn 90 degrees and continue propagating parallel to the weld direction through the region of high tensile transverse stress. The NIST study involved welded plates that were free of lateral constraints on skip welds. It is expected that the lateral constraint typically experienced in tank cars can produce increased transverse stress levels. This aspect was not investigated in NIST study.

Table 4-1

Specified Tensile Properties for tank car steels

Steel	Tensile Properties, Mpa, (ksi)	
	Yield Strength (min.)	Tensile Strength
A 212 B	260 (38)	485-585 (70-85)
A-515 grade 70	260 (38)	485-620 (70-90)
TC-128 grades A & B	345 (50)	558-696 (81-101)

Table 4-2

TENSILE PROPERTIES OF CURRENT SHELL PLATE MATERIAL

Sample	Test Location	H. T.*	Transverse Tensile Strength KSI	Transverse Yield Strength KSI	Elong.** in 2-in. %	Reduction of Area %	Hardness BHN
				AAR TC128-Grade B			
	Specified Values		81-101	50	19.0		
M-1	Mill	A	89.7	56.0	21.0		
	AAR	A,S	86.6	54.0	29.5	56.8	165
M-2	Mill	A	91.3	60.5	19.5		
	AAR	A,S	85.7	51.9	29.5	61.5	173
M-3	Mill	A	84.8	62.1	21.0		
	AAR	A,S	91.4	68.1	21.3	44.5	179
M-4A	Mill	A	91.4	64.6	19.0		
	AAR	A,S	90.6	63.5	29.5	61.7	183
M-4B	Mill	A	90.1	66.5	19.0		
	AAR	A,S	91.0	64.5	24.5	54.9	183
M-10	Mill	A,N	83.7	56.0	24.0		
	AAR	A,N,S	72.3	50.6	33.5	69.7	137
M-11	Mill	A,N	81.9	55.5	22.0		
	AAR	A,N,S	80.1+	57.2+	33.9	56.0	152
				ASTM A515 - Grade 70			
	Specified Values		70-85	38	21.0		
M-5	Mill	A	76.4	46.4	22.0		
	AAR	A,S	71.5	41.8	29.0	61.5	137
M-6	Mill	A	71.1	42.7	23.0		
	AAR	A,S	63.9	40.0	34.5	56.1	126
M-7	Mill	A	78.5	49.6	27.0		
	AAR	A,S	78.5	47.8	35.0	63.8	128
M-8	Mill	A	81.6	50.5	19.0		
	AAR	A,S	79.6	51.3	29.0	45.9	149
				ASTM A516 - Grade 70			
	Specified Values		70-85	38	21		
M-9	Mill	A, N	75.3	48.2	26		
	AAR	A,N,S	70.1	44.4	24.5	59.8	134

* Heat Treatment Code: A-As Rolled, S-Stress Relieved, N-Normalized

** All Mill Tests on 8 in. Specimens; + Data Modified from AAR Noncalibrated Test with Difference Between Mean of Calibrated and Mean of Noncalibrated Tests.

Table 4-3

TENSILE PROPERTIES OF CURRENT HEAD MATERIAL

Sample	Test Location	H. T. *	Transverse Tensile Strength KSI	Transverse Yield Strength KSI	Elong. ** in 2-in. %	Reduction of Area %	Hardness BHN
			AAR TC128-Grade B				
	Specified Values		81-101	50	19.0		
M-13	Mill	A, N	88.5	57.0	23.0		
	AAR	A, N, C, S	85.5+	53.9+	30.0	59.1	167
M-14	Mill	A, N	84.7	54.4	26.0		
	AAR	A, N, C, S	80.7+	54.6+	27.7	61.3	156
M-15	Mill	A, N(1)	83.7	55.8	24.0		
	AAR	A, H, N(2)	95.7+	63.9+	21.8	53.4	199
M-17	Mill	A	92.9	60.1	19.0		
	AAR	A, H, S	83.8	56.8	26.1	55.6	167
M-18	Mill	A, N(1)	90.8	64.7	20.0		
	AAR	A, S(3)	96.8	71.3	20.3	48.2	199
M-19	Mill	A, N(1)	83.7	55.8	24.0		
	AAR	A, H, S	92.4	55.7	21.9	50.7	192
			ASTM A515 - Grade 70				
	Specified Values		70-85	38	21.0		
M-12	Mill	A	73.4	45.0	25		
	AAR	A, C, S	70.5	47.5	34.0	59.1	140
M-16	Mill	A	75.4	45.6	28		
	AAR	A, H, S	73.9	45.8	29.5	55.3	134

*Heat Treatment Code: A-As Rolled, S-Stress Relieved, N-Normalized, C-Cold Formed, H-Hot Formed

**All Mill Tests on 8 in. Specimens: + Data Modified from AAR Noncalibrated Test with Difference between Mean of Calibrated and Mean of Noncalibrated Tests.

(1) Mill Test Specimens Normalized 1650° F, 1/2 Hour, Air Cooled.

(2) AAR Test Specimens Normalized at 1650° F in Laboratory Furnace. Maintained 1/2 Hour. Air Cooled.

(3) Head Square Trim Stock. Stress Relieved. No Forming.

Table 4-4

TENSILE PROPERTIES OF ACCIDENT SAMPLES

Sample	Car I. D.	Grade	Location	Tensile Strength KSI	Yield Strength KSI	Reduct. of Area %	Elong. in 2 in. %	Hard-ness BHN
			GLENDORA, MISS.					
A 11	SHPX 85069	TC128B	Shell	76.8	50.6	53.7	24.5	152
A 12	SHPX 85069	TC128B	Shell	84.2+	68.7+	53.2	19.8	187
A 31	SHPX 85069	TC128B	Shell	92.0+	63.7+	53.3	19.4	179
A 32	SHPX 85069	TC128B	Head	82.8	60.4	64.6	25.5	167
			TROUP, TEX.					
B 1	GATX 12807	A-515-70	Shell	82.5+	71.7+	51.1	16.3	170
			LEHIGH, KAS.					
C 1	UPCX 83641	A-212-B	Shell	78.8	46.8	-	28.3	-
C 21	UPCX 81505	TC128B	Shell	92.9	63.8	61.5	25.5	197
C 22	UPCX 81505	TC128B	Head	86.7+	60.3+	57.4	27.2	170
C 41	UTLX 38332	TC128B	Shell	76.0+	63.8+	55.2	29.5	149
C 42	UTLX 38332	TC128B	Head	89.5+	70.6+	60.6	21.6	183
			CRESCENT CITY, ILLINOIS					
D 2	SCMX 3445	TC128B	Shell	84.3	64.4	42.5	19.9	174
D 3	NATX 32025	A-212	Shell	76.7	57.1	52.2	21.0	156
D 8	SOEX 3037	A-212	Shell	77.1+	55.3+	52.1	23.4	156
D 10	SOEX 3037	A-212	Shell	77.8	44.7	44.9	25.6	156
D 11	NATX 32025	A-212	Shell	79.6	57.8	56.1	27.0	174
			SOUTH BYRON, NEW YORK					
EI-E2	PPGX 9990	TC128B	Shell	95.3+	76.3+	43.1	17.6	217
			CALLAO, MISSOURI					
F 1	GATX 94451	TC128B	Head	87.6+	65.0+	60.0	23.4	217
F 2	GATX 94451	TC128B	Shell	84.1	57.0	54.1	20.5	170
F 3	GATX 94451	TC128B	Shell	91.2+	64.3+	47.8	20.7	201
F 4	GATX 94451	TC128B	Shell	90.4	65.6	53.3	24.0	192
			KAMLOOPS, B.C.					
G 1	CGTX 63526	TC128B	Shell	95.4	81.7	60.0	21.2	217
			HOUSTON, TEXAS					
H 1	ESMX 4804	TC128B	Shell	88.2	54.8	-	26.5	-
H 2	ESMX 4804	TC128B	Shell	84.8	48.8	-	27.0	-

*All properties Transverse unless noted.

+Tensile Data Modified from AAR Noncalibrated Test with Difference Between Mean of Calibrated and Mean of Noncalibrated Tests.

Table 4-5

TENSILE PROPERTIES OF OLD TANK CAR STEELS

Specimen	Car	Class	Grade	Mill	Plate Thickness	Tensile Strength (ksi)		Yield Strength (ksi)	Red. of Area (%)	Elongation (% in 2")	Brinell Hardness
01	SHPX 362	105A500W	A212B Firebox	D	0.875	Spec. **	70-85	>38.0	-	>21.0	137
						Test L	69.7	49.7	66.0	31.6	
						Test T	69.5	49.7	56.5	29.8	
						Mill	72.4	47.8	-	28.0	
02	SHPX 362	105A500W	A212B Firebox	D	0.875	Spec. **	70-85	>38.0	-	>21.0	
						Test L	76.3	49.6	59.7	28.8	149
						Test T	76.1	47.0	53.8	27.5	
						Mill	77.0	53.0	-	25.0	
03	SHPX 14136	103W	A285C	A	0.520	Spec.	55-65	>30.0	-	>26.0	
						Test L	55.3	36.2	67.0	32.6	91*
						Test T	54.9	34.5	61.4	36.9	
04	SHPX 14136	103W	A285C	A	0.550	Spec.	55-65	>30.0	-	>26.0	
						Test L	62.3	40.8	66.2	32.3	109
						Test T	60.5	35.2	63.4	33.1	
05	SHPX 3686	105A500W	M115 Flange	G	1.125	Spec.	55-65	>1/2T.S	-	>1.5×10^6/T.S. in 8"	
						Test L	55.9	32.5	64.7	36.4	104
						Test T	55.9	34.3	62.3	36.1	
06	SHPX 3686	105A500W	M115 Flange	G	1.125	Spec.	55-65	>1/2T.S	-	>1.5×10^6/T.S. in 8"	
						Test L	50.8	31.8	68.8	39.0	
						Test T	50.7	30.1	65.2	38.5	85

* 1000 Kg load

** Spec. superseded in 1966 by ASTM A515-70

Table 4-6

Effects of decreasing the 10-minute lifetime stress on the rupture life.

		Increase in Rupture Life					
Temperature	10-Minute Lifetime Stress (MPa)	One Hour	Stress	Two Hours	Stress	Three Hours	Stress
593 C	234.3	-17%	194.5	-23%	180.4	-27%	171.0
621 C	190.0	-19%	153.9	-26%	140.6	-30%	133.0
649 C	157.2	-23%	121.0	-33%	105.3	-38%	97.5
677 C	123.8	-27%	90.4	-37%	78.0	-43%	70.6

Table 4-7

NDT Temperature Range for Seven Reference Structural steels

Steel	Design Reference Class	NDT Temperature Range, °F	NDT Temperature Range, °C
LIS, AR, CGP	1	0 - 70	-18 - 21
LIS, AR, CGP	2	0 - 50	-18 - 10
LIS, N, FGP	1	-50 - 10	-46 - -13
LIS, N, FGP	2	-50 - -10	-46 - -24
LIS Alloy, FGP+N	1	-70 - -10	-58 - -24
LIS Alloy, FGP+N	2	-50 - -30	-46 - -34
LIS Alloy, AR, FGP	1	0 - 70	-18 - 21
LIS Alloy, AR, FGP	2	0 - 50	-18 - 10
HS Low Alloy, Q&T	1	-90 - -50	-68 - -46
HS Low Alloy, Q&T	2	-90 - -30	-68 - -34
HS Low Alloy, Q&T, (excessive section Size)	1	-30 - 70	-34 - 21
HS Low Alloy, Q&T, (excessive section Size)	2	-30 - 50	-34 - 10
HS High (best) Alloy, Q&T	1	-160 - -80	-107 - -62
HS High (best) Alloy, Q&T	2	-160 - -100	-107 - -73
Cb (Nb) Control-Rolled		-90 - -50	-68 - -46
Cb (Nb) Control-Rolled, ICR		-120 - -80	-84 - -62
Cb (Nb) Control-Rolled, ICR&AC		-150 - -110	-101 - -79

Table 4-8

NDT Temperature Range for Five Generic Classifications of steels

Steel	NDT Temperature Range, °F	NDT Temperature Range, °C
Typical C/Mn, AR	20 - 60	-7 - 16
Best C/Mn & Alloy, AR	0 - 40	-18 - 4
Typical C/Mn, N	-40 - 0	-40 - -18
Best C/Mn & Alloy, N	-70 - -30	-58 - -34
Cb, FGP, N	-90 - -55	-68 - -48
"Future" Tank Car Steels		
Cb (Nb) Controlled-Rolled	-90 - -50	-68 - -46
Cb (Nb) Controlled-Rolled, ICR	-120 - -80	-84 - -62
Cb (Nb) Controlled-Rolled, ICR&AC	-150 - -110	-101 - -79

Table 4-9

NDT Temperature Data from NIST Reports

Steel	NDT, °F	NDT, °C
AAR TC 128 Grade B, N+ISC [6]	-40	-40
AAR TC 128 Grade B, N+ISC [7]	-60	-51
AAR TC 128 Grade B, N [9]	-40	-40
AAR TC 128 Grade B, N+SR [9]	-40	-40
"Future" Tank Car Steel		
A 8XX Grade B, CR+ISC [6]	-10	-23
A 8XX Grade B, CR+ISC [7]	-20	-29

N= Normalized, SR = Stress-relieved, CR = Control-rolled,
ISC = Inclusion shape control practice.
Reference [7] data is from retesting of the same steel plates as in Reference [6].

Table 4-10

FRACTURE TOUGHNESS PROPERTIES OF CURRENT SHELL AND HEAD PLATE MATERIALS

Sample	H.T.*	Charpy V-Notch Impact Test: 15 ft. lb. Temp °F	50% Shear Fracture, Temp. °F	15-mil Lateral Expan., °F	Trans. Shelf Energy ft. lb.	Long. Shelf Energy ft. lb.	Shelf Energy Ratio, L/T	Drop Weight Test: Nil-ductility Transition Temp., °F	Dynamic Tear Test: Long. Plateau Energy ft. lb.	Transverse Plateau Energy ft. lb.	50% Shear Area Trans. Temp. °F	50% Max. Energy Trans. Temp. °F	Drop Weight Tear Test: 80% Shear Area Trans. Temp. °F
AAR TC128 Grade B													
Shell Plate													
M-1	A,S	0	+80	+10	48	73	1.5	0	600	375	100	91	107
M-2	A,S	0	+65	-20	36	74	2.1	0	450	280	90	65	97
M-3	A,S	-10	+15	0	30	58	1.9	0	460	250	40	36	48
M-4a	A,S	+10	+50	+10	50	78	1.6		635	450	112	86	
M-4b	A,S	+10	+75	+20	42	79	1.9	-	625	300	118	98	
Average		+2	+57	+4	41	72	1.8		554	331	92	75	84
Shell Plate													
M-10	A,N,S	-75	-50	-50	70	85	1.2	-60	630	460	15	17	17
M-11	A,N,S	-70	-15	-50	45	113	2.5		990	340	55	32	
Average		-72	-32	-50	58	99	1.9		810	400	35	25	
Head Material													
M-13	A,N,C,S	-40	0	-45	53	74	1.4		470	400	38	20	
M-14	A,N,C,S	-50	-10	-40	55	60	1.1		500	400	4	20	
M-15	A,N	-10	+10	-35	47	64	1.4	-20	500	400	40	50	88
M-17	A,H,S	-45	-40	-20	44	73	1.7		600	400	28	4	
M-18	A,S (1)	+20	+40	+40	30	48	1.6		460	240	80	78	
M-19	A,H,S	+30	+20	+45	45	50	1.1	+20	480	340	120	105	80
Average		-16	+3	-9	46	61	1.4		502	363	51	46	83
ASTM A515 Grade 70													
Shell Plate													
M-5	A,S	-10	+50	0	35	62	1.8		600	325	112	105	
M-6	A,S	+35	+85	+35	36	87	2.4		500	280	109	102	
M-7	A,S	-5	+70	0	63	103	1.6	-20	560	320	72	92	
M-8	A,S	-10	-10	-5	25	60	2.4		360	200	12	10	
Average		+3	+49	+8	40	78	2.1		505	281	76	77	
Head Material													
M-12	A,C,S	+20	+70	+20	55	77	1.4	+30	530	400	112	108	125
M-16	A,H,S	+20	+40	0	38	66	1.7		415	250	76	65	
Average		+20	+55	+10	47	72	1.5		473	325	94	87	
ASTM A516 Grade 70													
M-9	A,N,S	-20	+5	-40	40	89	2.2	-40	640	340	55	33	85

NOTES: All Properties Transverse Unless Otherwise Noted.

* Heat Treatment Code: A-As Rolled, S-Stress Relieved, N-Normalized, C-Cold Formed, H-Hot Formed.

(1) Head Square Trim Stock - Stress Relieved, No Forming.

Table 4-11

FRACTURE TOUGHNESS PROPERTIES OF ACCIDENT SAMPLES

Tank Car	Sample[1]	Grade	Charpy V-Notch Impact Tests: 15 ft. lb. Temp °F	50% Shear Fracture Temp. °F	15-mil Lateral Expan., °F	Trans. Shelf Energy ft. lb.	Long. Shelf Energy ft. lb.	Drop Weight Test: Nil-ductility Transition Temp., °F	Dynamic Tear Test: Long Plateau Energy ft. lb.	Trans. Plateau Energy ft. lb.	50% Shear Area Trans. Temp °F	50% Max Energy Trans Temp. °F	Cause of Crack Initiation
							Glendora, Mississippi						
SHPX 85069	A-11-S	TC128-B	0	+10	-25	34	47	-10	360	275	67	86	
SHPX 85089	A-12-S	TC128-B	+15	+85	-25	28	50						Overheated area
SHPX 85069	A-31-S	TC128-B	+10	+80	+25	32	56			250	50	35	
SHPX 85069	A-32-S	TC128-B	-10	-30	-35	55	55						
							Troup, Texas						
GATX 12807	B1-S	A515-70	-115	+105	+110	29	57		480	275	133	112	Sudden overpressure (ethylene oxide)
							Lehigh, Kansas						
UPCX 83641	C1-8	A212-B	+75	+100	+65	-	48		800	380	128	140	Overheated area
UPCX 81505	C21-S	TC128-B	+25	+70	+35	40	68		575	300	125	90	
UPCX 81505	C22-H	TC128-B	-80	-15	-50	55	68		450	450	30	10	Overheated area
UTLX 38332	C41-S	TC128B	-60	+40	-50	67	83		725	500	98	75	Overheated area
UTLX 38332	C42-H	TC128-B	-45	-5	-35	42	68		575	360	38	45	Overheated area
							Crescent City, Illinois						
SCMX 3445	D2-S	TC128-B	+40	+40	+40	22	59		620	230	82	68	Overheated area
NATX 32025	D3-S	A212	+70	+70	+60	30	45		325	230	108	109	
SOEX 3037	D8-S	A212	+110	-95	+90	32	65						
SOEX 3037	D10-S	A212	+40	+65	+30	34	68		615	300	113	108	Overheated area
NATX 32025	D11-S	A212	-10	+110	+90	ND	ND		425	300	176	160	
							South Byron, New York						
PPGX 9990	E2-S	TC128-B	+70	+75	+80	25	43			260	83	85	Overheated area
							Callao, Missouri						
GATX 84451	F1-H	TC128-B	+85	+95	+80	40	40		510	350	35	40	
GATX 94451	F2-S	TC128-B	+10	+40	+10	36	76		640	340	78	72	Mechanical impact
GATX 94451	F3-S	TC128-B	+10	+40	+35	33	54	+20	435	250	84	62	
GATX 94451	F4-S	TC128-B	+70	+75	+70	31	54		280	325	122	102	
							Kamloops, British Columbia						
CGTX 63526	G1-S	TC128-B	+115	+120	+80	35	45		450	275	192	205	Overheated area
							Houston, Texas						
ESMX 4804	H1-S	TC128-B	+60	+50	+55	48	160		500	300	95	85	
ESMX 4804	H2-S	TC128-B	+15	+40	+35	48	180		600	300	102	90	Overheated area

NOTE: All Properties Transverse unless Otherwise Noted.

(1) S - shell sample location
H - head sample location

Table 4-12

FRACTURE TOUGHNESS PROPERTIES OF OLD TANK CAR PLATES

	CHARPY V-NOTCH IMPACT TEST					DROP WEIGHT TEST (NDT)	DYNAMIC TEAR TEST				DROP WEIGHT TEAR TEST
Sample	15 ft. lb. Temp. °F	50% Shear Fracture Temp. °F	15-mil Lateral Expan. °F	Trans. Shelf Energy ft. lb.	Long. Shelf Energy ft. lb.	Nil Ductility Temp. °F	Long Plateau Energy ft. lb.	Trans. Plateau Energy ft. lb.	50% Shear Area Trans. Temp. °F	50% Max. Energy Trans. Temp. °F	80% Shear Area Trans. Temp. °F
					ASTM A212B FIREBOX						
01	-30	20	-20	41	74	-10	525	300	40	60	95
02	-30	30	-30	36	55	-10	425	300	40	70	70
					ASTM A285C						
03	-40	40	20	44	103	-10	600	325	65	85	80
04	10	60	10	55	110	0	600	400	85	80	80
					AAR M115 FLANGE						
05	50	70	45	76	106	30	725	550	125	110	135
06	45	80	60	130	170	30	725	550	115	110	130

NOTE: All Properties Transverse Unless Otherwise Noted.

Table 4-13

Comparison of the CVN Impact Test Results Obtained at -50°F by the NIST and Those Reported by the Bethlehem Steel Corporation in its Certificate of Analysis. Values are in ft-lb.

	NIST				BETHLEHEM STEEL CORPORATION			
	A 8XX		AAR TC128		A 8XX		AAR TC128	
	LT	TL	LT	TL	LT	TL	LT	TL
	12.0							
	12.0	12.5	49.0	48	38		78	
	36.0	12.0	51.0	38	52		85	
	8.5	9.5	41.0	36	33		70	
Average	17.1	11.3	47.0	40.7	41.0		77.7	

Table 4-14

FATT Data

Steel	FATT, °F	FATT, °C
AAR TC 128 Grade B, N, L-T [9]	10	-12
AAR TC 128 Grade B, N, T-L [9]	20	-7
AAR TC 128 Grade B, N+SR, L-T [9]	10	-12
AAR TC 128 Grade B, N+SR, T-L [9]	25	-1

N= Normalized, SR = Stress-relieved
T-L and L-T designate specimen orientation (see Figure 4-4)

Table 4-15

Crack Initiation and Crack Arrest Fracture Toughness for Normalized and Inclusion Shape Controlled AAR TC128 Grade B Steel.

Specimen Number	Specimen Orientation	Test Temperature °C	Test Temperature (°F)	Fracture Toughness K_i^1 MPa*m$^{1/2}$	Fracture Toughness K_i^1 Ksi*in$^{1/2}$	Fracture Toughness K_a^2 MPa*m$^{1/2}$	Fracture Toughness K_a^2 Ksi*in$^{1/2}$
F1[3]	LT	-53	-63	319	290		
F2	LT	"	"	319	290		
F15	TL	"	"	266	242		
F16	TL	"	"	245	223		
H234	LT	-46	-50			56	51
H24	LT	"	"			74	67
H25	LT	"	"			60	55
H26	LT	"	"			75	68
F3	LT	-40	-40	265	241		
F17	TL	"	"	284	258		
H27	LT	"	"			55	50
H28	LT	"	"			77	70
H29	LT	"	"			70	64
H33	LT	-26	-15			86	78
H15	TL	"	"			57	52

1. Crack initiation fracture toughness, plane stress, ASTM E 813-89.
2. Crack arrest fracture toughness, plane stress, ASTM E 1221-88.
3. "F" specimens are compact tension type.
4. "H" specimens are modified compact tension type.

Table 4-16

Crack Initiation and Crack Arrest Fracture Toughness for Micro-Alloyed, Control-Rolled, and Inclusion Shape Controlled A 8XX Grade B Steel.

Specimen Number	Specimen Orientation	Test Temperature °C	Test Temperature (°F)	Fracture Toughness K_I^1 MPa*m$^{1/2}$	Fracture Toughness K_I^1 Ksi*in$^{1/2}$	Fracture Toughness K_a^2 MPa*m$^{1/2}$	Fracture Toughness K_a^2 Ksi*in$^{1/2}$
B3[3]	LT	-51	-60	71	65		
D37[4]	LT	-46	-50			58	53
D38	LT	"	"			52	47
D14	TL	"	"			41	37
D14	TL	"	"			51	46
B1	LT	-40	-40	76	69		
D33	LT	"	"			51	46
D34	LT	"	"			65	59
D36	LT	"	"			45	41
D11	TL	"	"			45	41
D12	TL	"	"			53	48
D13	TL	"	"			53	48
D30	LT	-34	-30			54	49
D31	LT	"	"			66	60
D32	LT	"	"			49	45
D8	TL	"	"			68	62
D9	TL	"	"			65	59
B2	LT	-29	-20			-76	69
D5	TL	-26	-15	67	61		
D25	LT	"	"		CRACK DID NOT RUN		
D26	LT	"	"		CRACK DID NOT RUN		
B4	LT	-17.8	0	248	226		
B5	LT	-6.7	+20	306	279		
B14	LT	+22.8	+73	363	330		

1. Crack initiation fracture toughness, plane stress, ASTM E 813-89.
2. Crack arrest fracture toughness, ASTM E 1221-88.
3. "B" specimens are compact tension type.
4. "D" specimens are modified compact tension type.

Table 4-17

Comparison of Fracture Toughness Results for Normalized AAR TC128 Grade B Steel and Control-Rolled A 8XX Steel using CTOD Test Results. Both Steels Were Made using Inclusion Shape Control Practice.

Specimen Number	Test Temp. °F	TC128 Plane Stress K^3	A 8XX Plane Stress K^3	TC128 Plane Strain K^4	A 8XX Plane Strain K^4	TC128 Plane Stress J^5	A 8XX Plane Stress J^5	TC128 Plane Strain J^6	A 8XX Plane Strain J^6	CTOD (inch) δc^7	CTOD (inch) δm^8
E8[1]	-82	251		290		2171		2894			0.0235
E9	-82	262		303		2373		3164			0.0257
A12[2]	-80		74		86		191		254	0.0017	
A9	-60		68		79		160		213	0.0014	
A11	-60		89		103		273		364	0.0025	
E10	-40	269		311		2493		3324			0.0272
E11	-40	269		311		2498		3331			0.0272
A14	-40		115		132		453		604	0.0042	
A17	-40		86		100		256		341	0.0024	
A18	-40		89		102		271		361	0.0025	
A15	-22		71		82		174		232	0.0016	
A16	-22		112		129		433		576	0.0004	
A20	-22		114		132		448		598	0.0042	
A22	0		175		202		1059		1412	0.0102	
A23	+20		194		224		1295		1727	0.0126	

1) AAR TC128 Steel - "E" specimens
2) A 8XX Steel - "A" specimens
3) $K=(1.2*E*\sigma_{flow}*\delta)^{\frac{1}{2}}$: Plane-stress where δ=CTOD, $(ksi\cdot in^{\frac{1}{2}})$
4) $K=(1.6*E*\sigma_{flow}*\delta)^{\frac{1}{2}}$: Plane-strain where δ=CTOD, $(ksi\cdot in^{\frac{1}{2}})$
5) $J=(1.2*\sigma_{flow}*\delta)$: Plane-stress where δ=CTOD, $(in\text{-}lb/in^2)$
6) $J=(1.6*\sigma_{flow}*\delta)$: Plane-strain where δ-CTOD, $(in\text{-}lb/in^2)$
7) CTOD at the onset of unstable brittle crack extension or pop-in.
8) CTOD at the first attainment of a maximum load plateau for fully plastic behavior.

Table 4-18

Comparison of Fracture Toughness Results using CT AND CTOD Test Results for Normalized and Inclusion Shape Controlled AAR TC128 Grade B Steel.

			CT			CTOD			
Method	Specimen Number	Test Temp. °F	J[3]	Plane Stress K[4]	Plane Strain K[5]	Plane Stress J[6]	Plane Strain J[7]	Plane Stress K[8]	Plane Strain K[9]
CT[1]	F1	-63	2904	290	304				
CT	F2	-63	2908	290	304				
CT	F15	-63	2012	242	258				
CT	F16	-63	1718	223	238				
CT	F3	-40	2000	241	252				
CT	F17	-40	2300	258	270				
CTOD[2]	E10	-40				2493	3324	269	311
CTOD	E11	-40				2498	3331	269	311

1) CT: Compact Tension Specimen
2) CTOD: Three Point Bend Specimen
3) From J-Integral Test (in-lb/in^2)
4) $K=(JE)^{1/2}$ using J obtained from CT test results (ksi$\cdot$in$^{\frac{1}{2}}$).
5) $K=(JE/(1-\nu^2))^{1/2}$ using J obtained from CT test results (ksi$\cdot$in$^{\frac{1}{2}}$).
6) $J=(1.2*\sigma_{flow}*\delta)$: Plane-stress where δ=CTOD (in-lb/in^2).
7) $J=(1.6*\sigma_{flow}*\delta)$: Plane-strain where δ=CTOD (in-lb/in^2).
8) $K=(1.2*E*\sigma_{flow}*\delta)^{\frac{1}{2}}$: Plane-stress where δ=CTOD (ksi$\cdot$in$^{\frac{1}{2}}$).
9) $K=(1.6*E*\sigma_{flow}*\delta)^{\frac{1}{2}}$: Plane-strain where δ=CTOD (ksi$\cdot$in$^{\frac{1}{2}}$).

Table 4-19

Comparison of Fracture Toughness Using CT and CTOD Test Results for Control-Rolled and Inclusion Shape Controlled A 8XX Steel.

Test Method	Specimen Number	Test Temp. °F	CT			CTOD			
			J[3]	Plane Stress K[4]	Plane Strain K[5]	Plane Stress J[6]	Plane Strain J[7]	Plane Stress K[8]	Plane Strain K[9]
CT[1]	B3	-60	147	65	68				
CTOD[2]	A9	-60				160	213	68	79
CTOD	A11	-60				273	364	89	103
CT	B1	-40	165	69	72				
CTOD	A14	-40				453	604	115	132
CTOD	A17	-40				256	341	86	100
CTOD	A18	-40				271	361	89	102
CT	B2	-20	164	69	72				
CTOD	A20	-22				448	598	114	132
CTOD	A15	-22				124	232	71	82
CTOD	A16	-22				433	576	112	129

1) CT: Compact tension specimen
2) CTOD: Three point bend specimen
3) From J-Integral Test (in-lb/in^2)
4) $K=(JE)^{\frac{1}{2}}$: Plane stress K (ksi$\cdot$in$^{\frac{1}{2}}$) obtained using J value from CT test.
5) $K=(JE/1-\nu))^{\frac{1}{2}}$: Plane strain K (ksi$\cdot$in$^{\frac{1}{2}}$) obtained using J value from CT test
6) $J=(1.2*\sigma_{flow}*\delta)$: Plane-stress where δ=CTOD (in-lb/in^2).
7) $J=(1.6*\sigma_{flow}*\delta)$: Plane-strain where δ=CTOD (in-lb/in^2).
8) $K=(1.2*E*\sigma_{flow}*\delta)^{\frac{1}{2}}$: Plane-stress where δ=CTOD (ksi$\cdot$in$^{\frac{1}{2}}$).
9) $K=(1.6*E*\sigma_{flow}*\delta)^{\frac{1}{2}}$: Plane-strain where δ=CTOD (ksi$\cdot$in$^{\frac{1}{2}}$).

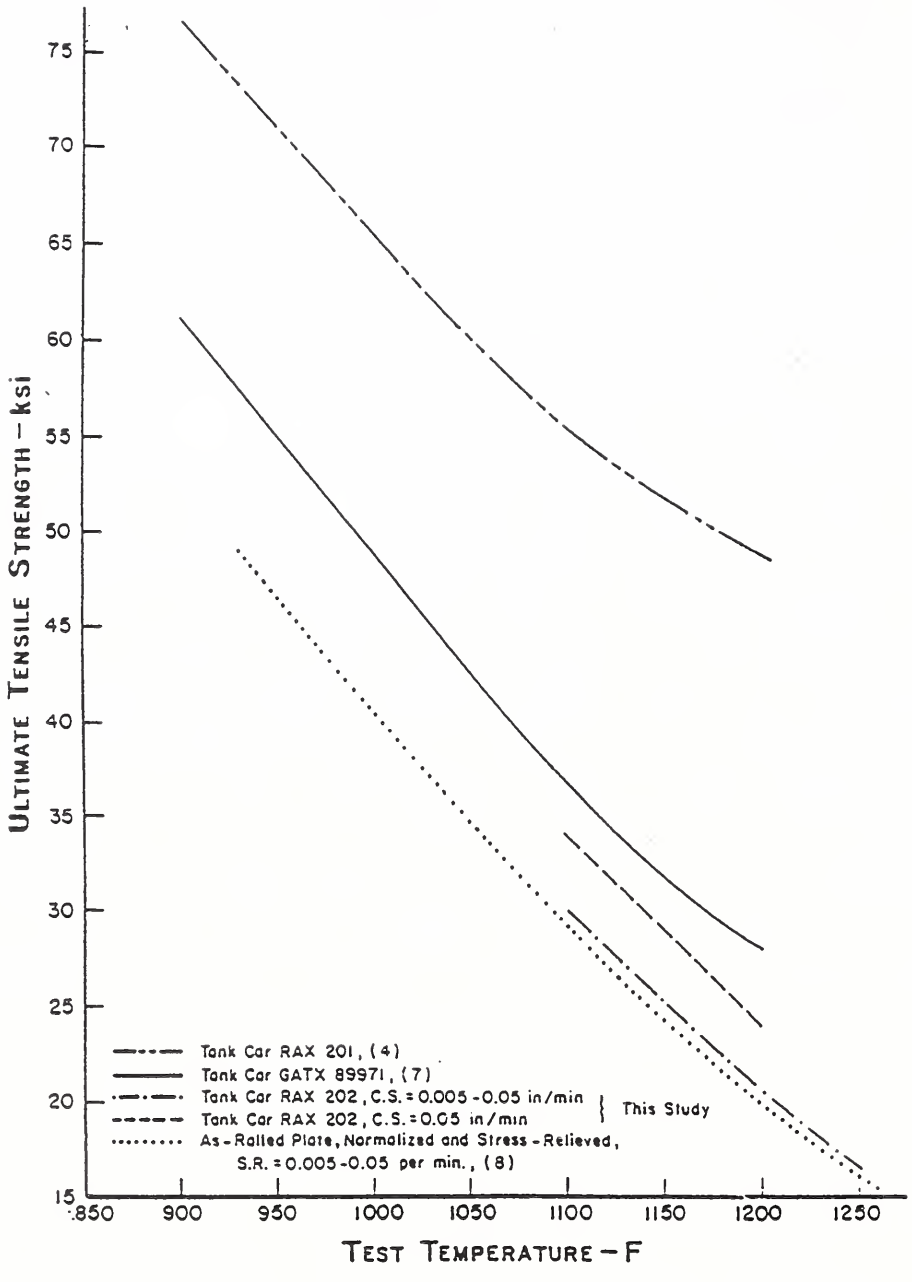

Figure 4-1. Elevated Temperature Ultimate Tensile Strength Properties of AAR M128-B Steel.

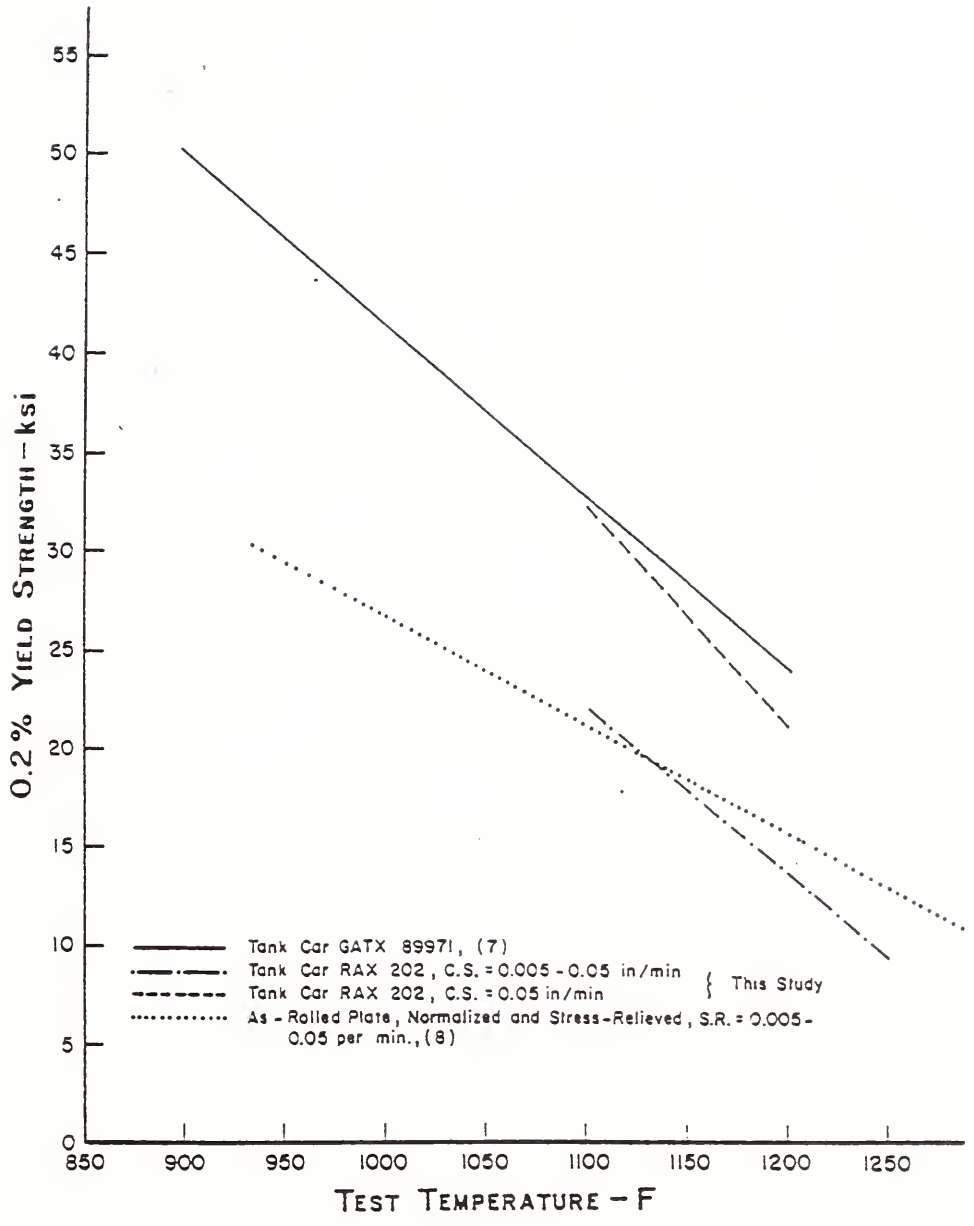

Figure 4-2. Elevated Temperature Yield Strength Properties of AAR M128-B Steel.

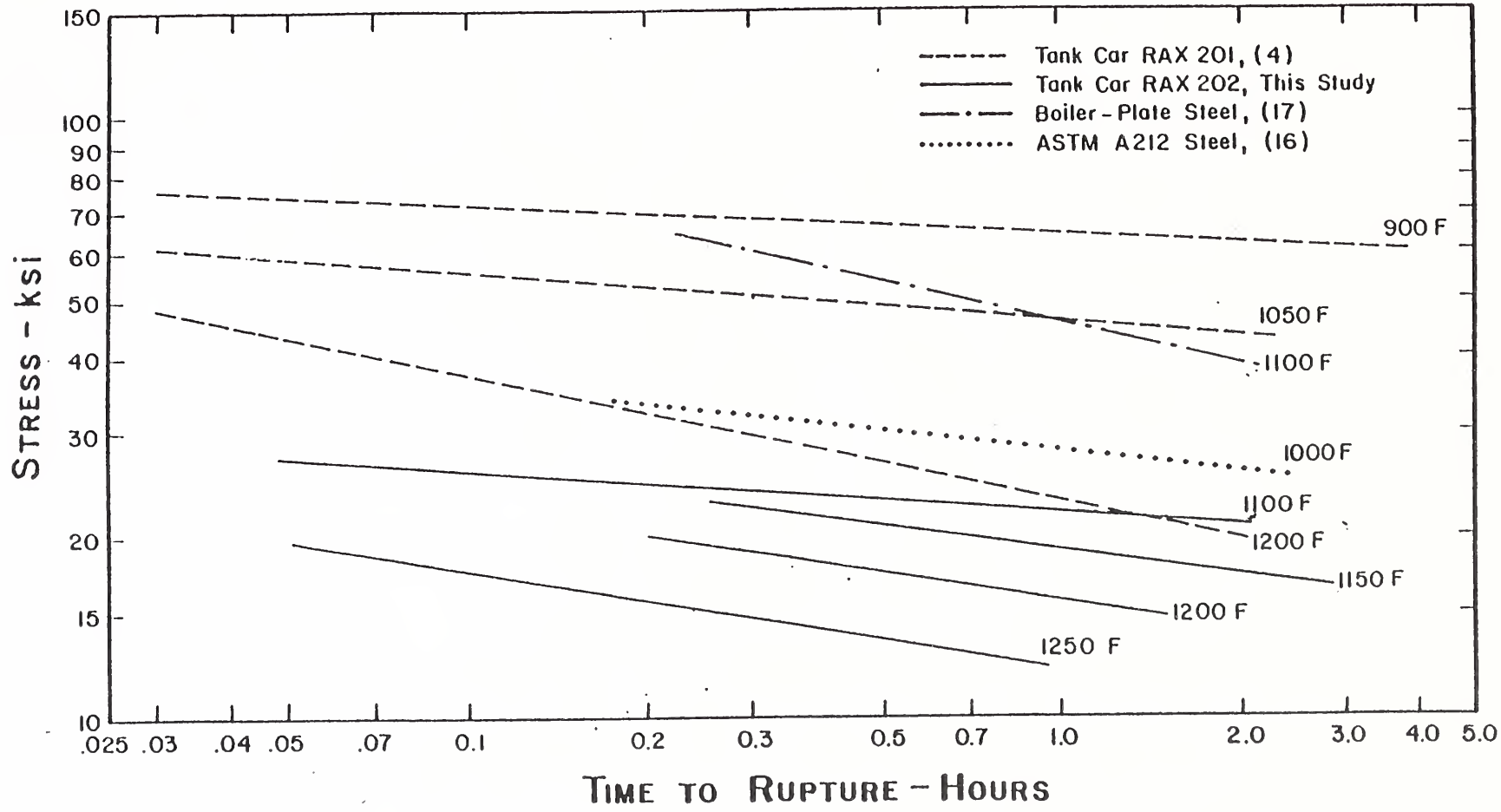

Figure 4-3. Stress-Rupture Data for Several Pressure Vessel Steels.

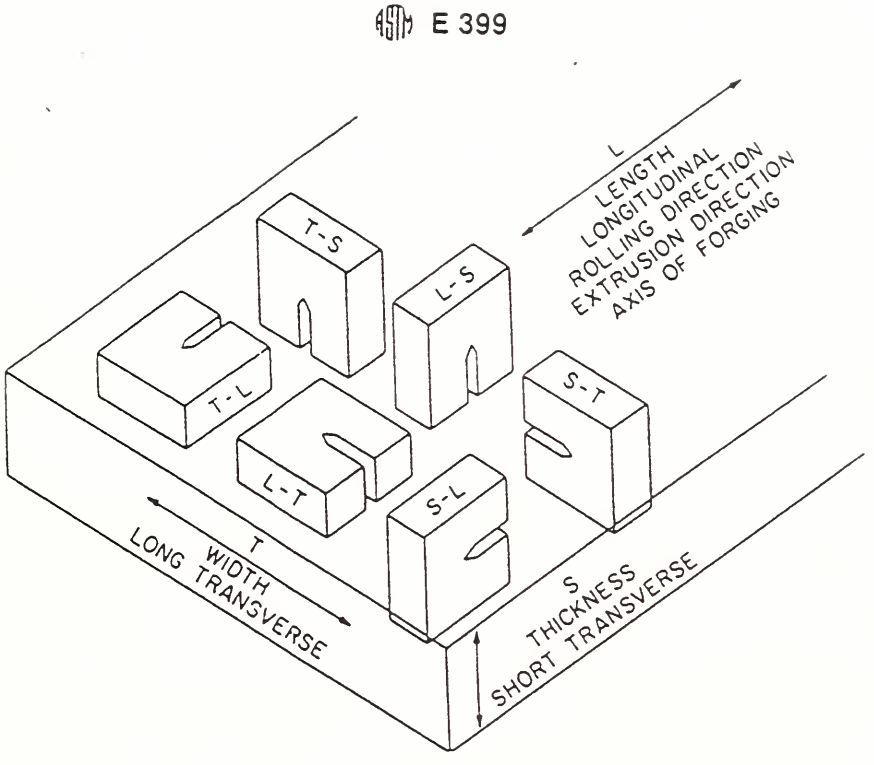

Figure 4-4. Crack Plane Orientation for Rectangular Sections.

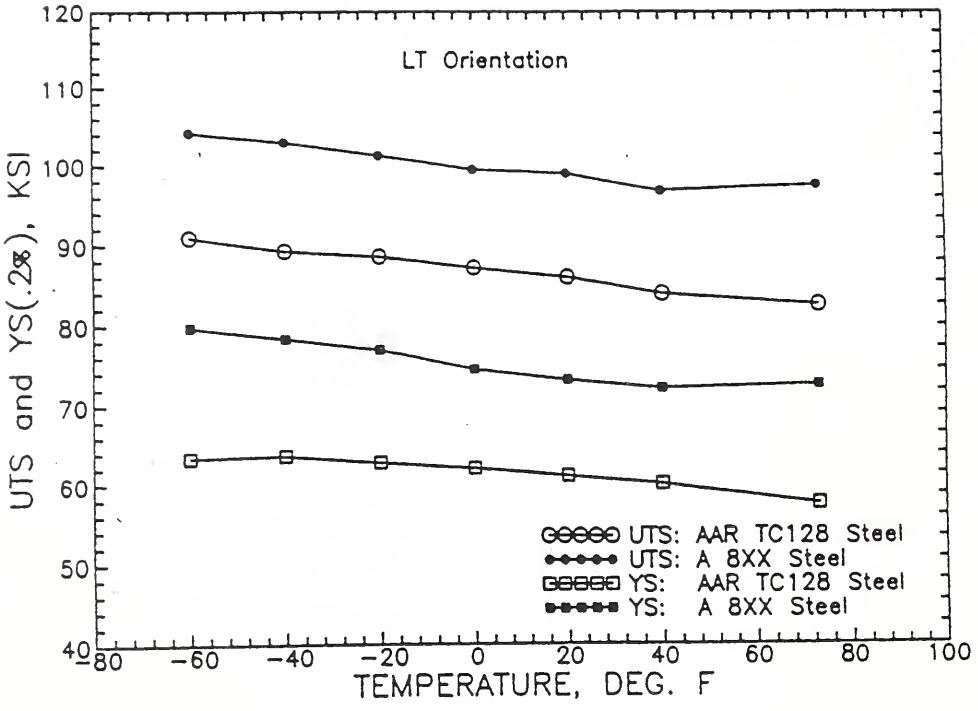

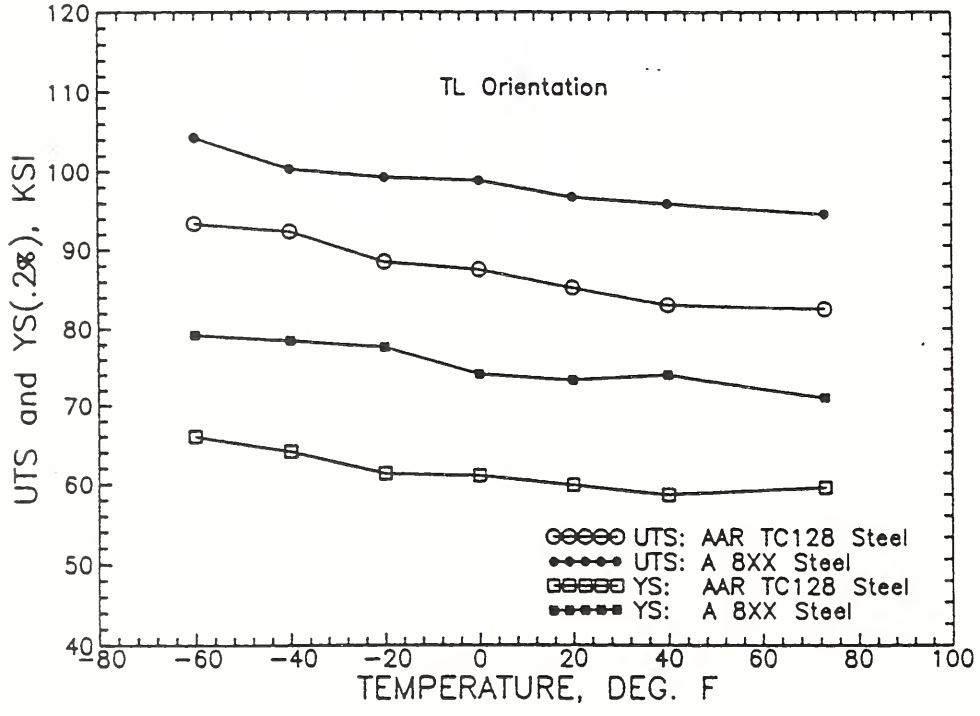

Figure 4-5. Yield and Ultimate Strength Data for LT and TL Orientations.

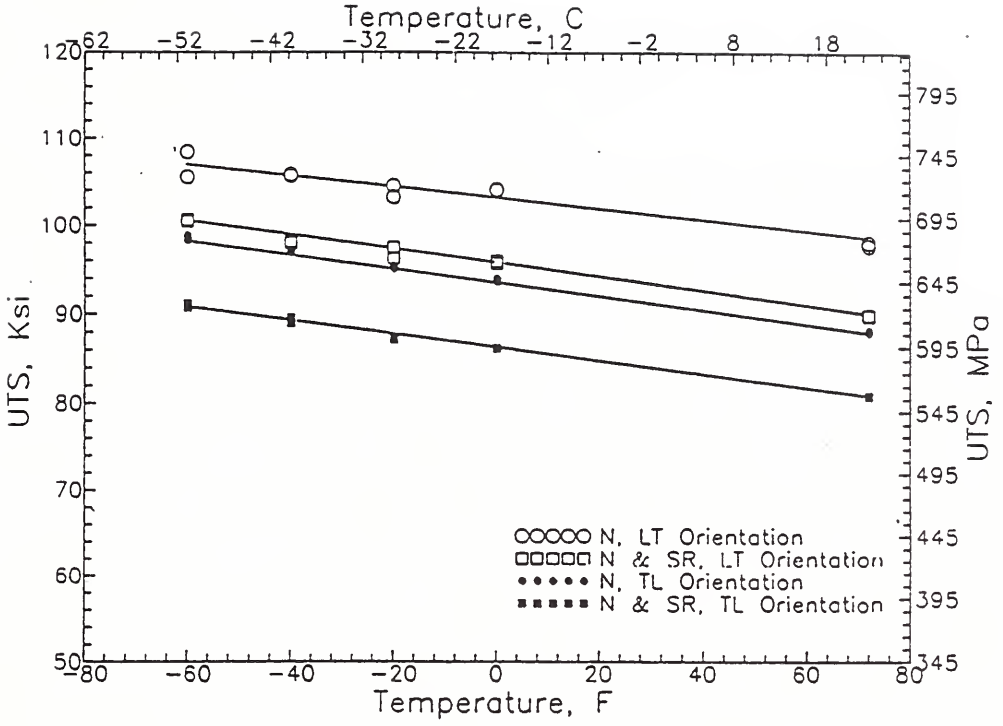

Figure 4-6. Ultimate Tensile Strength Versus Temperature for Normalized, and Normalized and Stress Relieved AAR TC128 grade B Steel.

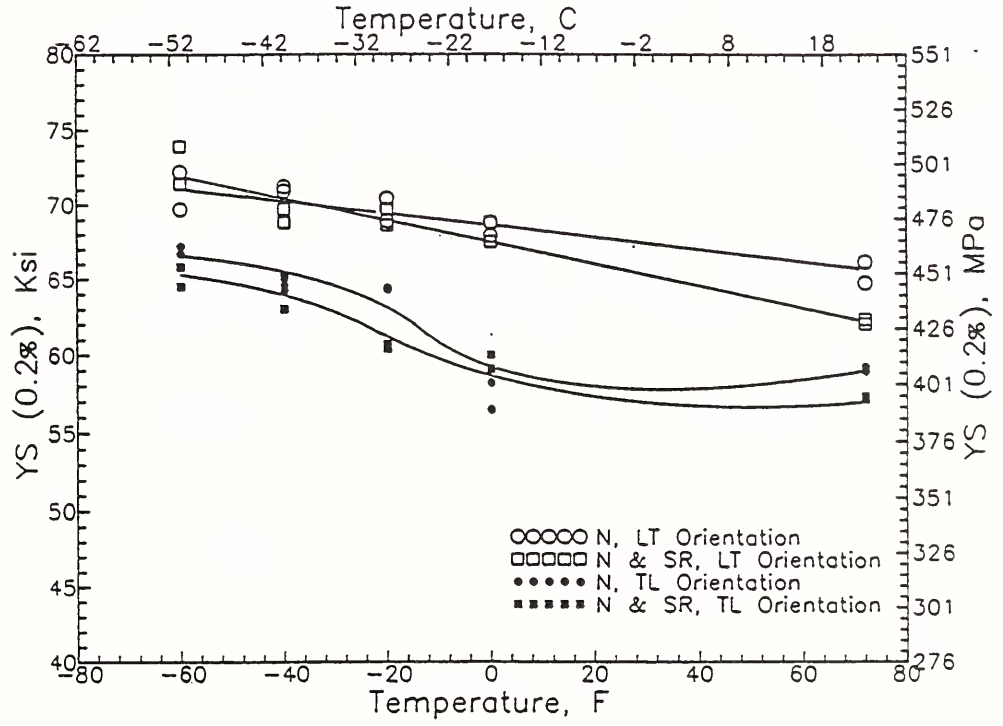

Figure 4-7. Yield Strength Versus Temperature for Normalized, and Normalized and Stress Relieved AAR TC128 grade B Steel.

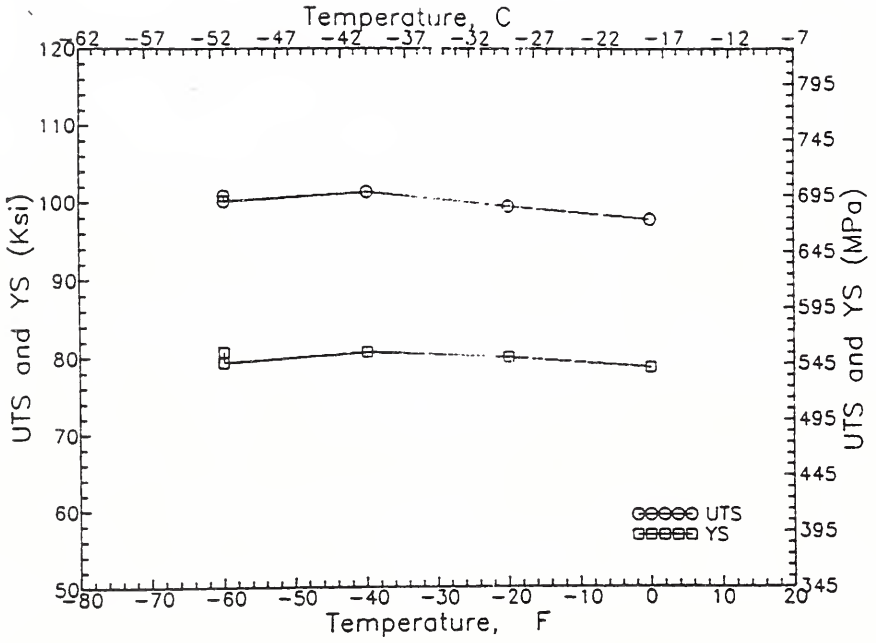

Figure 4-8. Tensile Test Results for All Weld Specimens.

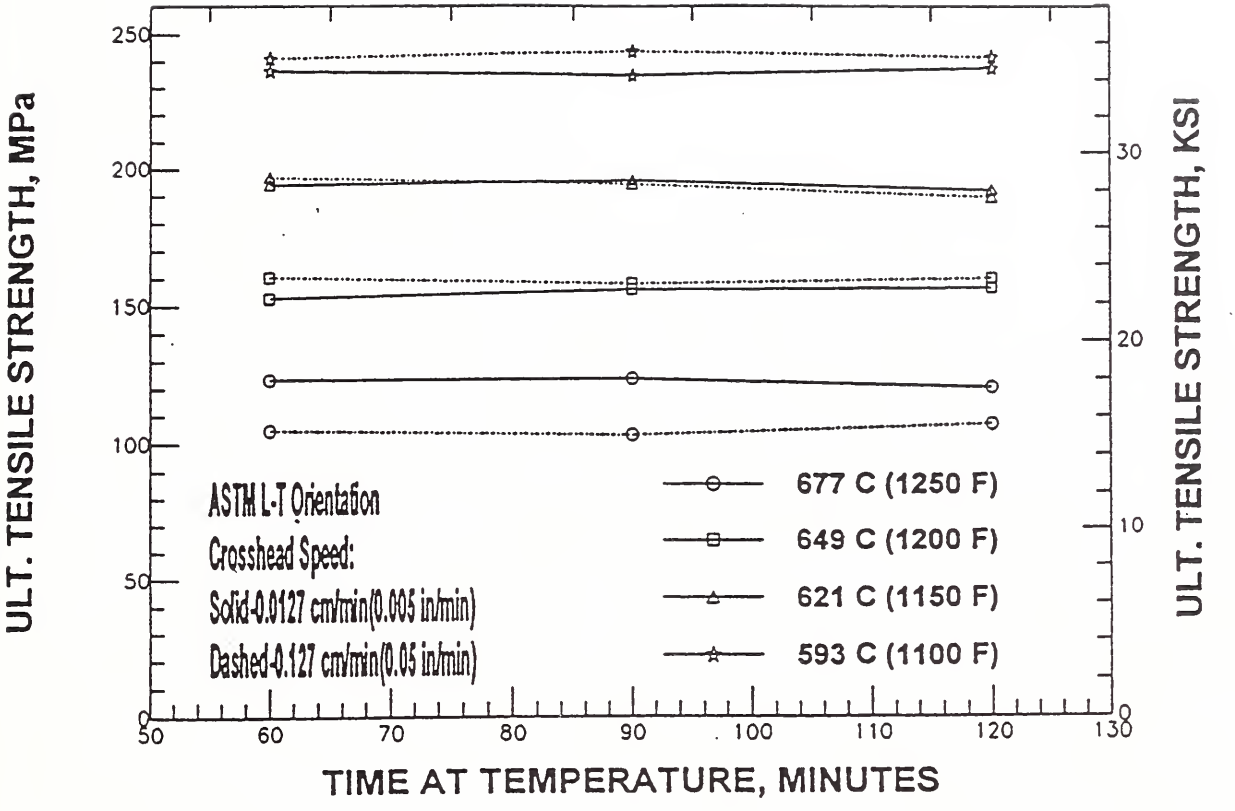

Figure 4-9. Effect of Crosshead Speed, Temperature, and Time on UTS, L-T Orientation.

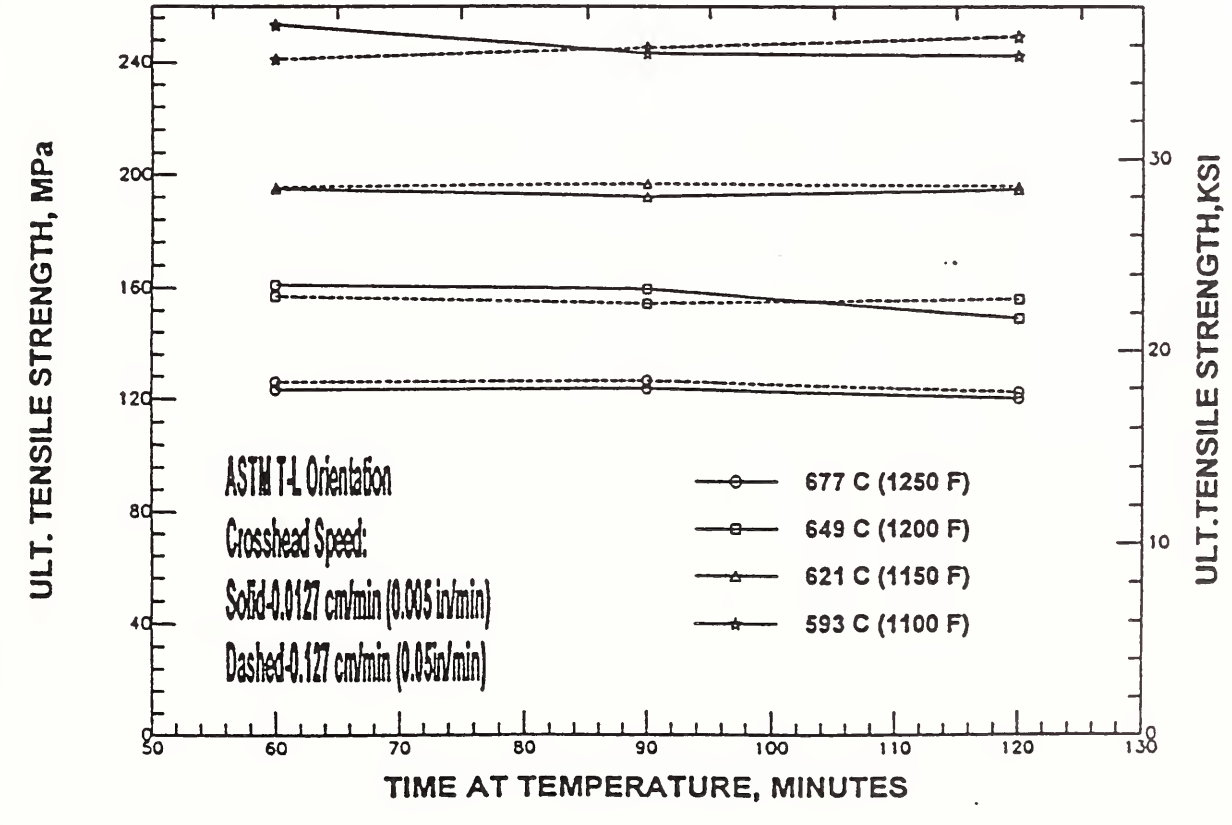

Figure 4-10. Effect of Crosshead Speed, Temperature, and Time on UTS, T-L Orientation.

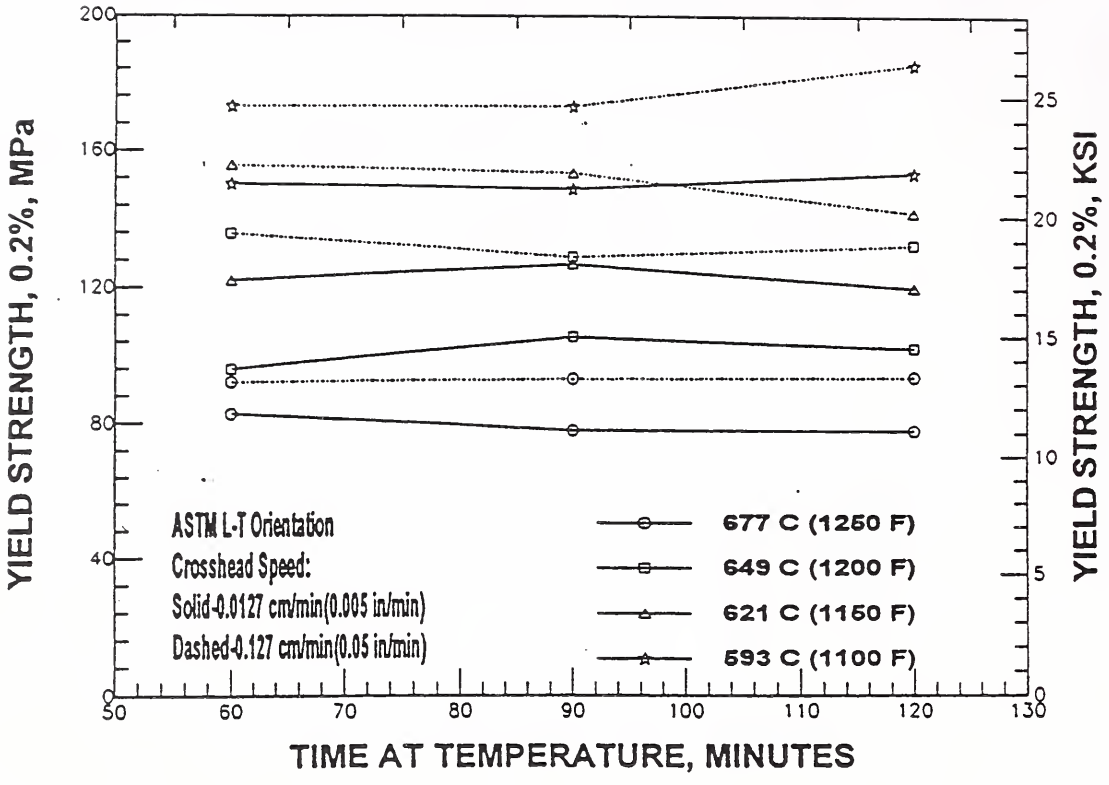

Figure 4-11. Effect of Crosshead Speed, Temperature, and Time on YS, L-T Orientation.

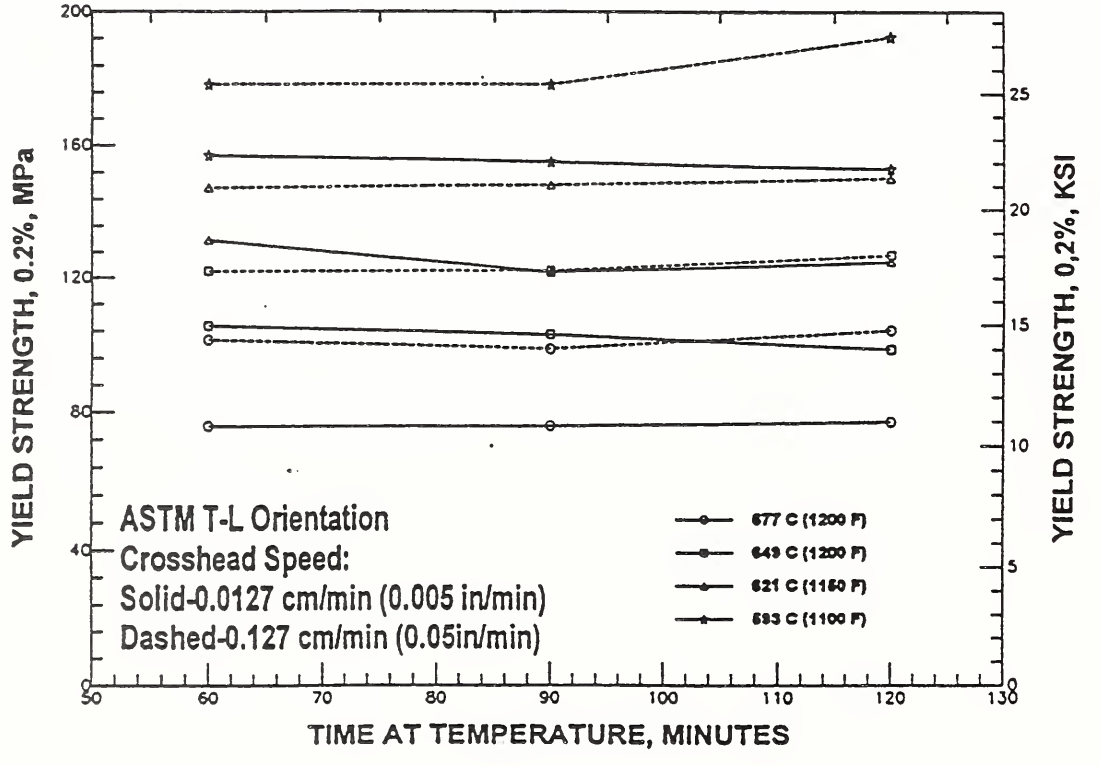

Figure 4-12. Effect of Crosshead Speed, Temperature, and Time on YS, T-L Orientation.

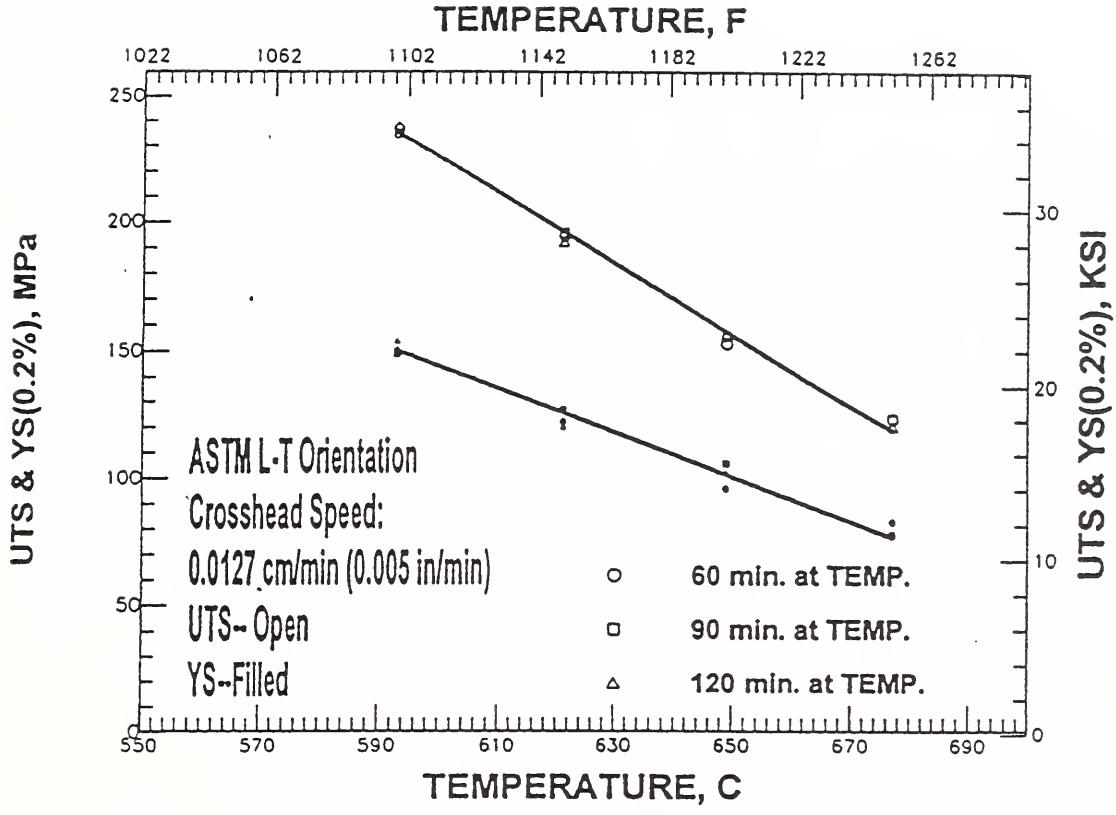

Figure 4-13. UTS and YS Versus Temperature, L-T Orientation, Crosshead Speed = 0.0127 cm/min.

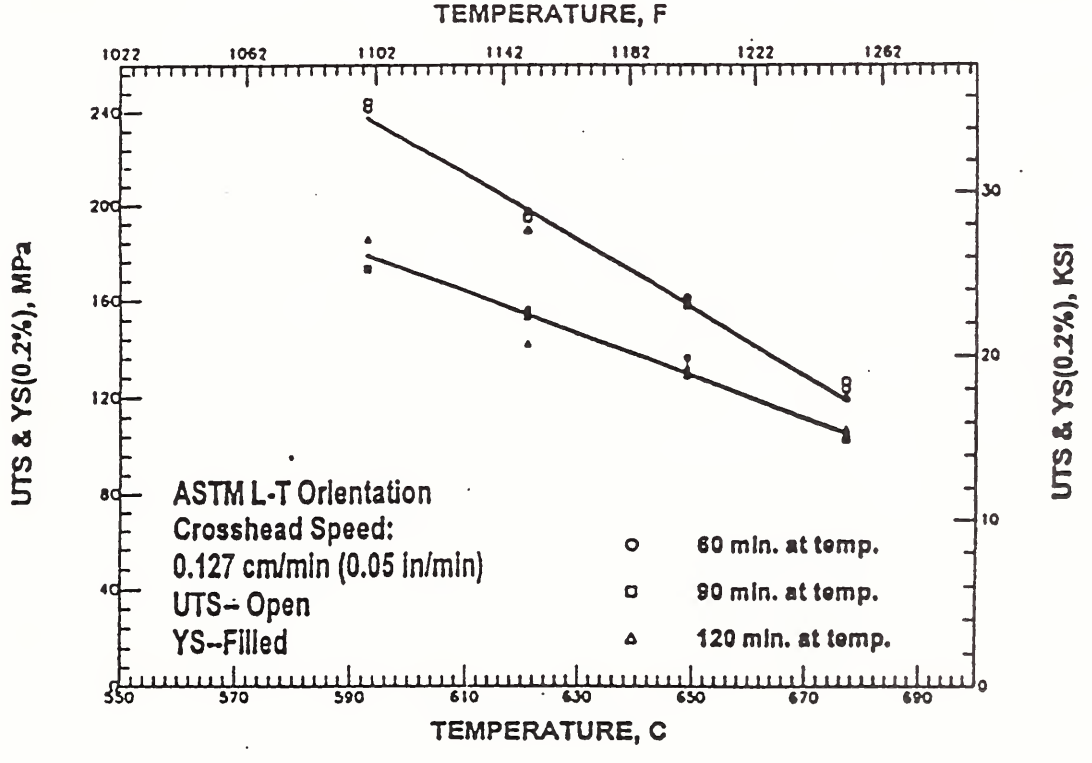

Figure 4-14. UTS and YS Versus Temperature, L-T Orientation, Crosshead Speed = 0.127 cm/min.

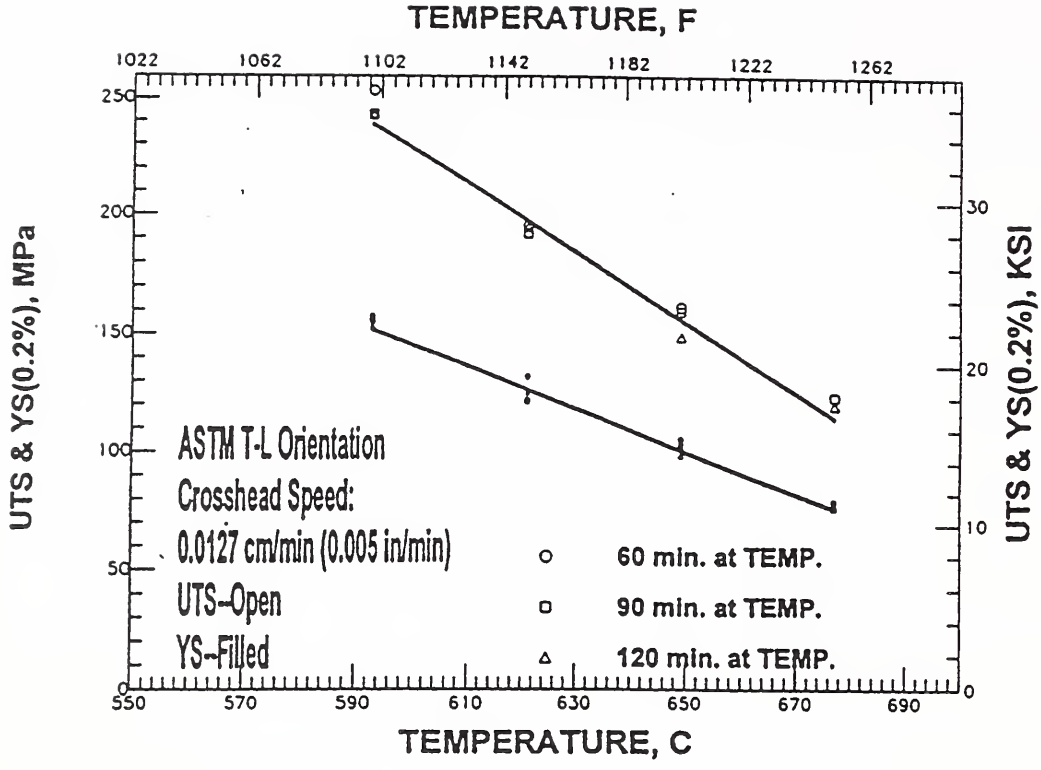

Figure 4-15. UTS and YS Versus Temperature, T-L Orientation, Crosshead Speed = 0.0127 cm/min.

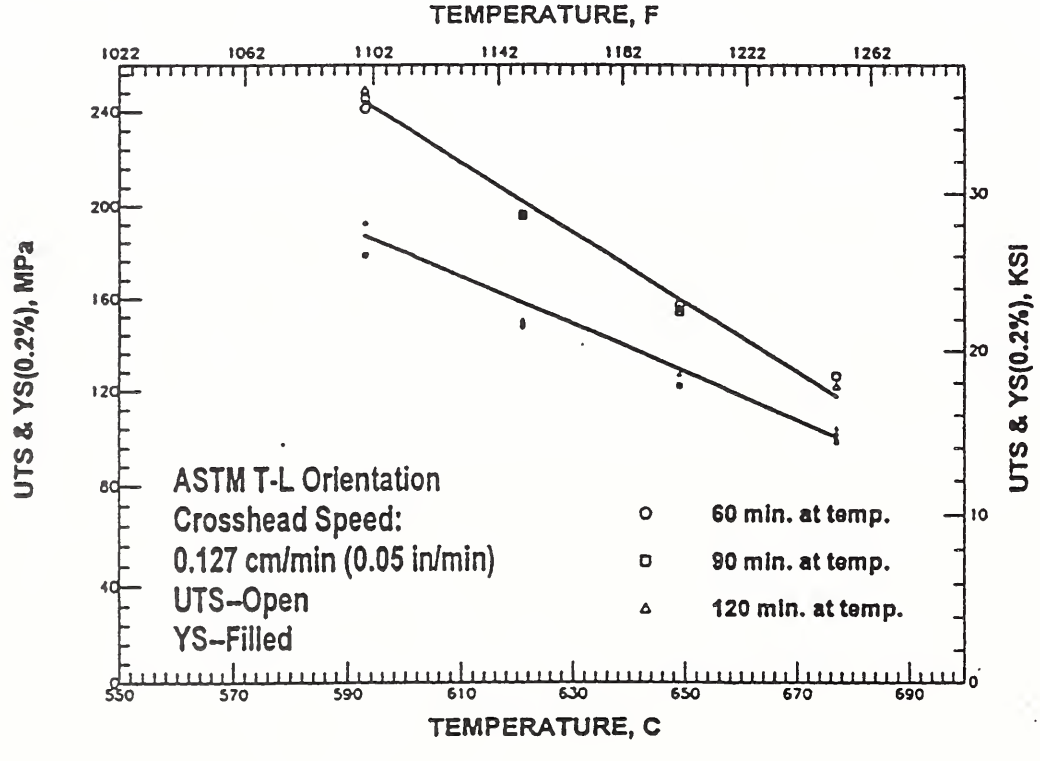

Figure 4-16. UTS and YS Versus Temperature, T-L Orientation, Crosshead Speed = 0.127 cm/min.

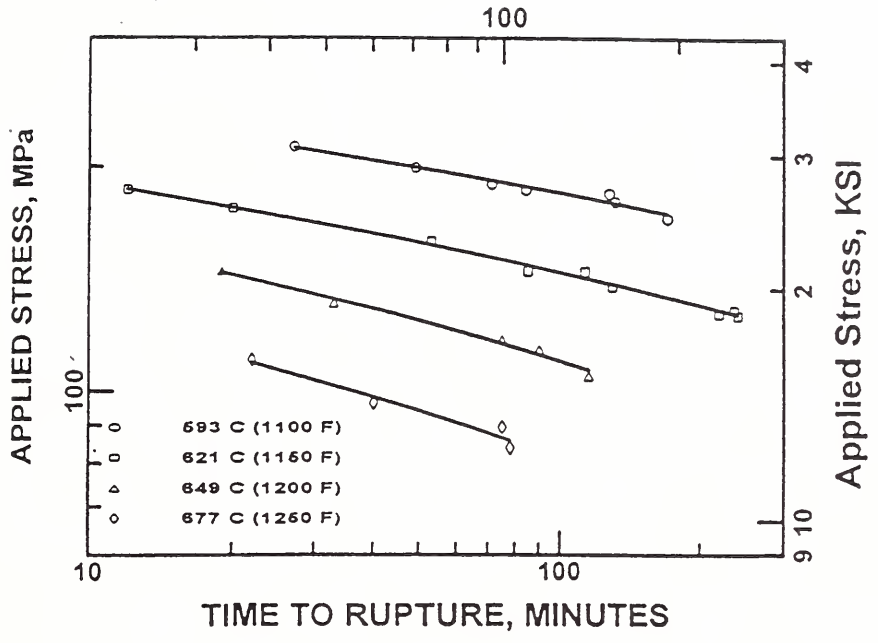

Figure 4-17. Applied Stress Versus Time to Rupture as a Function of Temperature.

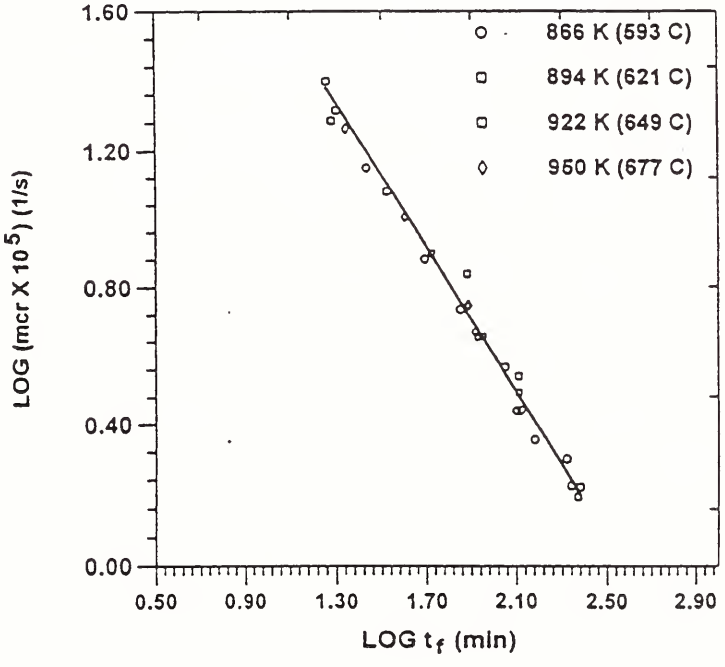

Figure 4-18. Minimum Creep Rate versus Time to Failure.

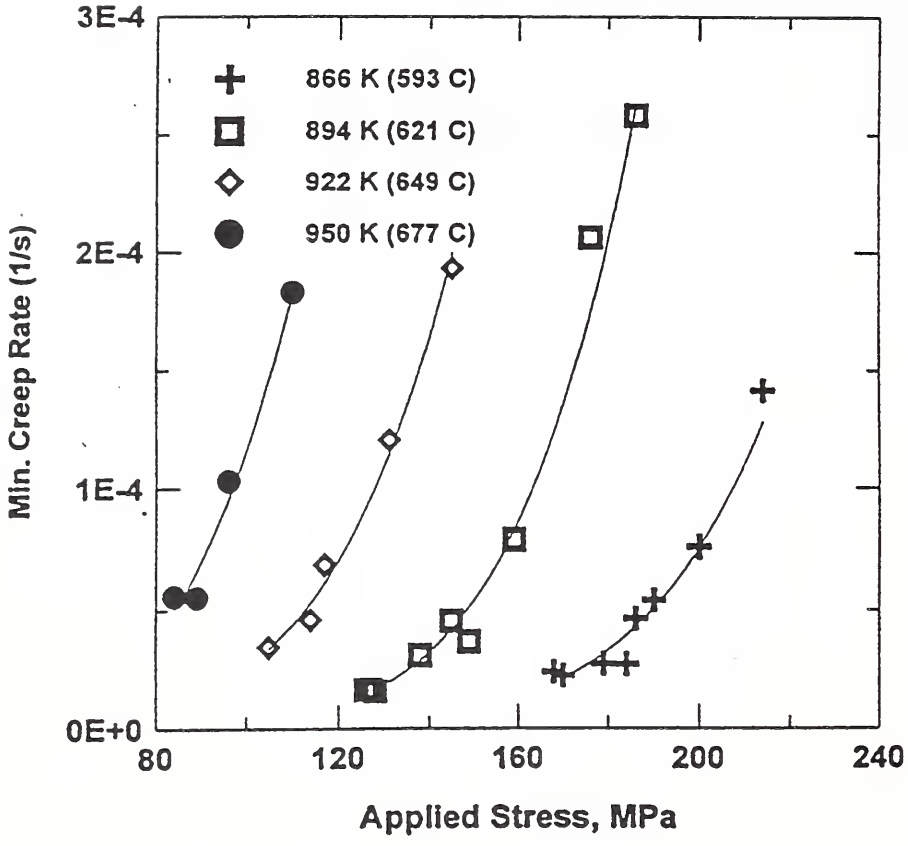

Figure 4-19. Minimum Creep Rate Versus Applied Stress as a Function of Temperature.

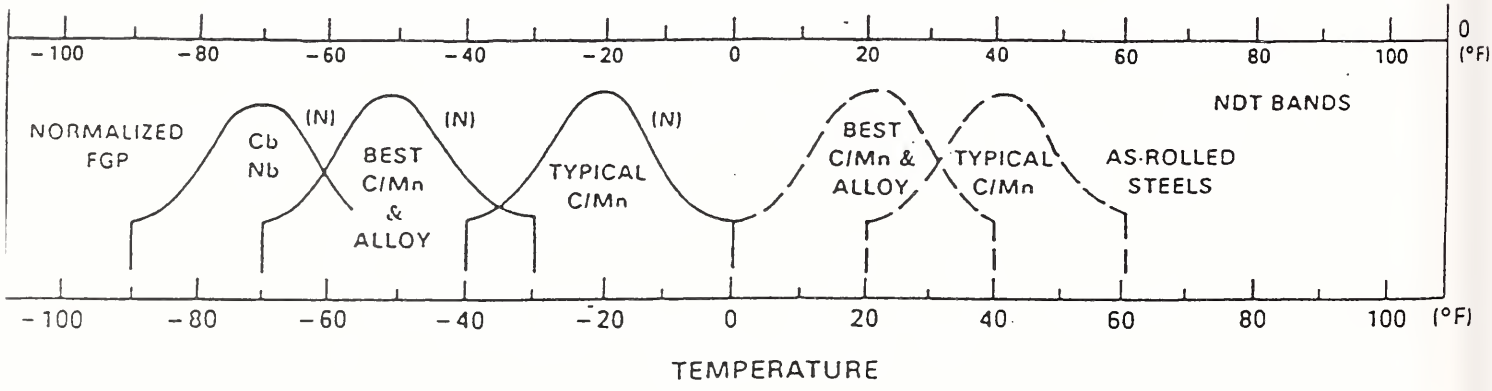

Figure 4-20. NDT Bands for Railroad Tank Car Steels.

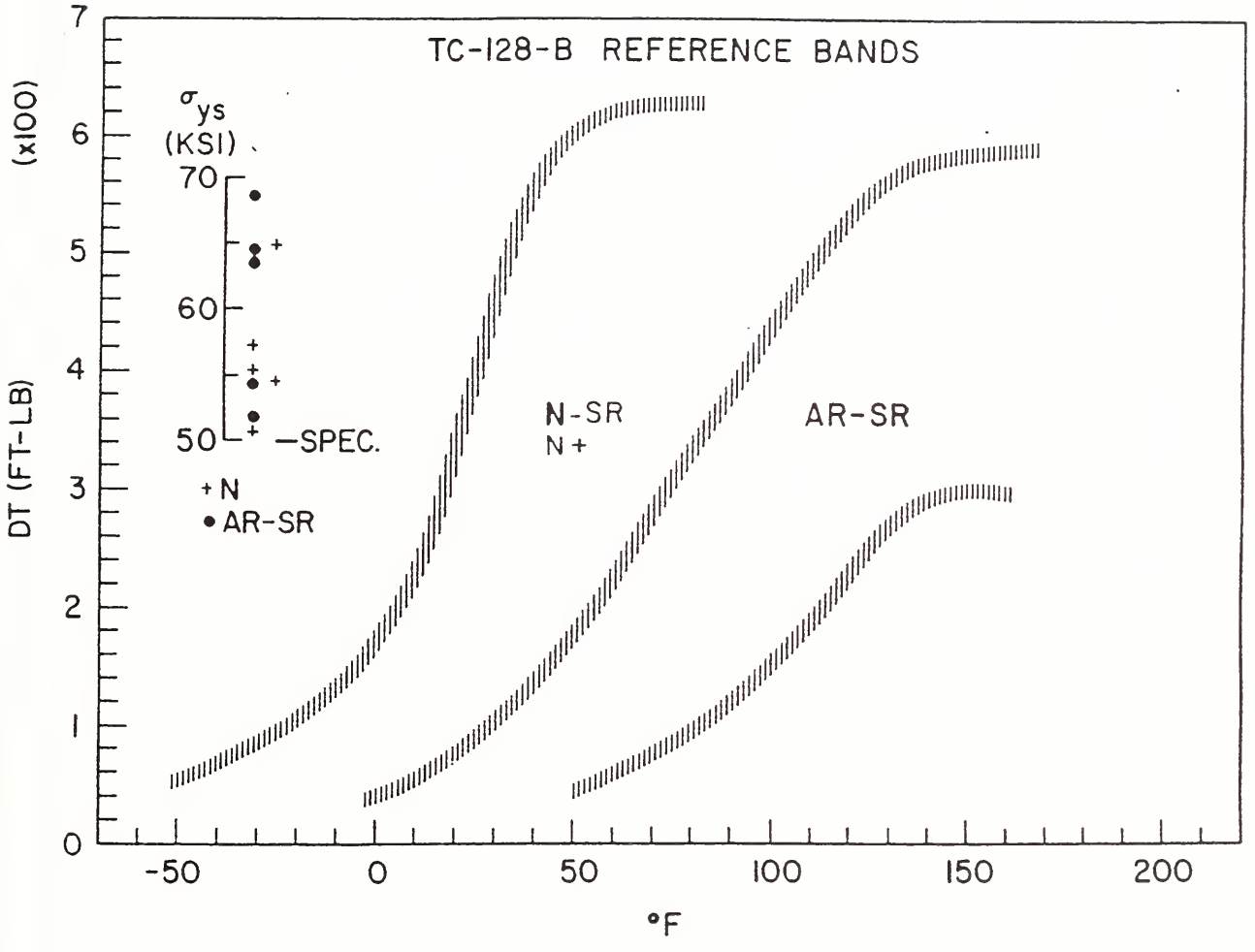

Figure 4-21. Summary of TC128B Reference Bands.

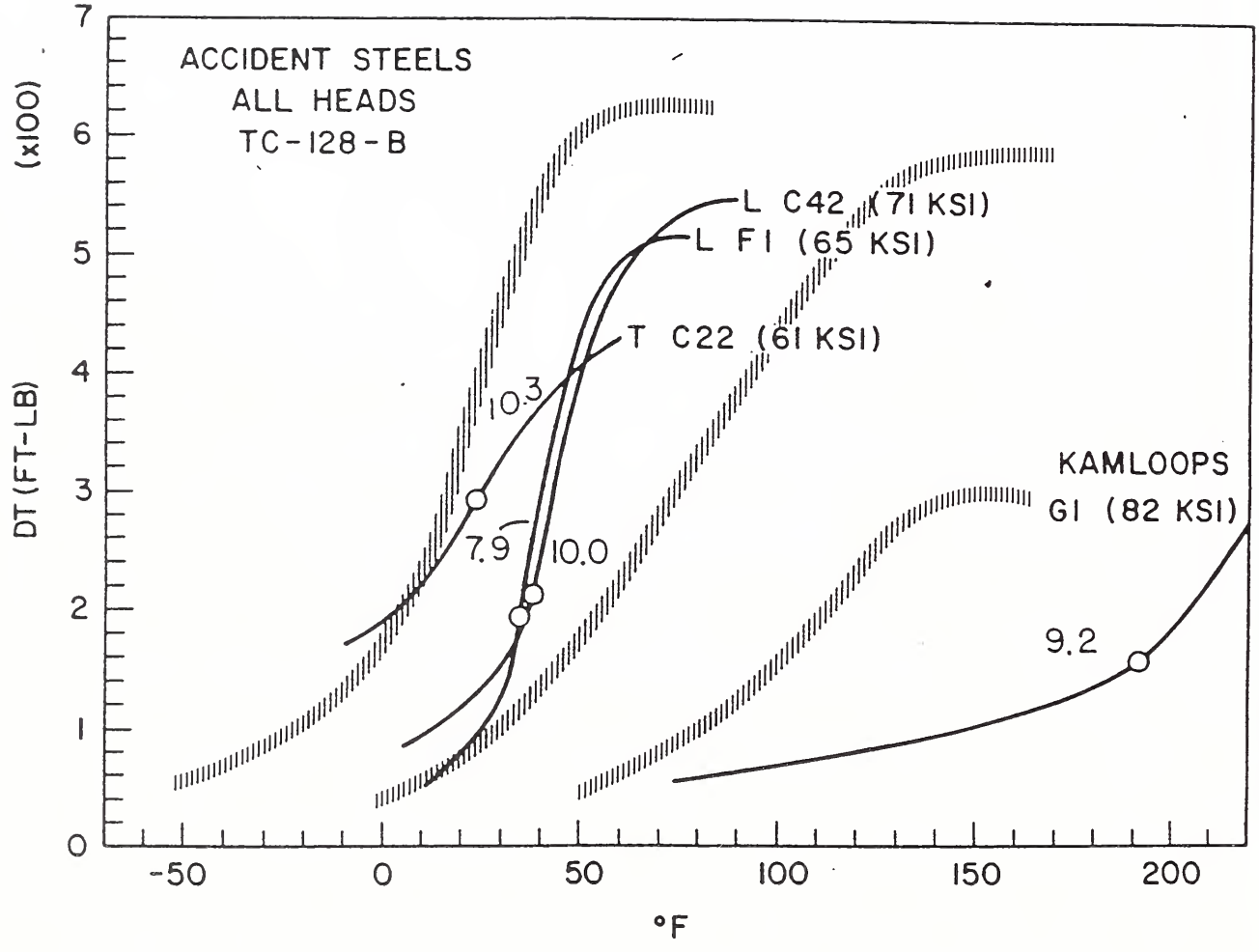

Figure 4-22. Accident DT Data, All TC128B Head Steels.

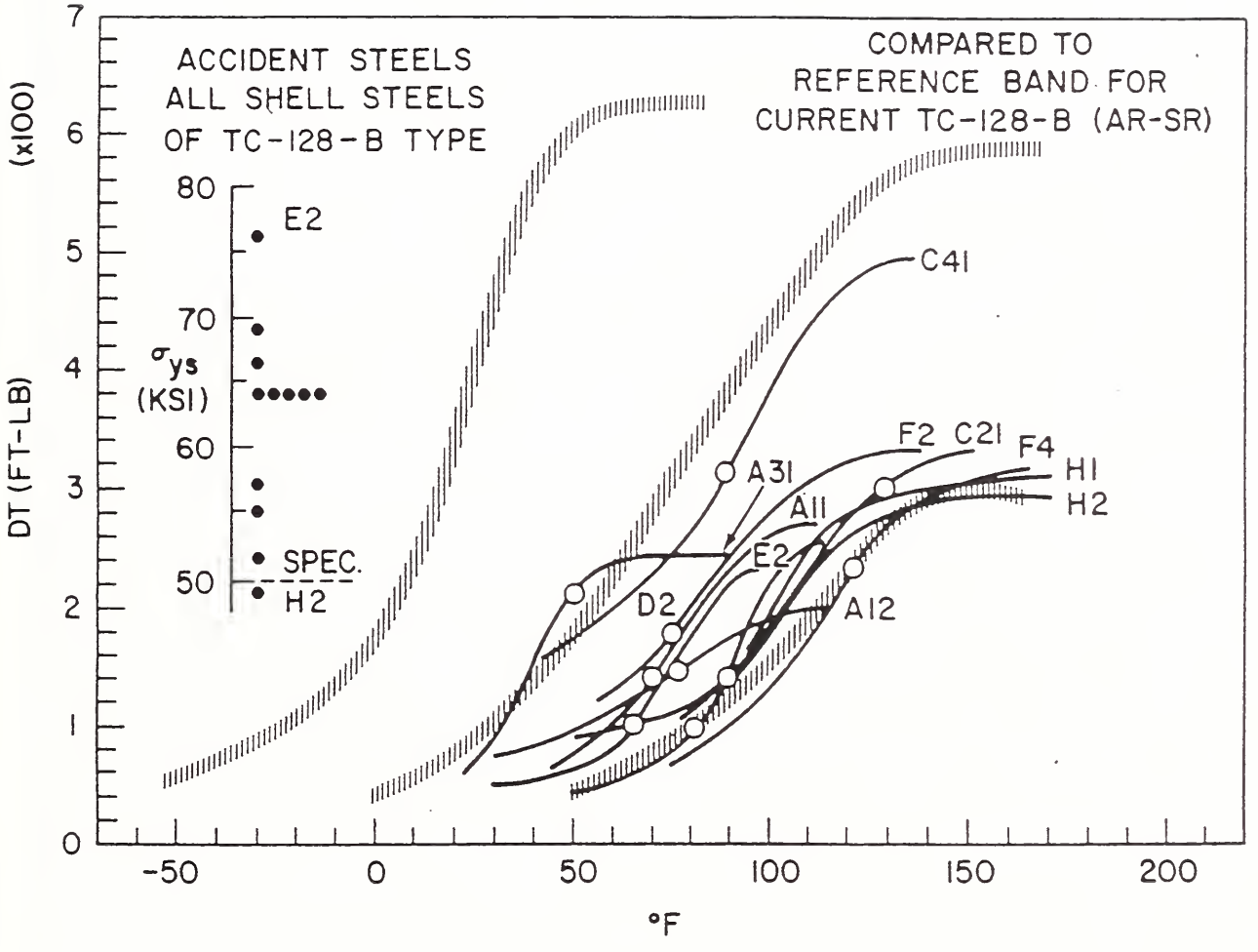

Figure 4-23. Accident DT Data, TC128B Shell Steels.

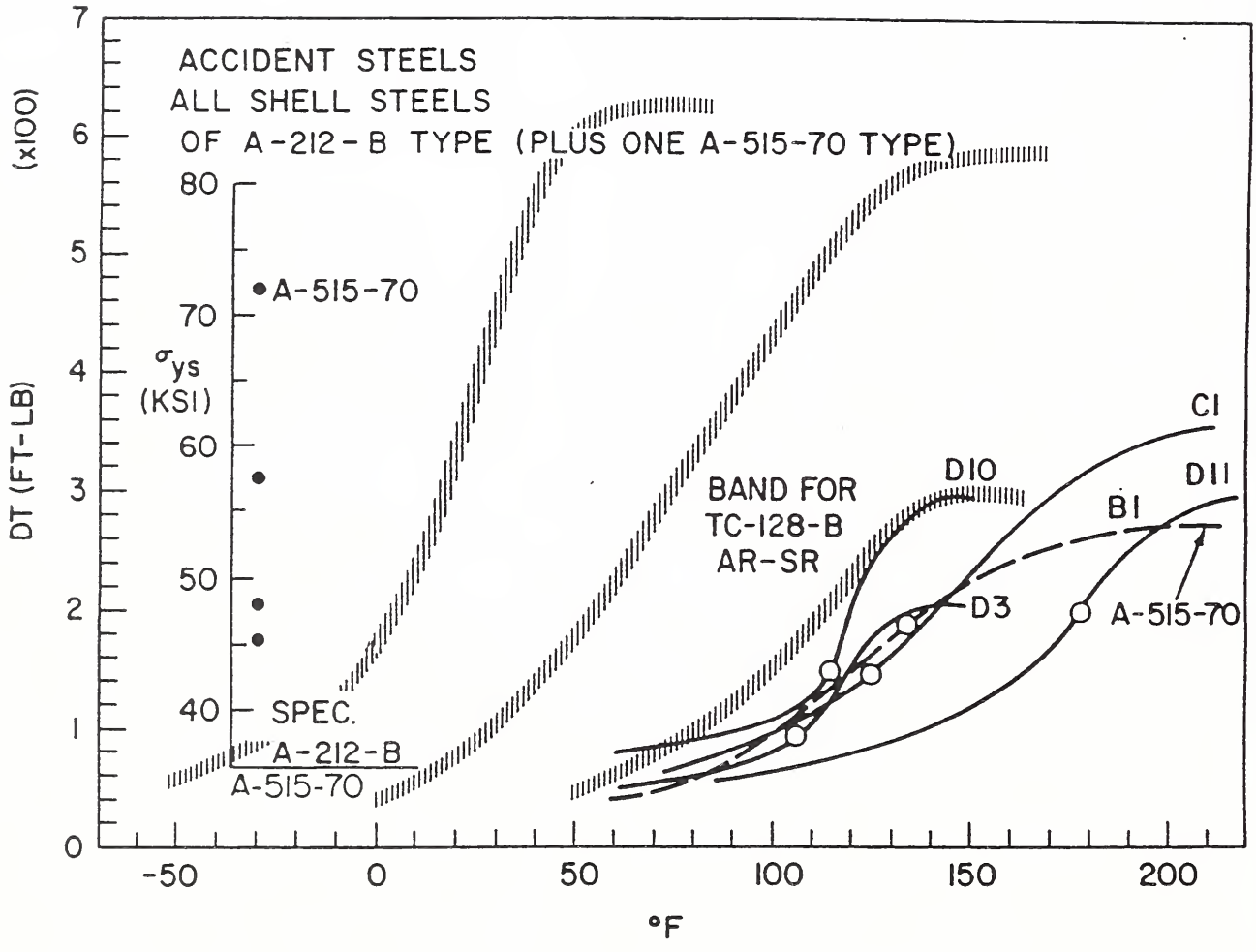

Figure 4-24. Accident DT Data, All A212B (A515-70) Shell Steels.

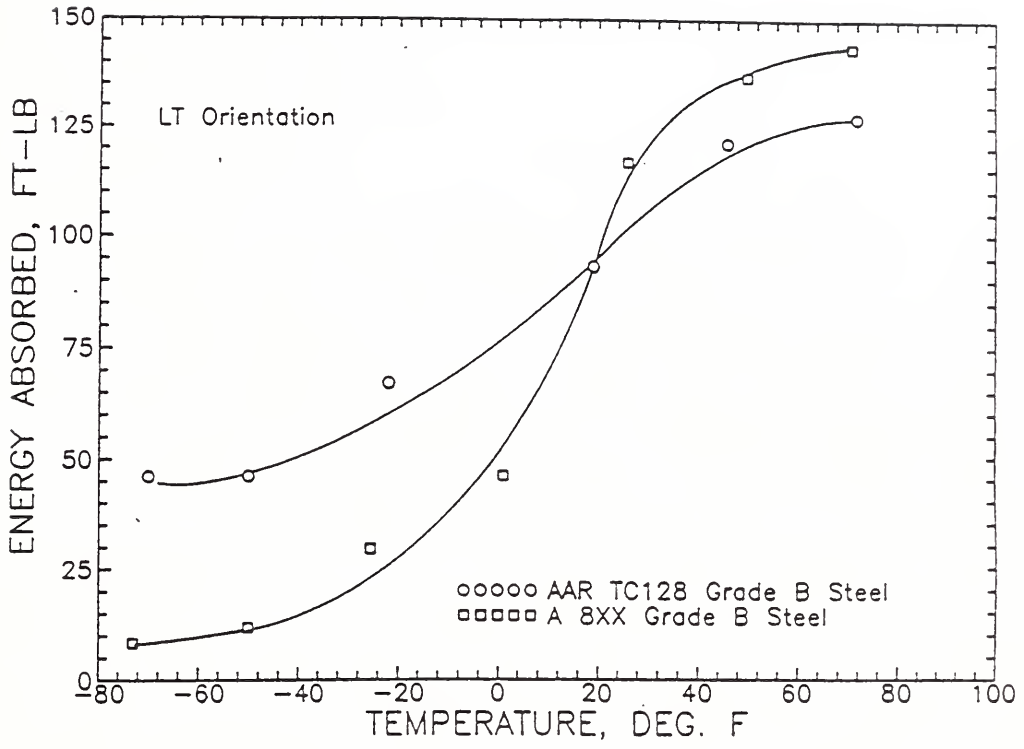

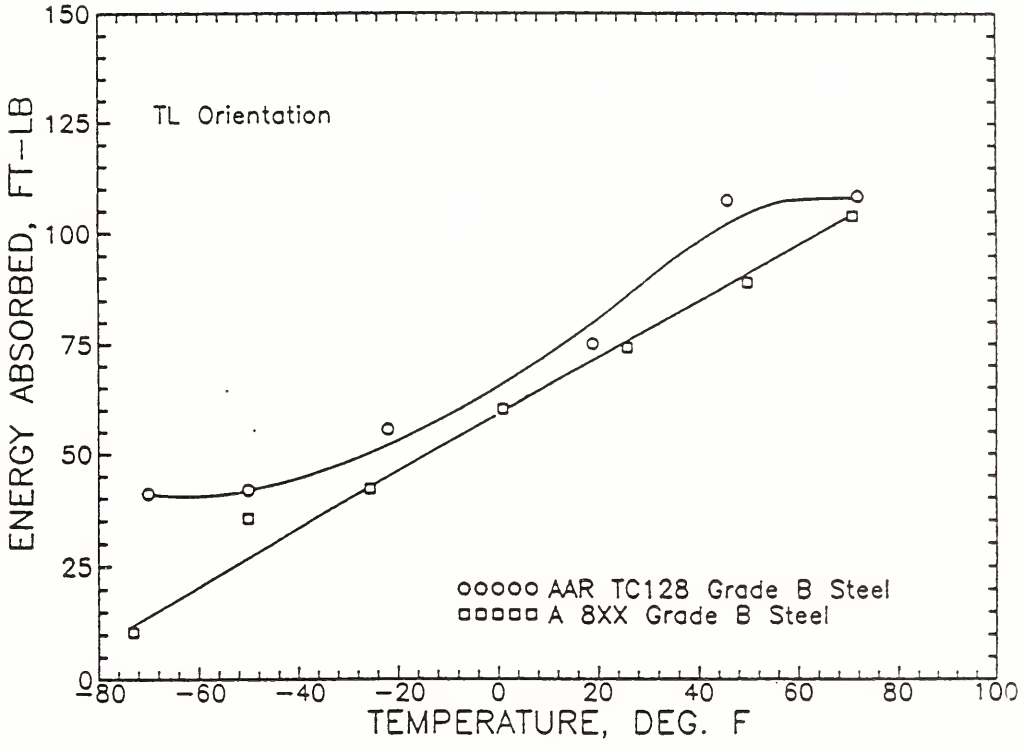

Figure 4-25. Energy Absorbed Versus Temperature for the A 8XX grade B Steel and the AAR TC128 grade B Steel.

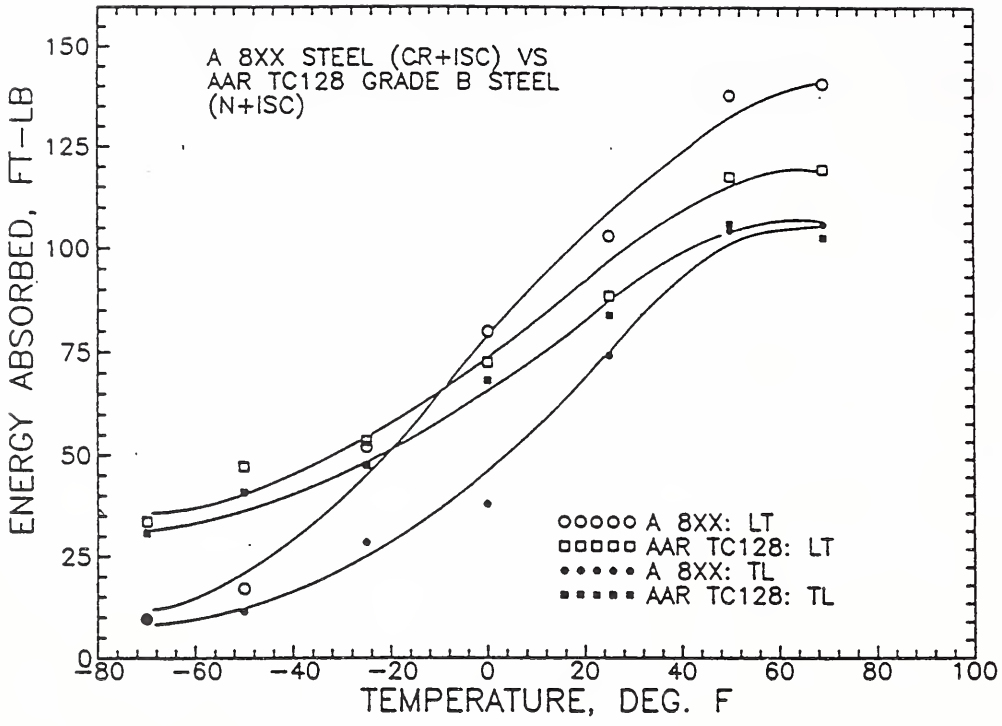

Figure 4-26. A Comparison of the Energy Absorbed as a Function of Temperature and Orientation for the A 8XX grade B Steel and the AAR TC128 grade B Steel.

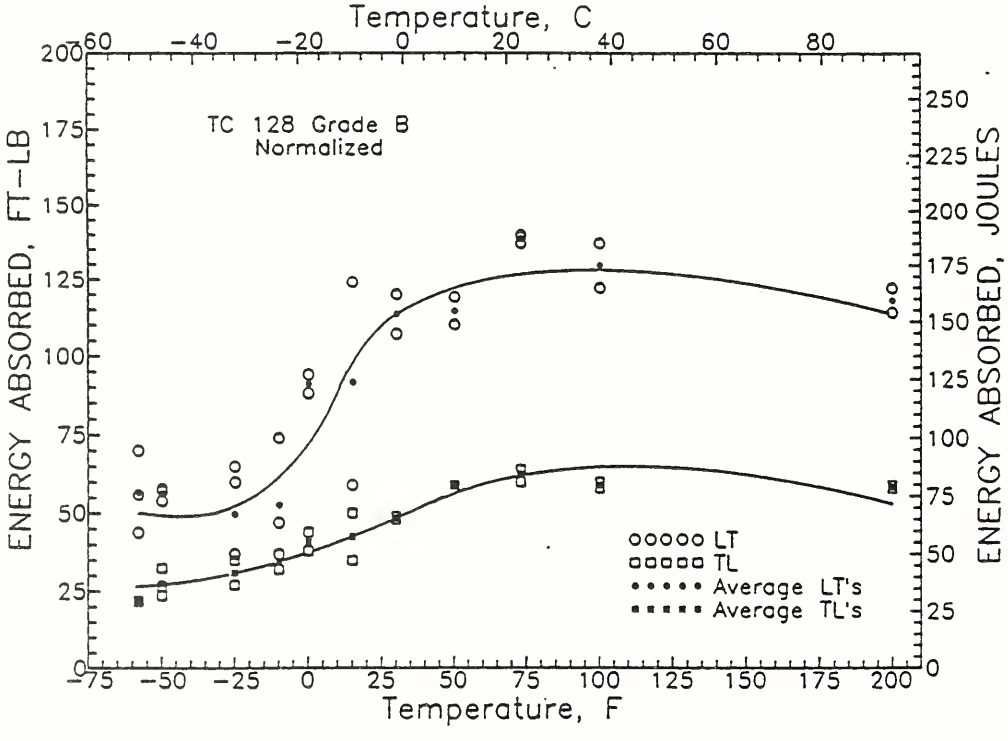

Figure 4-27. Charpy V-notch Impact Results for Normalized AAR TC128 grade B Steel.

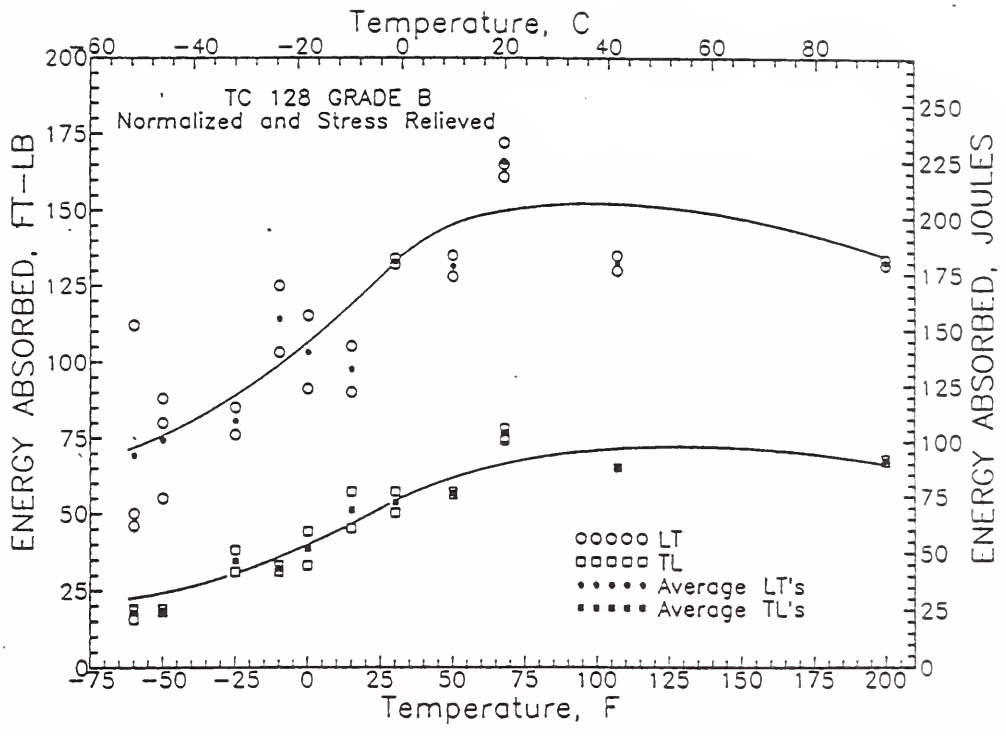

Figure 4-28. Charpy V-notch Impact Results for Normalized and Stress Relieved AAR TC128 grade B Steel.

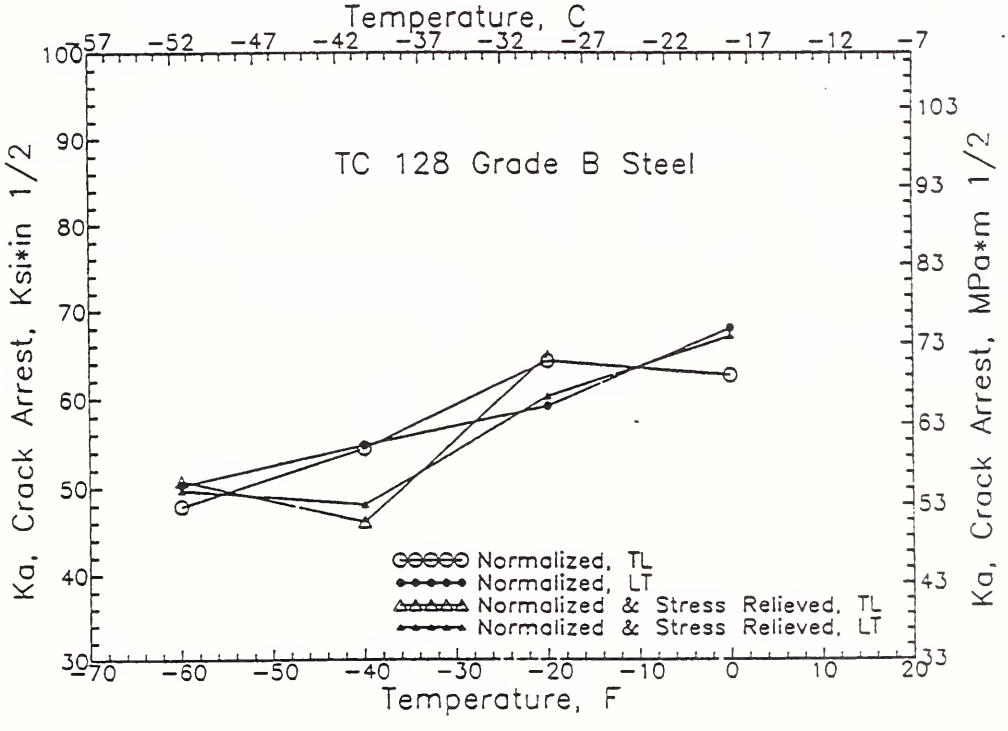

Figure 4-29. Crack Arrest Fracture Toughness for Normalized, and Normalized Stress Relieved TC128 grade B Steel, Both Orientations.

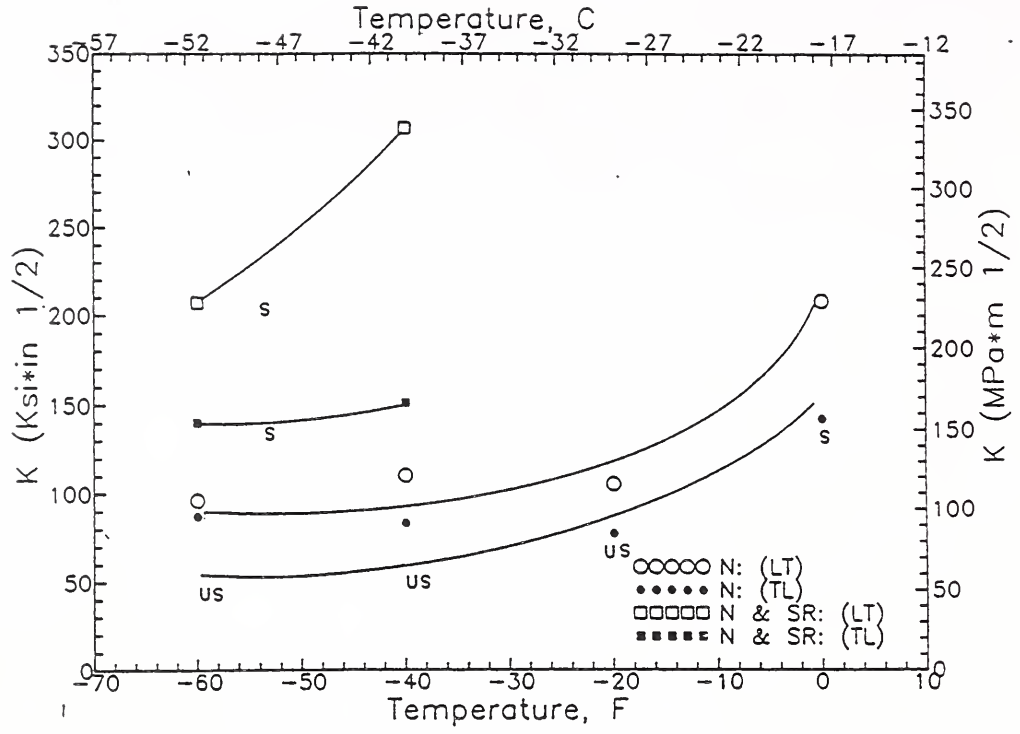

Figure 4-30. Fracture Toughness for Normalized, and Normalized Stress Relieved TC128 grade B Steel, Both Orientations.

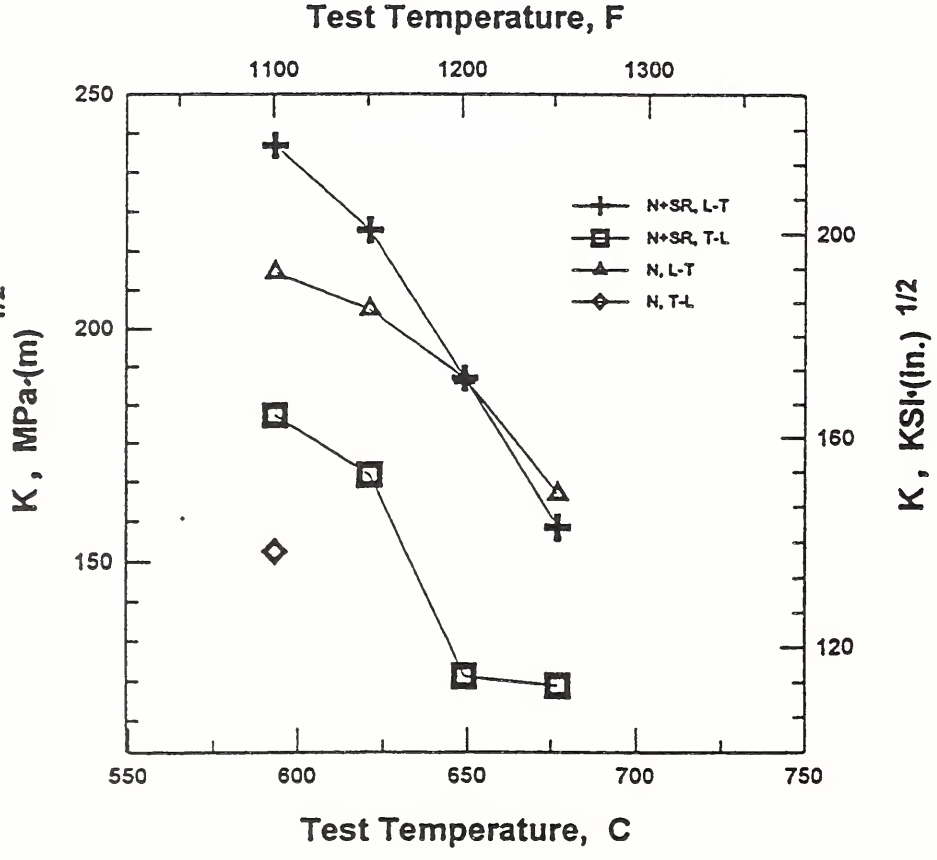

Figure 4-31. Fracture Toughness Versus Temperature for N and N+SR TC128B Steels.

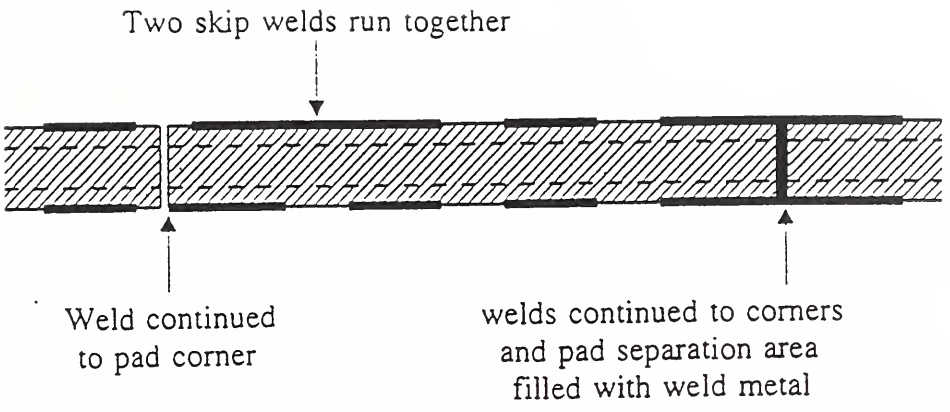

Figure 4-32. Examples of Nonconforming Welds.

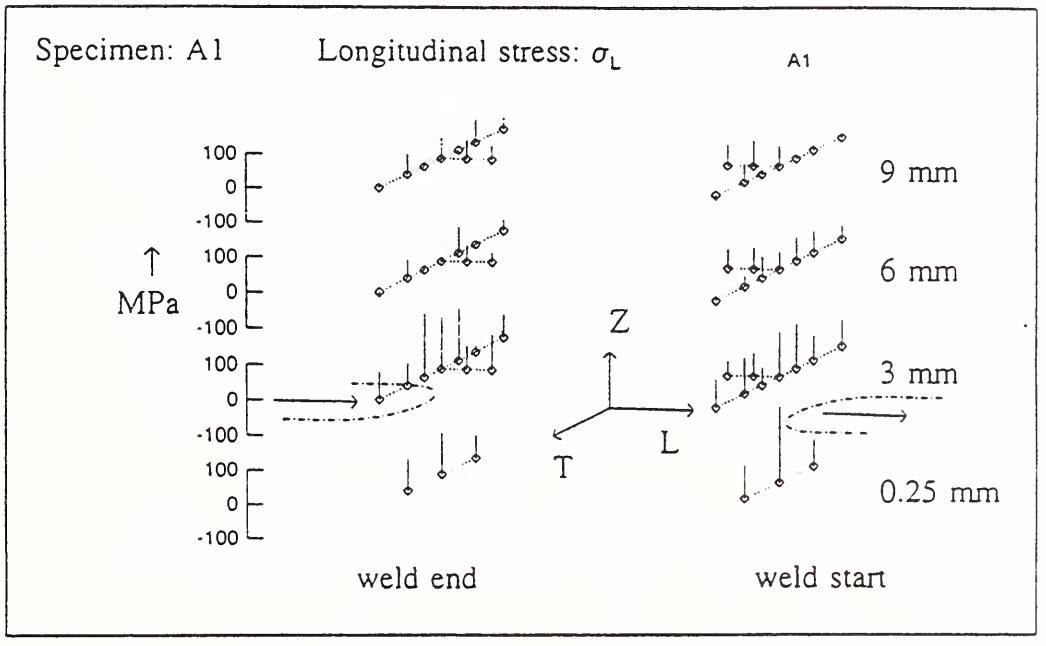

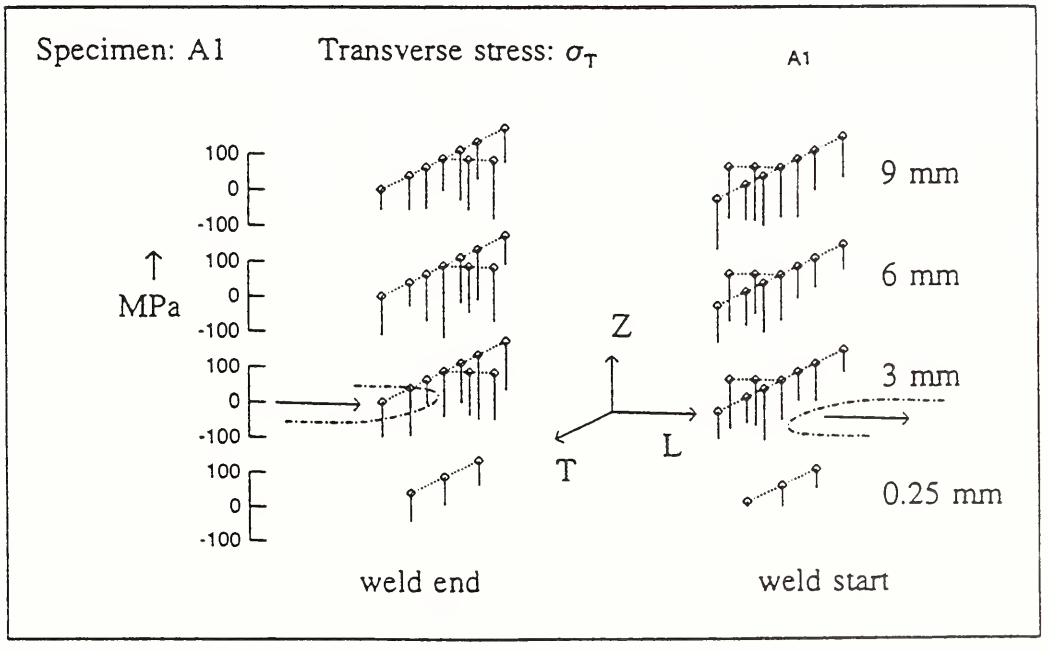

Figure 4-33. Longitudinal and Transverse Residual Stresses.

Section 5

SERVICE EXPERIENCE FOR PRESSURE TANK CARS

The behavior of pressure tank car steels in accidents is described in the RPI-AAR Tank Car Safety Project report [4]. This report covers tank cars in accidents over the sixteen-year period from 1965-1980. The accident data base was carefully developed and classified by type of car and cause of lading loss. Ten different causes of lading loss were identified, which included head puncture, shell puncture, rupture due to impact and rupture due to fire. Figure 5-1 shows the puncture types and identifies their location (shell or head) and geometry. The puncture geometry was classified into three types: generally round, elongated, and crack like punctures. Cases involving rupture due to impact or fire are shown in Figure 5-2. It identifies the type of fracture by number of circumferential fractures and by the number of tubs (section of tank with head).

5.1 BRITTLE FRACTURES (1965-80)

A total of 1345 loaded pressure cars suffered severe accident impacts during the 1965 to 1980 period [4]. Of these sixteen accidents involved brittle fracture. All of the brittle fractures occurred due to the development of a crack-like defect. A random sampling of the data indicated an average of 2.5 impact points for each car, i.e., 3362 total impact points. The number of lading loss cases due to ductile penetration of the tank greatly exceeded the number of brittle fracture cases. In many cases the tank cars suffered severe plastic deformation without rupture of any type. This experience indicated that tank cars then in service were mechanically "husky" fracture-resistant structures [4, 5].

Table 5-1 summarizes this service experience and also includes three brittle fracture cases outside this reference period. In all, nineteen brittle fracture cases were considered.

5.2 MAJOR LADING LOSSES DUE TO DUCTILE RUPTURES

A primary structural integrity objective for tank cars is the prevention of major lading loss in accident environments. Table 5-2 summarizes data for lading loss due to head and shell puncture, rupture due to impact and fire, and due to some combination of these causes.

The RPI-AAR Tank Car Safety Project [4] recommended the use of head shields and shelf couplers for head protection, and the use of thermal insulation for protection against fire-induced ruptures. These improvements are expected to substantially reduce the incidence of lading loss in the future.

Table 5-1

Summary of Tank Car Service Experience from 1965 through 1980

Type of Car and Service Record	Number
Pressure and non-pressure cars	180,000
Non-pressure cars	130,000
Pressure cars	50,000
Brittle fracture of pressure cars in normal service	None
Pressure cars impacted in accidents	1,345
Number of impact points (2.5 per accident)	3,362
Brittle fracture cases	16(+3)= 19

Table 5-2

Summary of Major Lading Losses for Pressure Tank Cars, Damaged in Accidents During the Sixteen-Year Period from 1965 Through 1980

Cause for Lading Loss	Total Number with Lading Loss	Number Involving Brittle Fracture
Head Puncture	128	4
Shell Puncture	68	1
Rupture Due to Impact	9	7
Rupture Due to Fire	95	3
Rupture Due to Multiple Causes	36	1
Totals	336	16

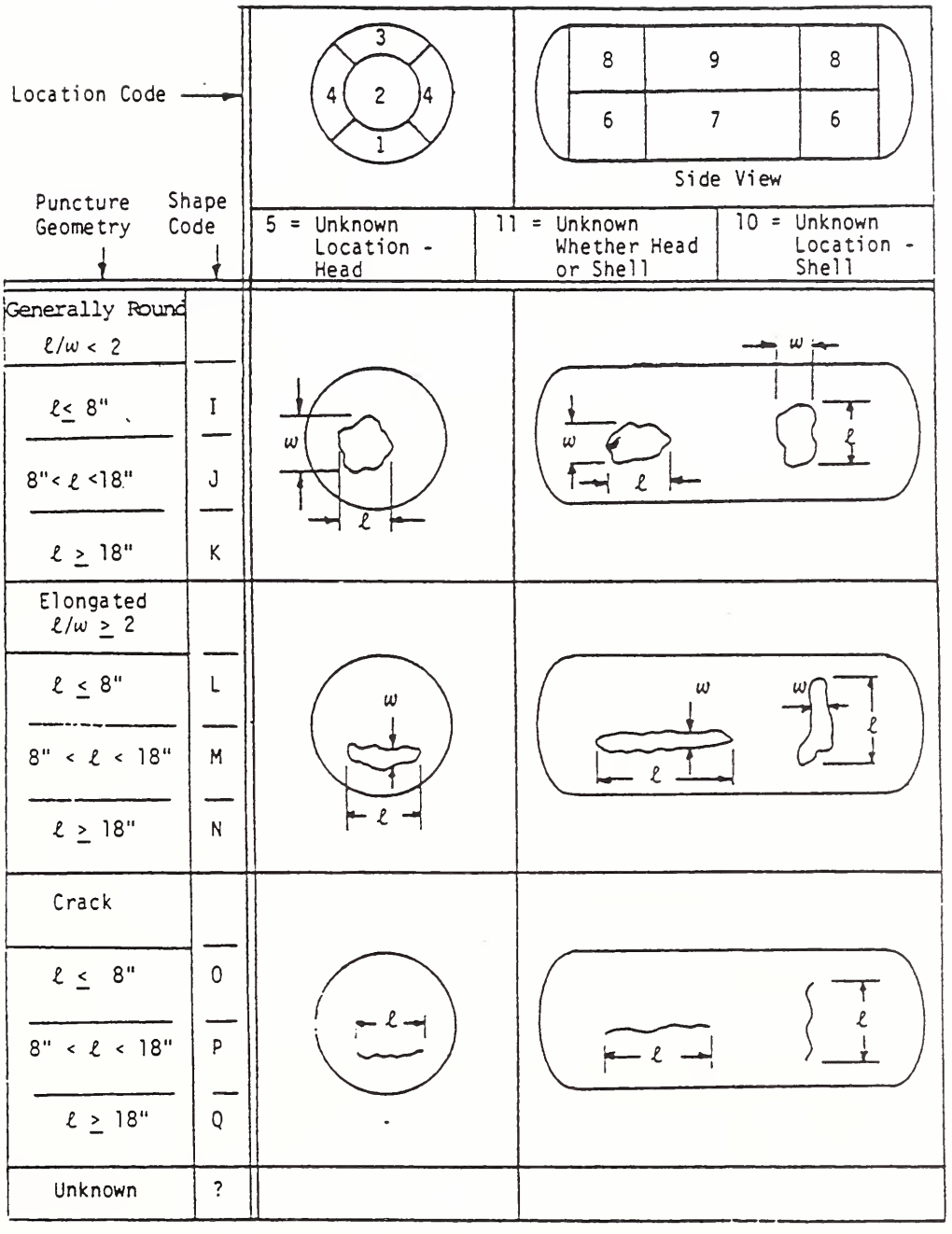

Figure 5-1 Puncture Types, Service Experience in Railroad Tank Cars.

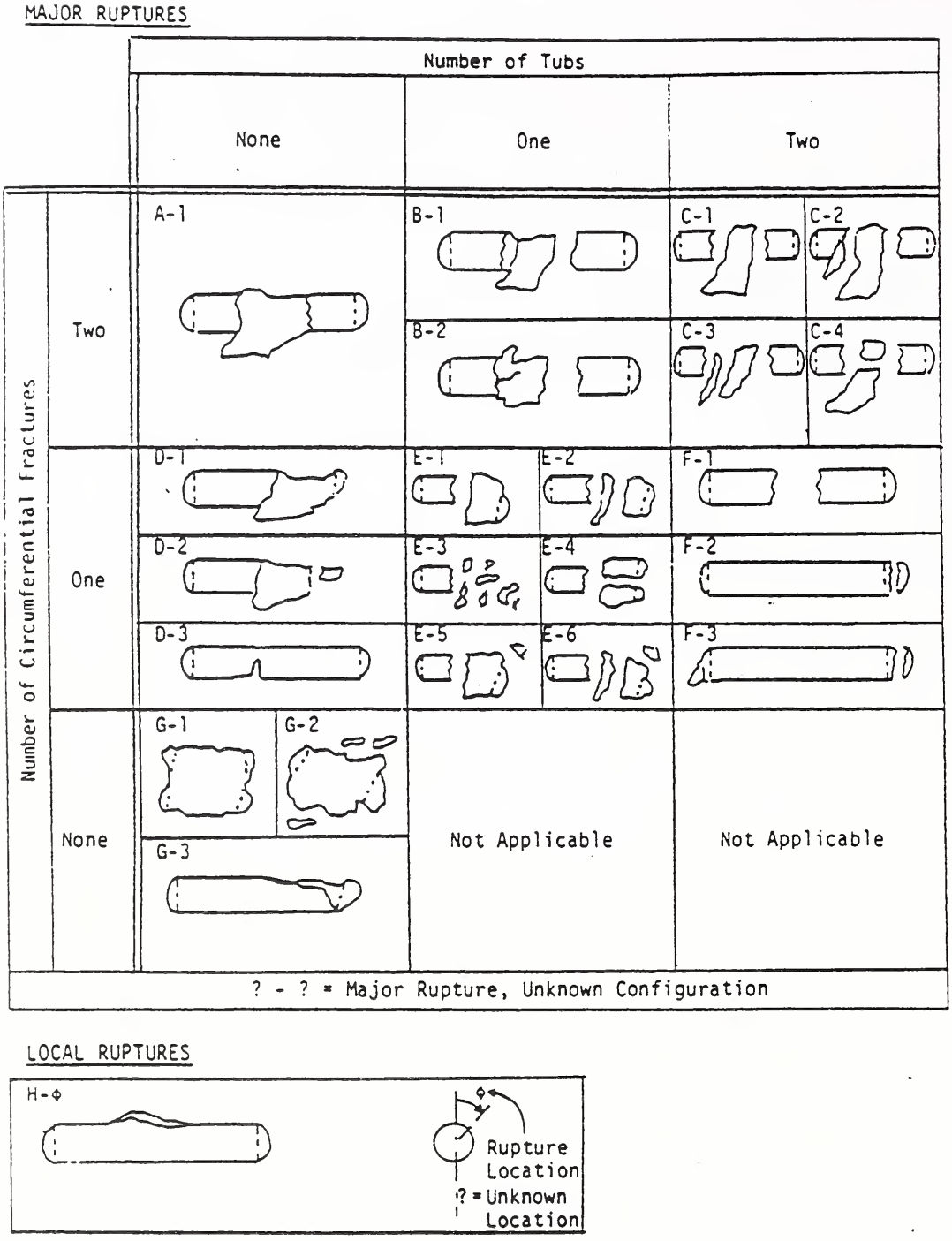

Figure 5-2 Rupture Types Due to Impact or Fire.

Section 6

FLAWS IN PRESSURE TANK CARS

6.1 SERVICE EXPERIENCE

Service experience on tank cars in accident [4] indicated that flaws had developed and propagated when tank cars experienced a rail-burn dent or impact. The Waverly TN and the Cumming IA accidents involved fracture due to the rail-burn dent. In the Belle accident, fracture was attributed to a preexisting flaw that opened upon impact by another car. Typically, a flaw initiates at a circumferential weld as shown in Figures 6-1 and 6-2. The surface flaw then penetrates through the wall and becomes a throughwall crack and continues to propagate some distance. The long crack then opens (bulges) sufficiently under internal pressure which results in flap development at both ends. The crack then turns in the circumferential direction.

In the case of LPG tank cars circumferential fracture has resulted in the development of two end-tubs, which were projected over a long distance. These types of fractures are termed 'BLEVE' (Boiling Liquid Expanding Vapor Explosion). Internal pressure and/or violent expansion of the liquefied lading is the primary cause of such fracture.

Figures 6-1 and 6-2 also show the flaw location at sub-arc girth welds that initiated the BLEVE fracture [4]. Also, shown in these figures are surface flaws and their size. A schematic of all types of tank car ruptures was shown in Figure 5-2 (Section 5).

Rail-burn, dent-induced brittle fracture experience in LPG and anhydrous ammonia cars [1, 4, 5] indicated that the length of the dents must be in excess of seven feet (2.1 M) in order to develop flaps and subsequent turning of the crack in the circumferential direction. Shorter dents have resulted in arrested fracture.

Service experience indicates other flaw locations in the HAZ of fillet weld, fatigue cracks at anchor welds in old designs, and crack at a reinforcement plate weld. These cases are shown in Figures 6-3 through 6-5 [4]. Flaw shape and size information was not available. Another potential flaw location is at skip welds.

6.2 FLAW POSTULATIONS IN FRACTURE MECHANICS ANALYSIS

Fracture mechanics analysis of tank cars requires a realistic assumption of the flaw shape and size, and flaw orientation. Service experience has demonstrated that most spectacular fracture cases involved propagation of a longitudinal flaw in the tank car shell. Fracture predictions for determining whether a leak or break would occur require postulations of both the surface flaw and the throughwall flaw. In the initial stage of fracture development, a longitudinal surface flaw is of interest. However, consideration of potential BLEVE fracture requires the postulation of circumferential

flaws. These cases are illustrated in Figure 6-6. The flaw shape and size postulations are typically based on in-service inspection or from accident investigations. None of the reports reviewed shed any light on flaw size and shape, other than those discussed in Section 6.1.

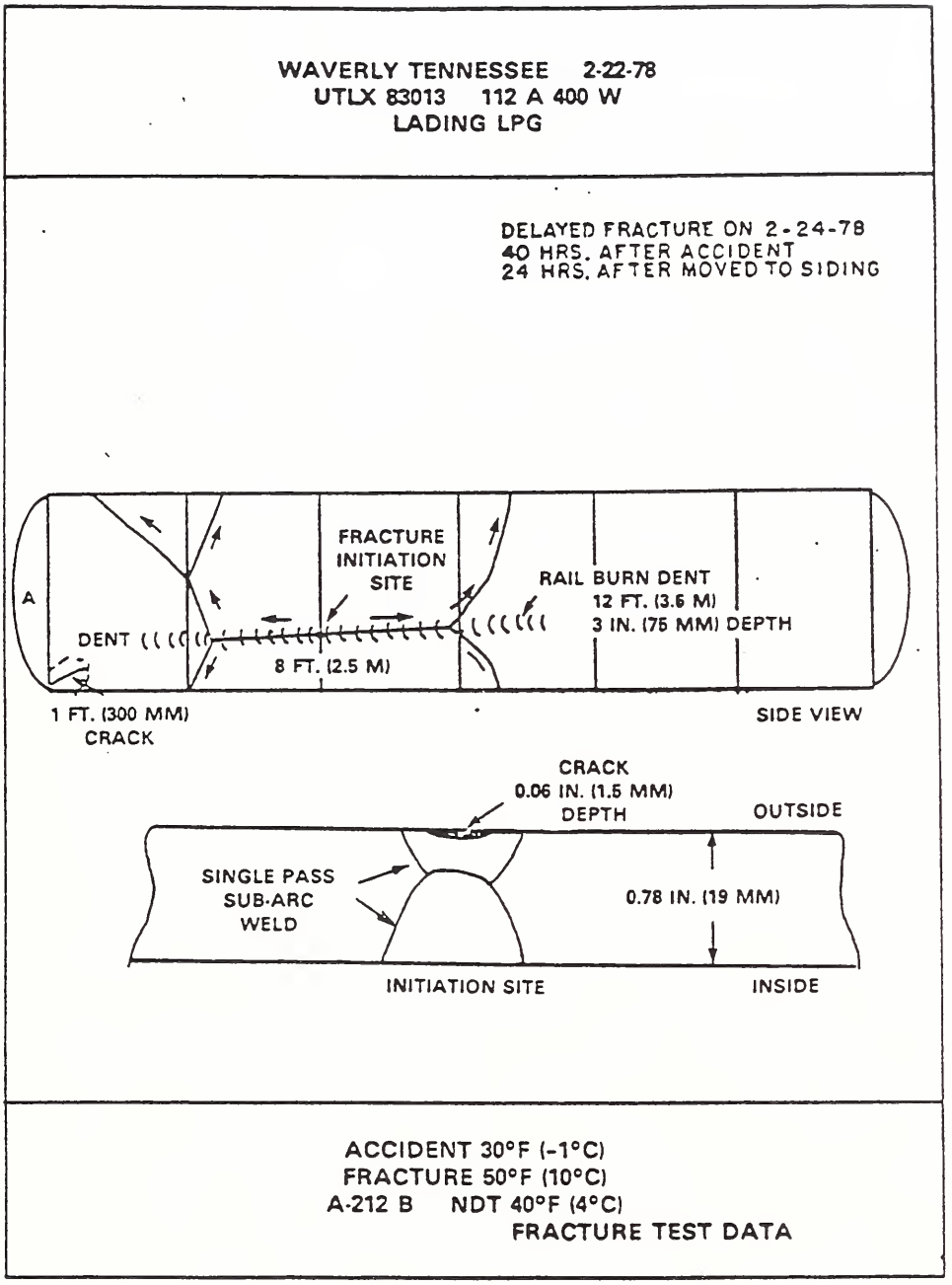

Figure 6-1 Flaw Propagation in Waverly, Tennessee Accident.

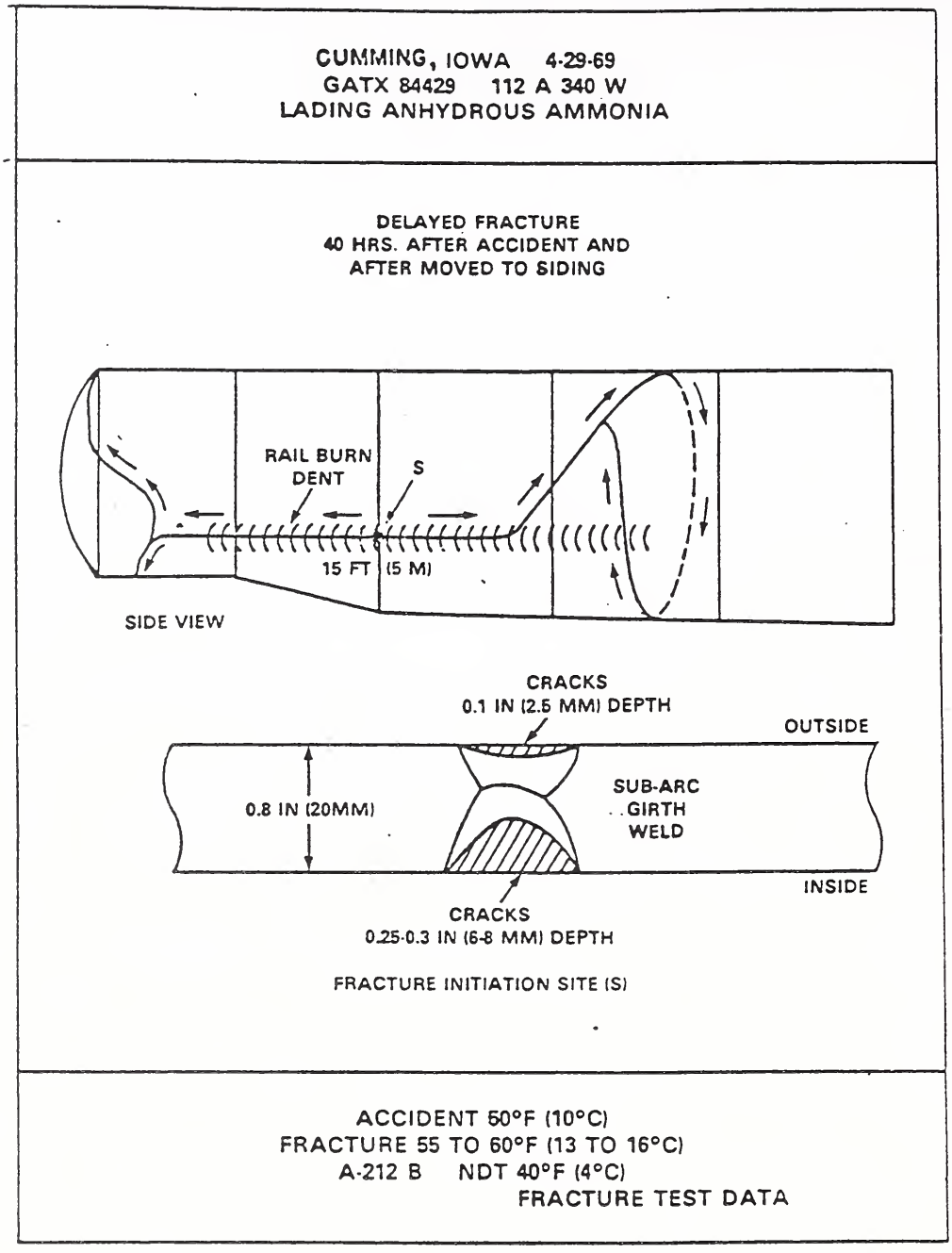

Figure 6-2. Flaw Propagation in Cumming, Iowa Accident.

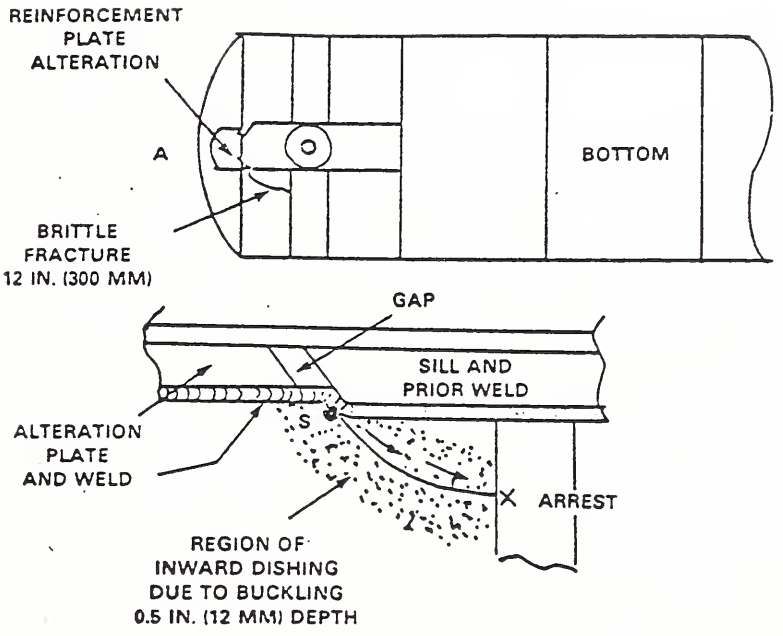

Figure 6-3. Fracture Initiation Sources at HAZ of Fillet Weld.

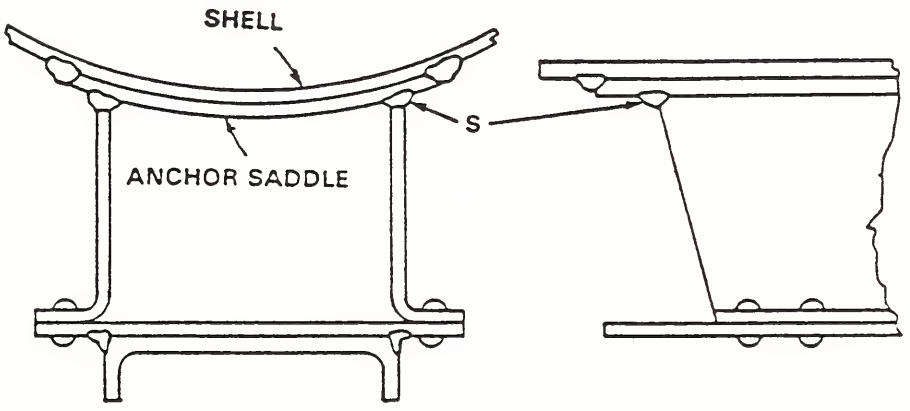

Figure 6-4. Fatigue Crack at Anchor Welds.

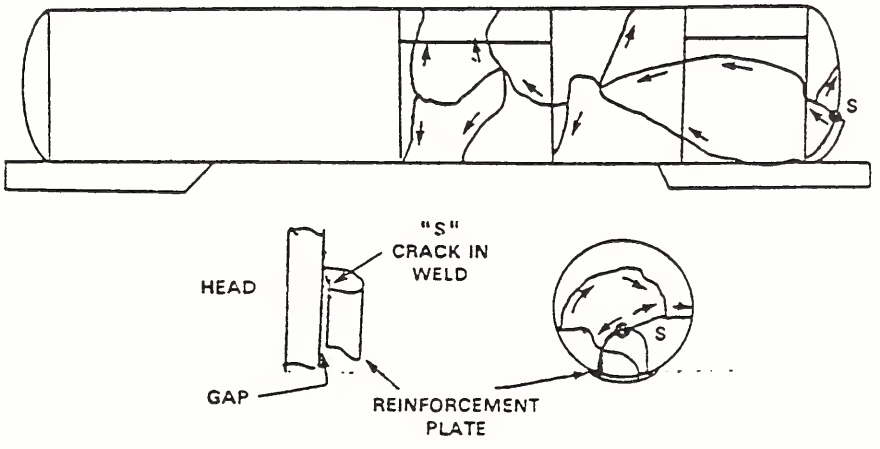

Figure 6-5. Crack at Reinforcement Plate Weld.

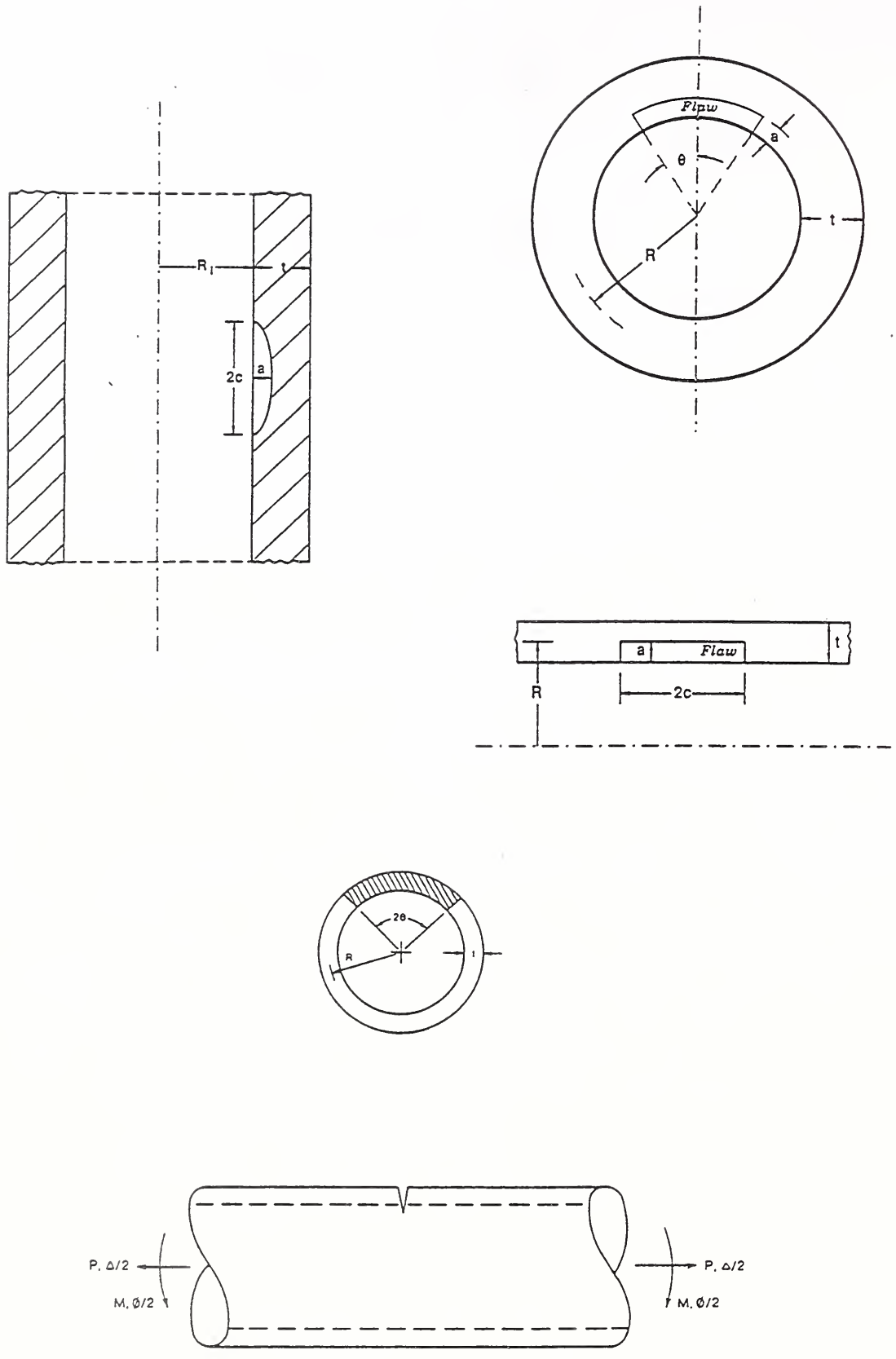

Figure 6-6. Circumferential and Axial Flaws.

Section 7

FRACTURE MECHANICS ASSESSMENTS FOR PRESSURE TANK CARS

7.1 SLIDE GRAPH METHOD

The slide-graph method [4, 5] is essentially a linear elastic fracture based method where several conservative assumptions for materials data are incorporated. It is a stress versus temperature graph, where the applied or operating stress at a location is normalized and expressed as a fraction of the material yield strength and the temperature is expressed relative to NDT. The indexed temperature scale allows several steels to be represented on one. Figure 7-1 shows a typical fracture analysis slide graph. Certain elements of this figure can be shifted (slid) along the indexed temperature scale depending upon the type of analysis and will be described a little later in this section.

A fracture analysis slide graph contains three major elements. The first element is the fracture/arrest curve which is derived from a combination of material's data and conservative assumptions based on past experience (1940's -70's) with structural steels used in the navy (and shipping industry). This fracture/arrest curve is shown as a bilinear curve, the beginning part of which has a fixed normalized stress value, just below 0.2, for all temperatures up to a T-NDT of 10°F (-12°C). After this temperature, the curve rises linearly and terminates at the normalized stress representing the yield stress (YC). It is argued that beyond this termination point fracture would occur by large scale yielding around the crack location and would require an elastic-plastic fracture analysis method. The slope of this curve can be determined from experimental data or by analysis or by a combination of both and will be described later.

The idea of such a bilinear curve originates from the early dynamic crack arrest temperature (CAT) curves developed from a number of tests, as shown in Figure 7-2 [1, 5]. The CAT fracture-arrest curve is determined by testing several plates over a range of temperature and stress levels. This figure shows that fracture does not occur below NDT temperatures when the applied stress is below 12% of yield strength (Y_s). Fracture generally occurs above $0.2Y_s$. For service temperatures above the NDT, the curve defines the boundary between fracture and no fracture (arrest after a short pop-in of the notch-tip crack). In this region, an applied stress falling below the curve would assure no-fracture. Therefore, the area below the curve represents crack arrest or no-fracture region and the area above the curve represents fracture region. The fracture-arrest curve shown in Figure 7-1 is equivalent to the CAT curve. Further details can be found in Reference [5] which also discusses the development of fracture-arrest design procedures during the period from 1950 to 1980.

The linear rising-part of fracture arrest curve is developed from a combination of analysis and crack arrest data. The procedure is illustrated in Figure 7-3. The lower part of this figure is a design reference curve base on K_{Id}. The K_{Id} represents dynamic loading fracture toughness and represents conservatism over slow or intermediate loading response of the material as shown in Figure 7-4. At any specified temperature, the K_{Id} represents a lower bound value for the material. The level of conservatism increases with temperature.

The upper part of Figure 7-3 is a fracture arrest curves which are developed from analysis of a part-through wall (surface) flaw in a plate. The LEFM solution for this geometry is:

$$K_I = 1.12\ S\ [\pi a/Q]^{0.5},$$

where S is the applied stress, a is the flaw depth, and Q is the shape factor which depends on the flaw aspect ratio a/2c, where 2c is the crack length. The stress intensity factor solutions for some common flaw geometries are shown in Figure 7-5.

The critical stress for a specified flaw depth and temperature is calculated by assuming $K_I = {}_{Kid}$. A series of calculations is performed for the entire range of flaw depth and temperature which produces the series of fracture arrest curves shown in the Upper part of Figure 7-3.

Two points L and YC (defined earlier) on the design reference K_{Id} curve are considered next. The point L represents the plane strain limiting K_{Id} value that can be measured from standard ASTM test specimen for K_{Id} determination. The L and YC point on the design reference curve (lower figure) are projected up on the calculated arrest curves to determine the intersection points and their corresponding stress (σ_n) value. A linear relationship between L and YC points is assumed. It should be noted that the point "L" depends upon test specimen thickness. A different fracture-arrest curve is developed for each thickness, giving curves such as those shown in Figure 7-6.

The second element of the slide graph method is fracture initiation curves. Two series of these curves are shown in Figure 7-1 for slow loading and dynamic loading conditions in service. They are separated by a fixed NDT indexed temperature scale. These curves are calculated using K_I solutions given in Figure 7-5.

The third element of the slide graph method is the inclusion of NDT scatter bands for railroad tank car materials. It is discussed in Section 4.3 and shown in Figure 4-20.

7.2 THE SLIDE GRAPH ANALYSIS PROCEDURE

The first two elements of the AAR slide graph method discussed above are presented in Figures 7-7 and 7-8. As discussed before, the fracture-arrest bilinear curve is the same in both figures. This curve is shown for the 1-inch (25-mm) section size which is assumed to represent tank car steels in the section size range of 0.5 inch (12.5 mm) to 1.2 inches (31 mm). The temperature difference between the NDT temperature and the YC temperature is 50°F (28°C). The only difference between the two figures is the analytical fracture initiation curve. The former figure is for the slow rate loading and the later for dynamic loading. Either one is used depending upon the type of analysis being performed for determining the potential for fracture. It has two reference lines: one indicating the yield stress level and the other the reference NDT index (vertical) line. The normalized stress and indexed temperature axes are removed because one of these figures is positioned on top of the NDT reference band diagram of Figure 7-9. These figures are reproduced as transparencies and used as 'slide graph' to position it on Figure 7-9 for the appropriate material being investigated. The slide graph is aligned first to match the yield stress line on Figure 7-9, then the vertical NDT index line is matched to the

peak bell curve of the specific material by sliding the graph along the temperature scale. Figures 7-10 show the alignment position for as-rolled Typical C/Mn steels and includes the fracture initiation curves for slow loading rates. Figure 7-11 shows the same case for dynamic loading.

Alternatively, if the analysis is aimed at selecting a suitable material then the YC point (ductile rupture at yield stress) on the slide graph is matched to the lowest anticipated service temperature (LAST) for the tank car, this then leads the index reference line pointing to the material and the NDT requirement for the material. If the analysis is for the temperature range where fracture initiation or fracture arrest would occur then the NDT index line on the slide graph is positioned to match the NDT band curves for specific steel. Once positioned thus the family of fracture initiation curves indicate the range of temperatures where such an event might occur. In order to obtain a specific answer, one needs to enter the flaw size and applied stress on this graph.

Typically, the flaw size is deduced from the flaw inspection data or assumed as some conservative size. The applied stress is the appropriate stress acting on the flaw. Pellini [5] makes separate assumptions for fracture initiation and propagation analyses. He suggests that local stress at the crack site should be considered for fracture initiation analysis, whereas through-thickness average stress should be used for fracture propagation analysis, see Table 7-1. The basis for this assumption is not indicated in Reference [5]. It introduces some conservatism in the analysis but the degree of conservatism built into each case is not known when making a relative assessment of the most critical location in the tank car.

7.3 DISCUSSION ON SLIDE GRAPH METHOD

Several assumptions in the slide graph method need to be examined when fracture is predicted to occur at service operating conditions or accident conditions. These apply to the development of fracture initiation and propagation curves of Figures 7-7 and 7-8. These curves were developed assuming a surface flaw in an infinite plate. This assumption does not allow a distinction between a longitudinal and circumferential flaw. Separate solutions are now available for surface flaws in either direction. Also, solutions are now available for internal as well as external flaws. The method assumes local (point) stress as applied stress. Solutions are now available for stress gradient loadings in cylindrical structures. Beyond the stress distribution and flaw geometry issues, it appears that the K_I calculations do not include the effects of plasticity ahead of the crack tip. This would underestimate the calculated K_I value for the flaw. This underestimation would not be significant for shallow flaws under low applied stresses but be appreciable for higher stresses particularly for accident loading conditions.

The YC point on the crack-arrest diagram is clearly well into the elastic-plastic fracture regime. Consequently, an elastic-plastic fracture parameter should be used to define this point. Further, the L-YC curve is assumed as a straight line. This linear curve needs to be reexamined for stress levels above the 0.5 yield stress level. This is because significant plasticity is generated in the flaw region and fracture mechanics calculations must include plasticity effects correctly, otherwise conservatism introduced in other places would be diminished and may even lead to nonconservative predictions particularly for accident conditions.

7.4 SLIDE GRAPH FRACTURE EVALUATIONS

7.4.1 Normal Operating Conditions

Railroad tank cars are designed and fabricated to assure structural integrity under normal operating conditions. Three factors that contribute to this feature are conservative design stresses, well designed structural configuration and stress relief heat treatment.

The design hoop stresses for welded pressure vessels are generally limited to 50 percent of the yield stress. The hoop stress versus temperature curves for pressure tank cars designed for various liquefied gas ladings is shown in Figure 3-2, Section 3. A large number of tank cars transport propane (LPG) and anhydrous ammonia (AA). The hoop stresses for these tank cars are between 10 and 20 percent of the yield stress. These very low hoop stresses significantly contribute to structural integrity. The tank cars with carbon dioxide and hydrogen chloride ladings experience hoop stresses close to 50 percent of the yield stress. However, the internal pressure is limited by the valve discharge setting, which is maintained even in accident conditions as long as the valve continues to function to its design specifications.

Fracture initiation concerns from these stresses can be investigated by comparing the fracture initiation curves of Figure 7-10 against the design hoop stresses (Figure 3-2) as shown in Figure 7-12 [1, 5]. It is seen that fracture initiation is not possible for the four lading cases that produce low design hoop stress levels. The hoop stresses for tank cars with carbon dioxide and hydrogen chloride ladings are also below those required for fracture initiation, although the margin is much less. An accident loading combined with a malfunction of discharge relief valve would be required for fracture initiation. These conclusions are valid only for smooth regions of the tank cars.

Tank cars are designed to avoid any type of tank rupture that could result in the release of flammable, explosive or toxic materials. The thin-walled shell construction favors deformation in preference to fracture. The shell yields easily when impacted. In addition, the tank cars have relatively few regions of severe stress/strain concentrations. Such points are, however, susceptible to fracture initiation. Brittle fracture has been a concern. However, service experience indicates the vast majority of failure by severe plastic deformation. One thousand three-hundred forty-five loaded pressure cars were involved in severe accident impacts between 1965 and 1980. Of these only sixteen brittle fracture cases were experienced. These accidents involved an average of 2.5 impact points per car. Many cases involved severe plastic deformation of tank car without rupture of any type [4].

Another factor for good structural integrity performance is the stress relief heat treatment. Welded tank cars are required to be stress relieved by furnace heat treatment to temperatures of 1150°F (620°C). Consequently, the HAZ regions of welded tank cars have fracture resistance and ductility comparable to that of the base material.

The weld-toe regions of fillet welds (in reinforcement plates and attachments) experience intense localized plastic stresses under accident loading and are subject to fracture initiation. Furnace stress relief of these regions has alleviated brittle fracture concerns as indicated by the very low incidence of brittle fracture. Fracture initiation due to hard-brittle HAZ regions has been recorded only for

repair welds that were stress relieved by torch heating.

7.4.2 Accident Loading Cases

Service experience for LPG and anhydrous ammonia tank cars has indicated that brittle fracture is developed by two stages of crack propagation. Fracture is developed due to external forces (such as a rail-burn dent impact) from the accident. This typically initiates at a circumferential weld as shown in Figure 7-13. The surface flaw penetrates through the wall and becomes a throughwall crack and continues to propagate some distance. The long crack then opens (bulges) sufficiently under internal pressure which results in flap development at both ends. The crack then turns in the circumferential direction. In the case of LPG tank cars circumferential fracture has resulted in the development of two end-tubs, which were projected over a long distance. Internal pressure and/or violent expansion of the liquefied lading is the primary cause of such fracture. An explosion inside the tank is possible only for auto-oxidizable compounds, such as ethylene oxide. Prolonged heating in fires may initiate the explosive decomposition of such compounds.

Rail-burn, dent-induced brittle fracture experience in LPG and anhydrous ammonia cars [4, 5] indicates that the length of the dents must be in excess of seven feet (2.1 M) in order to develop flaps and subsequent turning of the crack in the circumferential direction. Shorter dents have resulted in arrested fracture.

Figure 7-14 shows the advantage of normalized condition over the as-rolled condition for the TC-128B steel [5]. The fracture arrest curves for the two conditions with their average and high limit NDT properties are shown by dashed lines. The normal hoop stress plots are shown by solid curves. The crack arrest behavior is predicted for those curves falling below the dashed lines. The following conclusions are derived from this figure.

(1) Fracture propagation outside regions of accident dent deformation is possible for the case of high hoop stress curves that lie to the left of the specific fracture arrest curves. These include the curves for carbon dioxide, hydrogen chloride and hydrogen sulfide.

(2) Fracture propagation outside the regions of accident dent deformation is not possible for low hoop stress curves. These include the curves for propane (LPG), anhydrous ammonia (AA), chlorine, vinyl chloride, and sulfur dioxide.

7.4.3 Liquefied Carbon Dioxide Cars

The hoop stress for liquefied carbon dioxide (CO_2) tank cars is the largest of all other cars (Figure 7-14). At normal service temperatures, the hoop stresses in these tank cars are above the stress level required for fracture arrest (i.e., above the flat-part of the bilinear fracture arrest curve). This implies that fracture arrest cannot be expected for CO_2 tank cars. Therefore, prevention of fracture initiation is a major objective for CO_2 cars.

There are no known cases of brittle fracture of CO_2 cars that were fabricated according to AAR requirements for the use of normalized TC-128B steel. The average NDT temperature for this steel is normally -50°F (-46°C) and the maximum NDT temperature is expected to be approximately -30°F (-34°C). The shell temperature of CO_2 cars which also have thick thermal insulation is between -20 and 0°F (-29 to -18°C). The analysis indicates that fracture initiation is not possible for slow loading rates and for cracks that are significantly less than 0.5 in. (12 mm) size (see Fig. 7-12) [5]. Fracture initiation under dynamic loading is possible only if the steel plate at the crack location is of statistically high -30°F (-34°C) NDT properties [5]. These cases need to be reanalyzed for reasons discussed in Section 7.3.

7.4.4 Cases of Pressurization-Induced Stress Systems

The potential for fracture of a pressurized tank car depends on its condition in service or accident. Table 7-2 ranks the analysis priority for three broad categories of tank condition and two broad categories of loading. The low, medium, and high ranking is meant for prioritizing the fracture mechanics analysis.

Crack-free or undamaged cars are routinely tested at hydrostatic test pressures. No failure has been recorded. No cases of rupture have been experienced for accidental pressurization of crack-free or undamaged tank cars to safety valve pressure levels. There has been no tank car rupture at calculated burst pressures in Service [5].

Tank car failures have been recorded for accident-induced deformations or where cracks were present. In all cases, failure analysis indicated that the fracture originated at locations of stress/strain concentrations primarily due to the presence or development of crack defects at these locations [22]. Reference [23] concludes from an NTSB study that sudden, total tank car failure might result from an after-the-accident overpressurization, involving pneumatic conditions. The slide graph fracture analysis [5] predicts that leakage would result for conditions of gradual (slow) hydrostatic overpressurization. Analysis details were not provided for either pneumatic or hydrostatic loading. This conclusion is most likely derived from service experience. Another condition of overpressurization is the shell-full condition which results from the elimination of the vapor space by partial crushing of the tank shell in accidents. Other conditions are safety valve malfunction due to damage in accidents and improper practices in tank car filling. No cases of brittle failures have been recorded for shell-full condition or safety valve malfunction [5].

7.4.5 Accidental Overpressurization During Tank Car Filling Operations

The total failure for tank cars in present service is possible only when: (1) flaws/cracks are present, and (2) gross deviations from customary safety measures result in overpressurization. Service experience documents only one known case of total tank car failure during filling operations. This case is discussed in [5] and shown in Figure 7-15. A combination of adverse conditions is required for the initiation of brittle fracture as the result of overfilling to shell-full conditions. These are: (1) Presence of crack-like defects, (2) Shell-full overfilling that results in high hoop stresses (hard filling),

and (3) Fast (dynamic) increase of the hoop stresses developed from pump-induced pressure surges. The probability for all three conditions happening at the same time is very low [5].

Although no details are provided in Reference [5], the slide graph fracture analysis predicts that (a) hydrostatic overfilling (shell-full) should normally be expected to result in short (arrested) fracture due to depressurization caused by leakage and (b) pneumatic overfilling that results in overpressurization may cause a total tank failure. Reference [5] also concludes that tank cars with straight-line, rail burn should not be a cause of concern in filling operations.

7.4.6 General Conclusions

As a result of the AAR-RPI analyses (discussed in Sections 7.4.1 through 7.4.5), the following observations and conclusions were made. Brittle fracture of tank cars has never developed in normal service. Service experience for pressure tank cars in present use demonstrated a high degree of resistance to brittle fracture. For the tank cars that suffered impact-deformation loading, the incidence rate of brittle fracture is less than 1 percent. This applies for tank cars that did not have the presently used protection systems of head shields, shelf couplers and insulation. With the required use of such protection systems [3], the incidence rate for brittle fracture in accidents is expected to be less than 0.1%.

The AAR-RPI studies conclude that certain unusual conditions must be developed in order to initiate and propagate brittle fractures. These are:

(1) A crack-like defect must be present or developed as the result of loading.

(2) The loading rate at the site of the crack-like defect must be dynamic. The crack-tip must be subjected to a fast application of crack-opening stresses in order to initiate cleavage (brittle) fracture.

(3) Brittle fracture cannot be expected to propagate through regions of low hoop-stress levels. For example, the stress levels for propane (LPG) and anhydrous ammonia are too low for fracture extension.

(4) For ladings involving low hoop stresses, brittle fracture can only propagate through regions of abnormally high elastic or plastic stresses.

The high quality design and fabrication standards for tank cars are the primary reason for the observed low incidence rates. Also, the low probability of the presence or development of crack-like defects contributes to the structural integrity of tank cars.

7.5 STEELS WITH IMPROVED LOW TEMPERATURE FRACTURE PROPERTIES

Reference [19, Pellini] reviews the fracture properties of presently used and possible "future" tank

car steels. It discusses the metallurgical, fabrication (weldability) and availability considerations. The AAR Tank Car Committee suggested that the "future" tank car steel should demonstrate fracture-safe behavior at the lowest service shell temperature for loaded propane (LPG) tank car, which is -30°F (-34°C). This meant that the "future" steel should have YC fracture properties at -30°F (-34°C). The slide graph analysis (Figure 7-11) indicated that the NDT temperature of the material should be -80°F (-62°C) to satisfy the hypothetical requirement for a YC of -30°F (-34°C).

As of early 1984 the steel used for propane (LPG) tank car fabrication was as-rolled TC-128B. At that time, the specified LAST need of -30°F (-34°C) was still being debated and this resulted in two positions [5]. One position cited the low incidence of brittle fracture for as-rolled steels (which have 50 to 90°F (10 to 32°C) YC fracture properties) and the other position was based on the premise that the use of normalized TC-128B steel would decrease the incidence of brittle fracture from 19 to 5. It is noted from Figure 7-11 that the normalized TC-128B steel did not meet the NDT requirement of -80°F (-62°C). The normalized Cb (Nb) steel also did not fully meet the NDT requirement. The attention was then focused on three Cb (Nb) control-rolled steels. The estimated NDT bands for these future steels are shown in Figures 7-16 and it can be noted that the ICR band meets the NDT requirement for "future" steel. This type of Cb (Nb) steel is produced by "intensive cold rolling (ICR)" practices and it means finish rolling at relatively low temperatures [19]. Additional issues identified with the selection of control-rolled steels were the submerged arc welding and stress relieving.

7.6 ASSESSMENT OF STEELS IN TANK CAR ACCIDENTS

Analyses of fracture behavior of pressure tank car steels in accidents were conducted in Reference [4]. The service experience described in this reference is summarized in Section 5 of this report. Here, the results of fracture analyses of nineteen brittle cases are summarized from Reference [4]. The objective of these analyses was to estimate the reduction in brittle fracture cases and the reduction in lading loss if the cars were fabricated of steels with improved fracture properties. The reduction in failure rates was defined by "true index of the resistance to brittle fracture (B.F.)." It is defined in terms of the percentage of impact points that resulted in brittle fracture. Using this definition, the Table 5-1 (section 5) data gives a BF = (19/3362) x100 = 0.6%, i.e., only 0.6 percent of impact points resulted in brittle fracture.

The Appendix B to Reference [4] presents the analysis and results which are summarized below. The steels considered in the analysis were the as-rolled TC-128B, normalized TC-128B and a "future" steel. The "future" steel is discussed in Section 7.5. The fracture propagation assessment was based on the slide graph method. According to this method, the potential for development of brittle fracture is defined by the YC temperature of the steel. If the tank shell temperature is above the YC temperature of the steel, brittle fracture cannot be developed, irrespective of the rate of loading or the degree of plastic deformation that occurs during the accident [4]. The YC temperature for each steel was compared against the specified accident temperature to determine if brittle fracture is possible.

It was estimated that the use of normalized TC-128B steel would reduce the brittle fracture cases

from 19 to 5, a reduction by a factor of approximately five over as-rolled condition. The "Future" steel featuring ductile behavior at the lowest service temperature, thus eliminating brittle fracture, requires maximum NDT temperature of -80°F (-62°C), see Section 7.5. Reference [19] discusses this aspect and concludes that this requirement is not presently (as of 1983) attainable in large plates of normalized or controlled-rolled steels. Table 7-3 summarizes all results in terms of the BF index.

It was concluded that additional factors must be considered to weigh the potential benefits of using the normalized TC-128B steel. These include specific analyses for fracture initiation and propagation, fracture prevention, development of statistical data base, additional cost for change to normalized condition, and lading loss considerations. Some of these were investigated by NIST [6-13].

At temperatures below the YC temperature, the initiation of brittle fracture may occur due to a crack-like defect already present or one that developed as a result of loading. It was suggested that this problem can be eliminated by appropriate fatigue design and by proper fabrication quality control practices. Pop-in cracks, due to hard HAZ (heat-affected zone) weld regions, can be precluded by proper use of stress relief practices [4]. The potential for fracture initiation was assessed on qualitative rather than quantitative basis. Table 7 of Reference [4] lists fracture initiation causes and prevention methods.

7.7 ELASTIC-PLASTIC FRACTURE MECHANICS METHOD

In general, a fracture mechanics analysis consists of two components: the crack driving potential and the material's resistance to crack extension. The crack driving potential is computed from fracture mechanics solutions that depend on the applied load, component geometry, service temperature, and stress-strain properties of the material. The material's resistance to crack extension is measured from laboratory specimens. The crack driving potential is then compared to the material's resistance to assess the structural integrity of the component.

When plastic deformation surrounding a crack is small compared to relevant dimensions in the location of the crack, the methods of linear elastic fracture mechanics (LEFM) are used. In this case the stress intensity factor, K_I, is used where appropriate adjustments are made for plastic deformations. However, when plastic deformation ahead of the crack is no longer small a nonlinear or elastic-plastic fracture mechanics (EPFM) analysis is used. This case is best handled by the J-integral fracture parameter, J. The J is identical to K_I in a linear elastic fracture mechanics analysis and it is for this reason many analyst use J for both the LEFM and EPFM fracture regimes. When the crack location involves large plastic deformation typical of ductile materials, it may be convenient to consider yet another fracture criterion such as the crack based net-section yielding criterion.

7.7.1 Analysis Method

Calculation of Crack Driving Potential (J)

The crack driving potential of the structure is a calculated quantity and is expressed as the sum of two

parts J_e and J_p [25]. The J_e is the elastic J modified for small scale yielding. The elastic J for tank cars can be computed from K_I^2/E, where K_I is the stress intensity factor and E is the elastic modulus of the material. The second part J_p is the plastic component of the J-integral, which depends upon the applied load, crack size, component geometry, and plastic characteristics (stress-strain curve) of the steel.

The elastic and elastic-plastic J solutions for part-throughwall and throughwall cracks in cylindrical geometries are reported in Ductile Fracture Handbook [25]. It contains solutions for wide range of crack sizes and loading cases. In general, fracture mechanics solutions for shell geometries with large radius-to-thickness ratio (R/t greater than 20) are available only for linear elastic analysis. The J-integral solution for circumferential throughwall cracks in tank cars was developed by Zahoor and reported in Reference [12].

Material Fracture Resistance, The J-Resistance Curve

The J-resistance curve is most commonly generated from compact tension, CT, specimens following the procedures set forth in ASTM E1152-87 [8]. The specimen size is selected to either match the thickness of the component or use a thickness that would produce a conservative estimate of the material's resistance to crack extension. The crack orientation in the specimen is selected to match that of the flaw in the application. Figure 4-4 (section 4) shows examples of crack orientation in CT specimens.

The J-T Method

The J-integral tearing modulus (J-T) method is increasingly used for determining the condition under which unstable crack extension would occur. The analysis method compares the crack driving potential (J) to the material resistance (J-R curve). During stable crack growth these two parameters are equal until a stability limit is reached. The J-T procedure for determining the load at incipient crack instability (fracture) is described below. Suppose that the maximum load (e.g., axial load or pressure) is to be computed for a specified circumferential throughwall crack length in a cylinder. First, the applied J-integral is calculated for the specified crack size and a range of applied loads. The applied J as a function of load is shown schematically in Figure 7-17. Next, applied tearing modulus (T) is computed as a function of J for the same crack size and loads [25]. The applied J and T pairs computed for each load are then plotted to establish the applied J-T line shown schematically in Figure 7-17.

A J-T curve representing the material's crack extension also is determined and plotted on Figure 7-17. The material J-T curve is developed from an experimental J versus crack extension curve (J-R curve). The value of the material T at any specified value of J is determined by multiplying the slope of the J-R curve with E/σ_f^2, where E and σ_f are the elastic modulus and flow stress, respectively. The flow stress is a reference stress usually defined as one-half the sum of yield and ultimate tensile strengths.

The intersection of the applied and material J-T curves illustrated in Figure 7-17 defines the J and T values corresponding to crack instability (fracture). The maximum load is then determined from the J versus load curve by entering the J at crack instability and determining the corresponding value of load. An iterative procedure is used to account for crack extension implied in the result. This procedure can be used for any flaw geometry and loading type. Further details are given in Volume 3 of Ductile Fracture Handbook [25].

7.7.2 Screening Criteria for Fracture Mechanics Analysis

It is possible to perform reliable fracture mechanics analyses for the three broad categories of yielding, i.e., predominantly elastic, elastic-plastic and net-section yielding at the crack location. The applicability regime for each fracture analysis method (K, J, net-section yielding criterion) is established by a series of calculations covering a wide range of flaw size, loading cases, and material properties of the structure. In principle, after conducting a series of calculations, it is possible to establish a simple screening criterion or guideline that can be used to define the correct analysis method (K, J or net-section yielding). It has been successfully developed and implemented for nuclear piping [Vol. 3 of Reference 25].

As an illustration, the screening criteria (SC) for nuclear piping application are shown in Figure 7-18. The SC is defined as the ratio of K_r' and S_r. The K_r' is the applied K_I normalized to a reference toughness such as a K_{Ic} or K_c, whereas the S_r' is the ratio of applied load to a reference design load. For carbon steel piping, it was determined that when SC is greater than 1.8 the linear elastic fracture mechanics (LEFM) method can be used to determine the critical flaw size or critical load for a specified flaw size. At the other extreme when SC is less than 0.2 the net-section yielding or limit load analysis can be used. In between the two limits, the correct analysis method is that based on the elastic-plastic fracture mechanics. Such a screening criterion has not been developed for railroad tank cars.

7.7.3 Cases Requiring EPFM Analysis

The tank cars are subjected to a wide range of temperatures, from very cold temperatures in normal service at one extreme to as high a temperature as 680°C in the case of accident involving fire. Over this temperature range, the material's strength and toughness performance varies considerably. Consequently, the use of proper fracture mechanics method is essential to assuring structural integrity. Bounding analyses for a range of flaw and loading combinations should be performed for normal service and accident temperatures. Two major categories can be identified for further analysis. The first includes all cases where the net-section stress exceeds 50% of yield stress, and the second is case where potentially higher temperatures than those in normal service are involved. In the latter case, the normal applied stresses will produce sufficient yielding thus necessitating an elastic-plastic fracture analysis. The review of the reports revealed that such analyses have not been performed. The only analyses reported are based on stress-rupture considerations which do not account for performance degradation from a pre-existing flaw.

7.8 CRITICAL FLAW SIZE RESULTS

The critical flaw size calculations were not found in any of the reports reviewed except for NISTIR-5179 [12]. This report used the latest fracture mechanics analyses method based on the J-integral fracture parameter [Reference 25; see Section 7.7.1]. The analyses were conducted for railroad tank cars that are made from normalized AAR TC128 grade B steel and for two service temperatures of –40°C and 22 °C. Circumferential throughwall cracks in the tank car shell region were postulated to determine the critical crack size for axial tension loadings anticipated in service or accident. Although desired, analyses for part-throughwall flaws were not conducted and it was assumed that the part-throughwall flaw after penetrating the tank shell remains stable, i.e., produces leak-before-break condition for the tank car. The validity of this assumption should be examined for all service and accident temperatures.

Fracture mechanics analyses were performed for five loading cases: (1) Coupler Impact, (2) Test Pressure, (3) Start-to-discharge Pressure, (4) Bursting Pressure, and (5) Vapor Tight Minimum Pressure. These analyses used the procedure described in Section 7.7.1. The critical crack size was determined for the condition when the applied J value matched the material's initiation (J_i) value. The material J_i values, extracted from Reference [9] were 41 and 121 KJoules/M^2 (240 and 700 in-lb/in^2) at –40°C and 22°C, respectively. The J calculations were performed for a large number of crack lengths. The critical crack size results are summarized in Table 7-4.

The critical crack lengths for discharge pressure were 43.4 and 74.2 cm at service temperatures of –40°C and 22°C. These crack lengths are approximately 30 to 50 times the tank car shell wall thickness. The results also indicate that the critical crack length for 22°C is 1.5 to 2 times greater than that calculated for –40°C. Among the loading cases investigated, the critical crack length was determined to be the largest for the impact force case. The analysis results showed that at the burst pressure throughwall cracks up to four times the tank shell thickness can be tolerated. If a part-throughwall flaw upon penetrating the shell wall has a length less than four times the wall thickness, the resulting throughwall crack will be stable, otherwise unstable fracture will result from a part-throughwall flaw (i.e., no leak-before-break). The implications of this result should be investigated further. The effect of lowering the relief valve discharge setting can be investigated in terms of critical flaw size but this was not investigated.

Service failure data indicated that the cracks initially ran in the axial direction. Analyses have not been conducted to determine the critical crack size for axial cracks. It would be desirable to conduct such predictive analyses and compare the results against the service data.

Table 7-1

Crack Location geometry and Event	Assumed Applied Stress
Fracture Initiation Analysis	
Complex Geometry and As-Welded Structures	Near-Yield Stress
Smooth Geometry	0.5 Yield Stress
Accident Loading	Yield Stress
Fracture Propagation Analysis	
Conventional structures.	0.5 Yield Stress
Accident Loading.	Yield Stress

Table 7-2

	Normal design Level of Pressurization	Abnormal, high Level of Pressurization
Defect-free, undamaged tank	Low	Medium
Deformation-damaged tank in an accident, with probable development of crack-like defects	High	High
Structurally weakened Tank due the effects of fires following an accident.	Thermal Insulation	Thermal Insulation

Table 7-3

BF Index Values for different Tank car steels

Steel	BF Index Value per Impact Point	BF Index Value per Car
As-rolled TC-128 grade B	17/3362 = 0.5%	17/1345 = 1.3%
Normalized TC-128 grade B	5/3362 = 0.1%	5/1345 = 0.3%
"Future" steel	0%	0%

Table 7-4

Critical Crack Size for Normalized AAR TC128 grade B Tank Car Shell

Loading Category	Critical Throughwall Crack Length, cm For –40°C	Critical Throughwall Crack Length, cm For 22 °C
Impact Force	85.3	127.3
Test Pressure	31.5	55.9
Start-to-discharge Pressure	43.4	74.2
Bursting Pressure	6.4	14.7
Vapor Tight Minimum Pressure	55.9	90.0

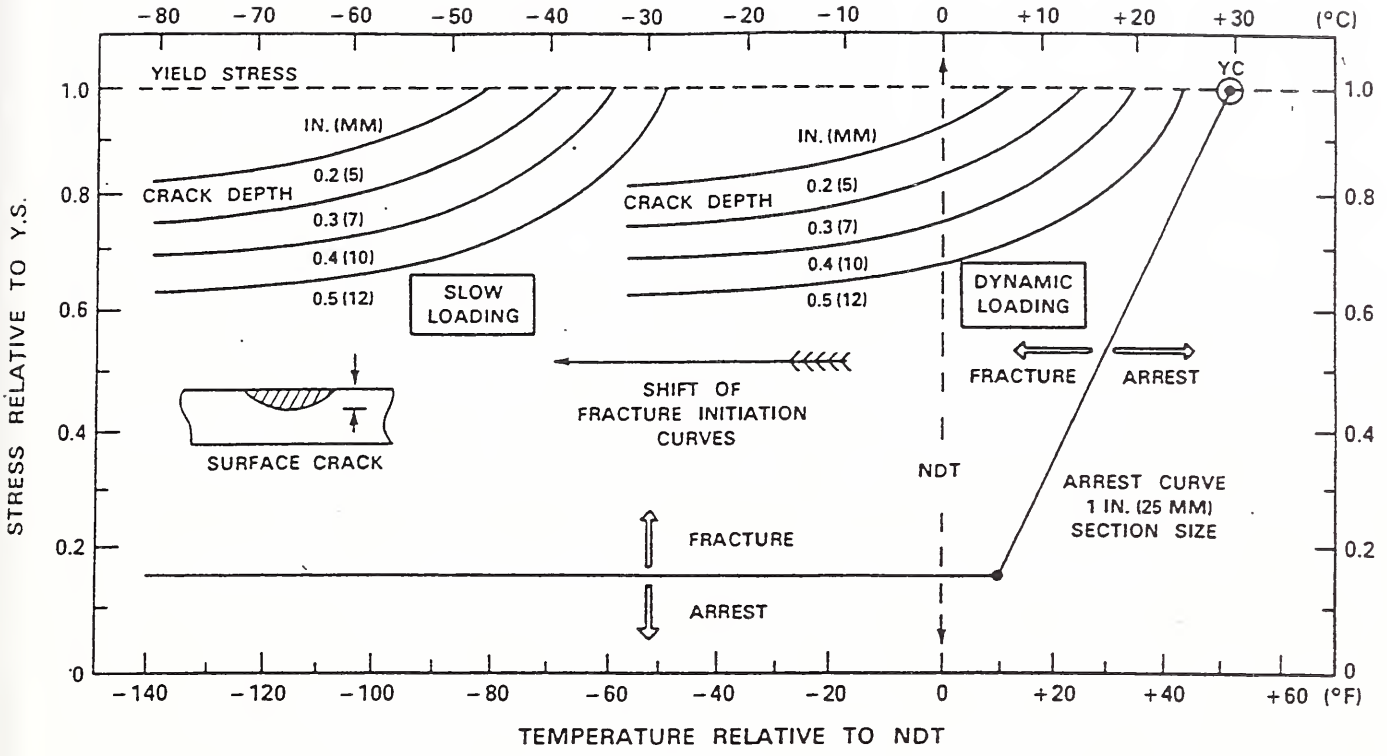

Figure 7-1. Fracture Analysis Slide Graph.

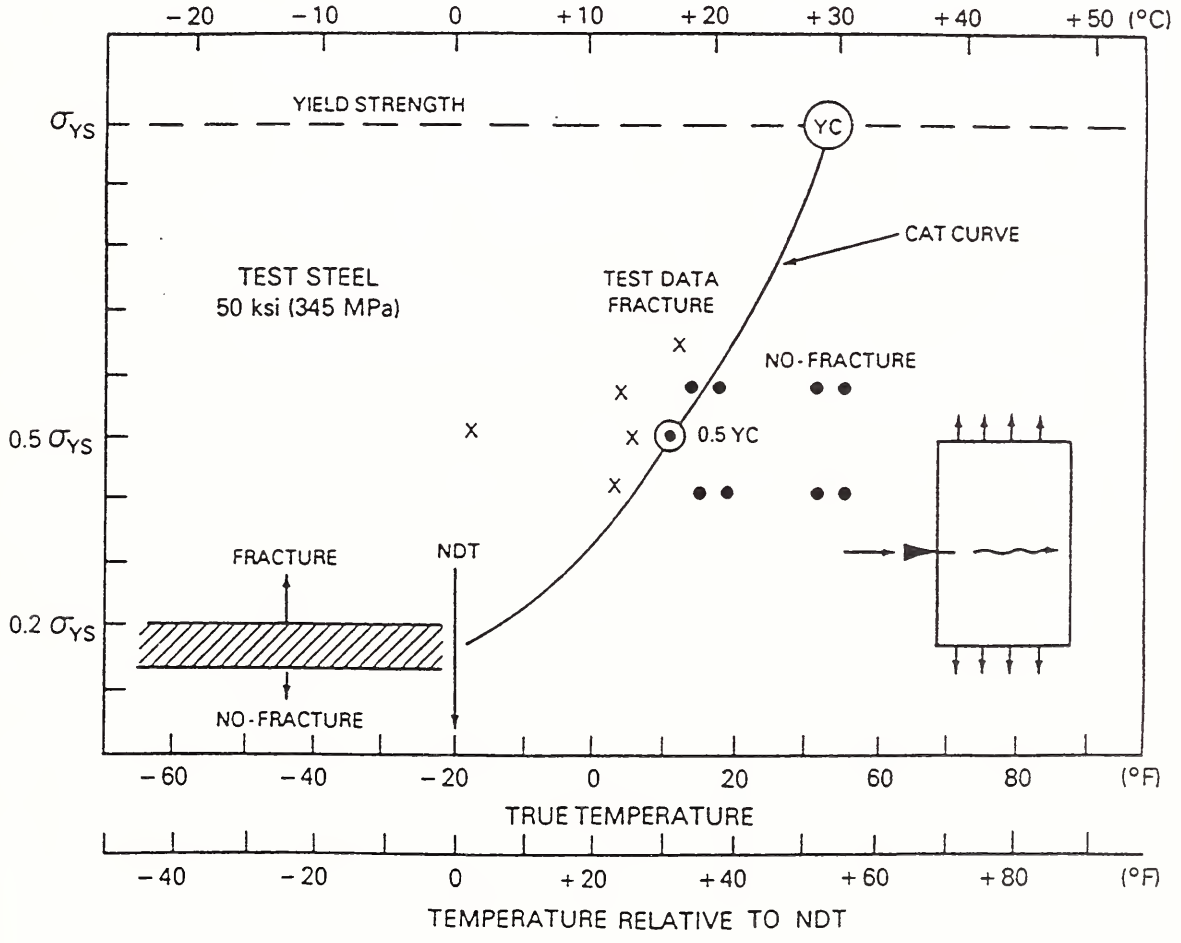

Figure 7-2. Fracture Arrest Curves, CAT.

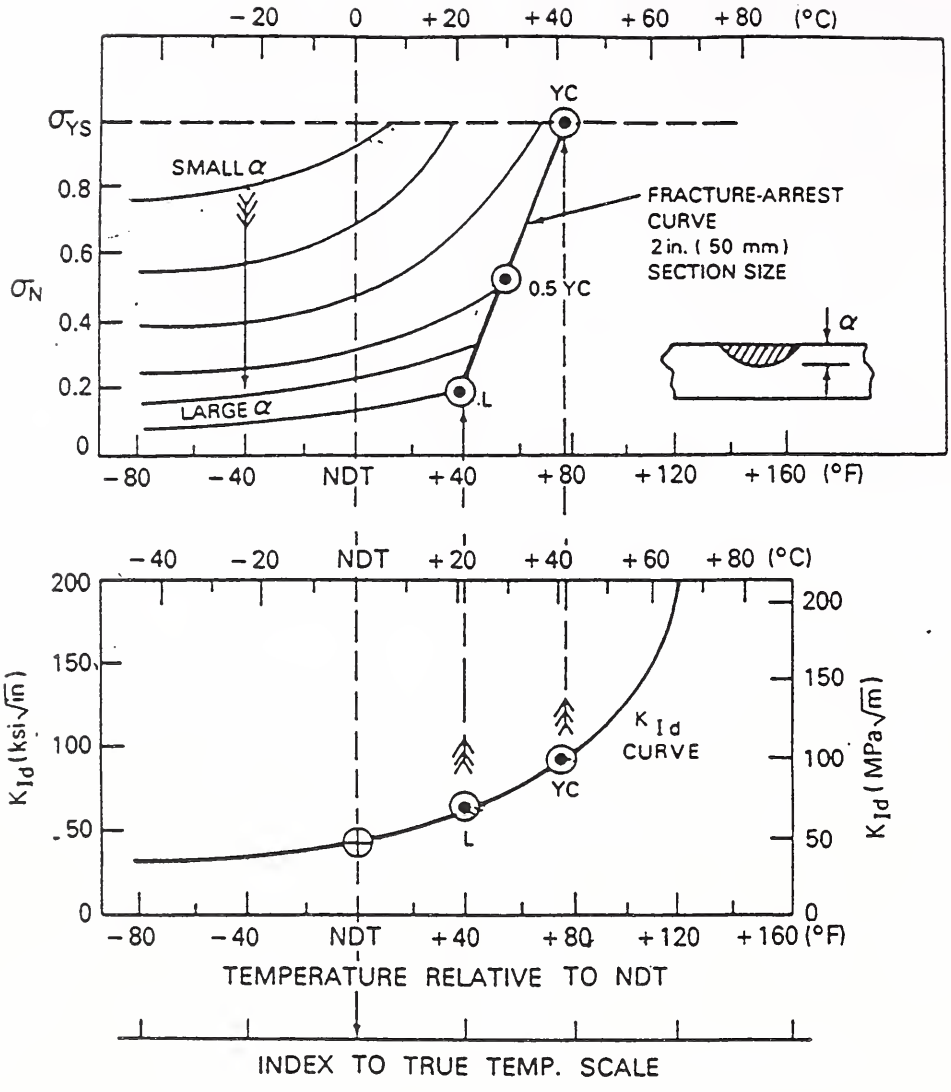

Figure 7-3. Procedure for Determination of L and YC on Fracture Analysis Graph.

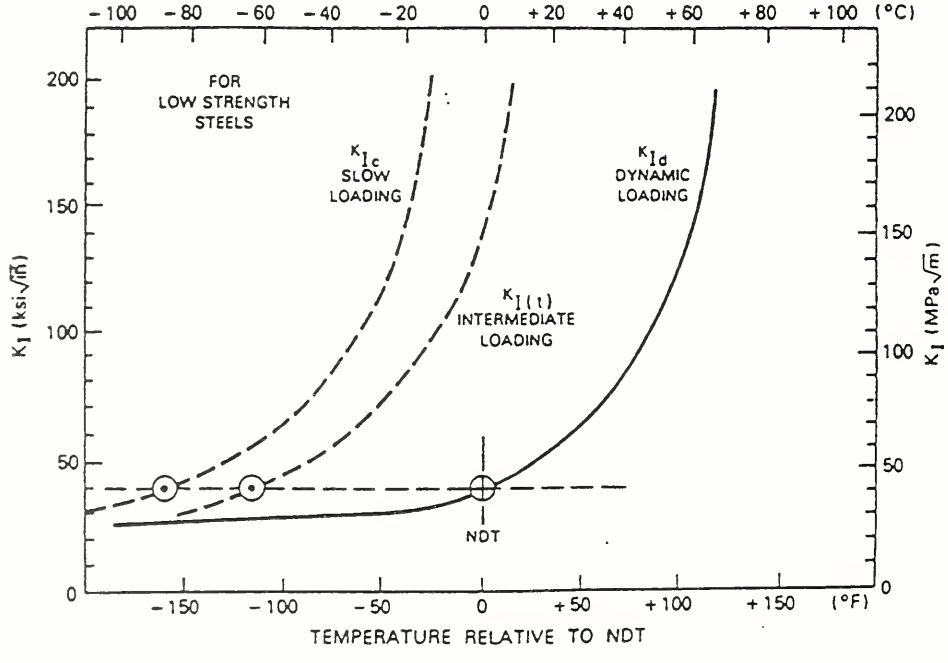

Figure 7-4. K_I Curves for Slow, Intermediate and Dynamic Loadings.

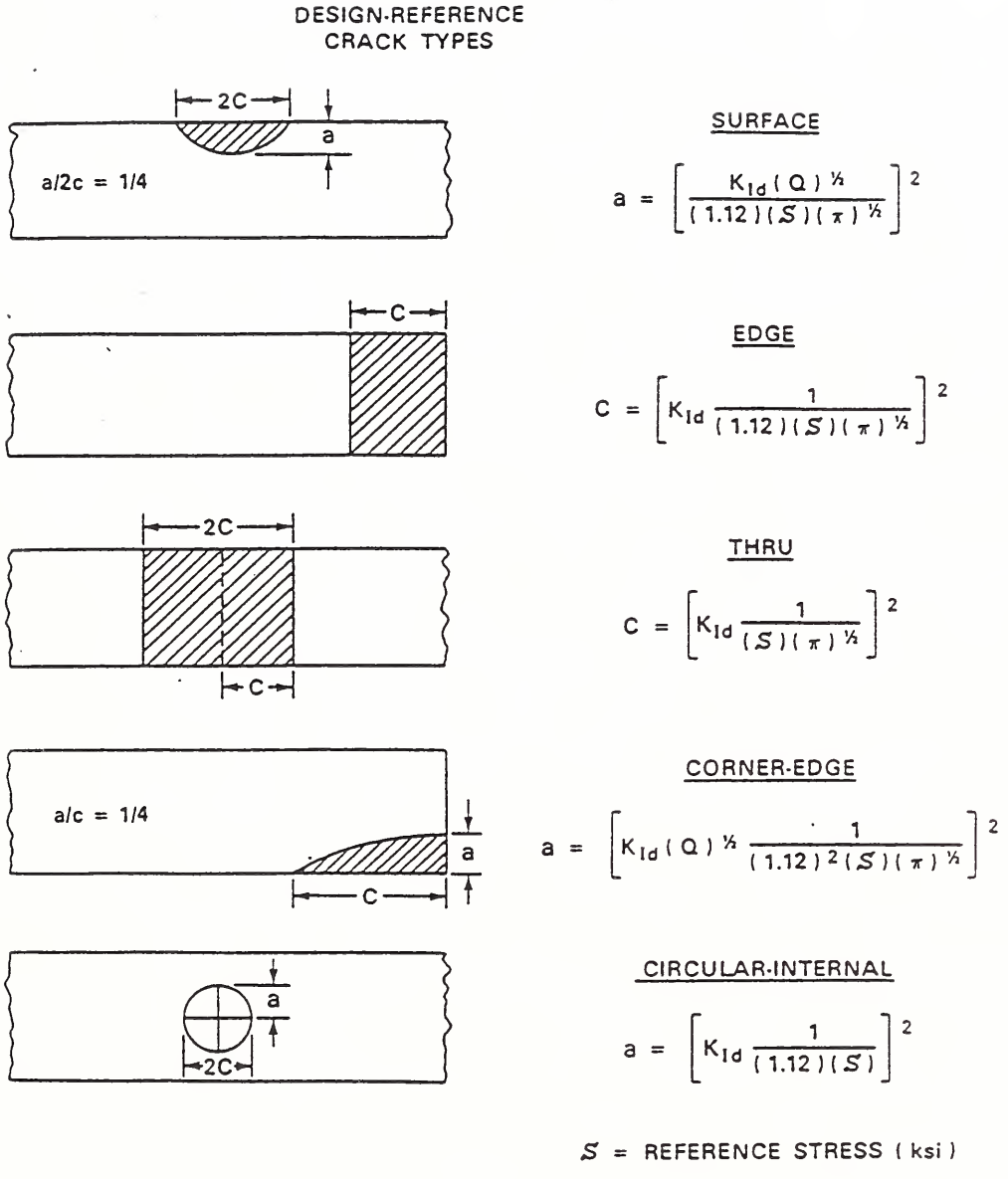

Figure 7-5. Critical Crack Size Solutions for Several Crack Geometries in Infinite Plates.

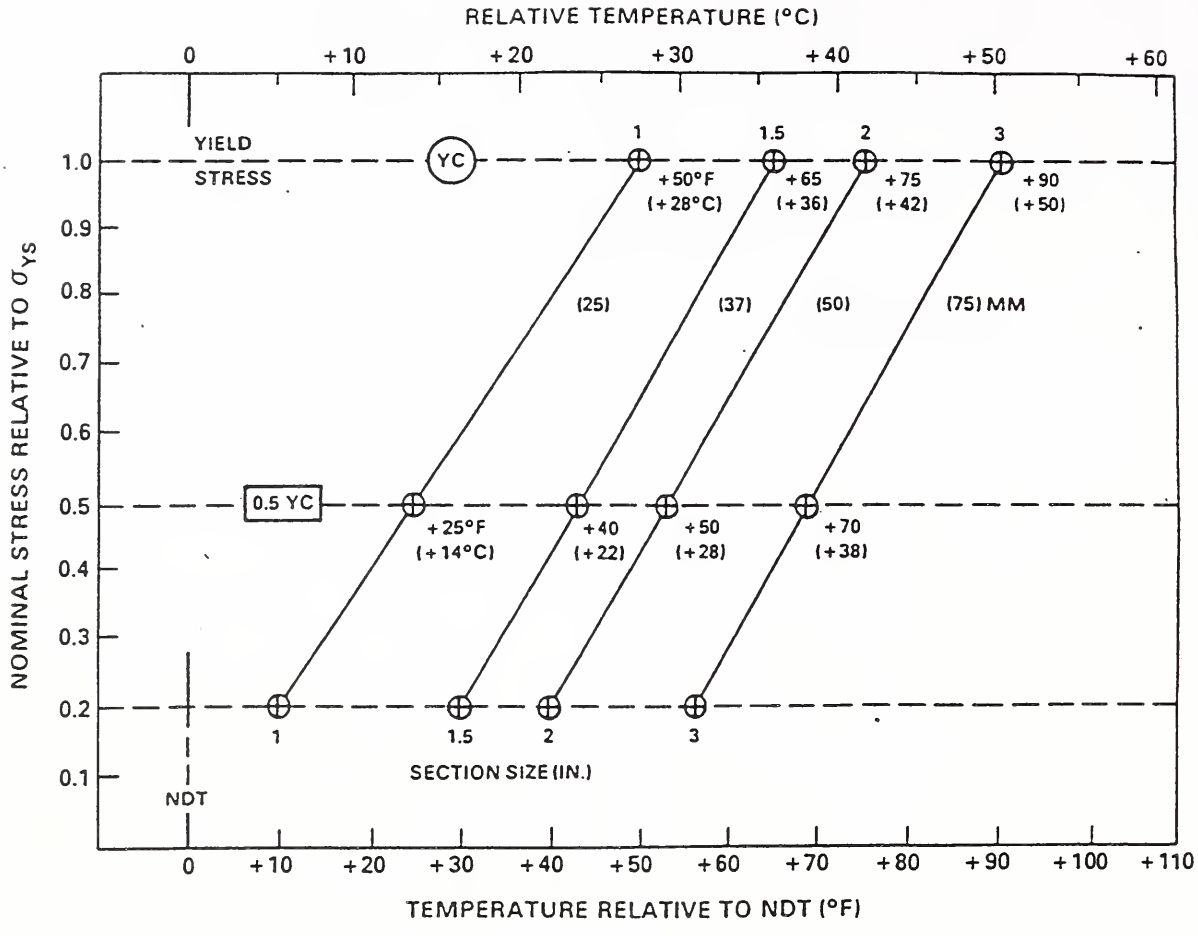

Figure 7-6. Design-Reference Graph for Fracture Arrest Curves.

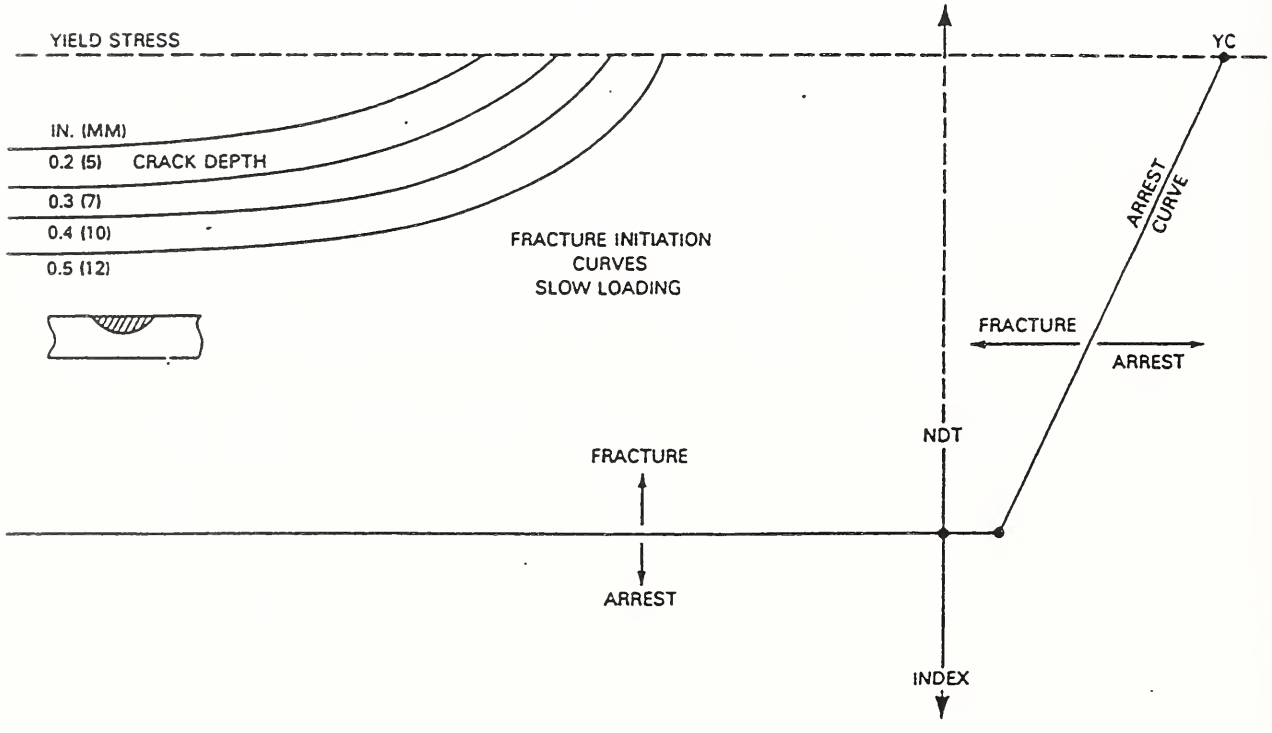

Figure 7-7. Slide Graph for Slow Loading.

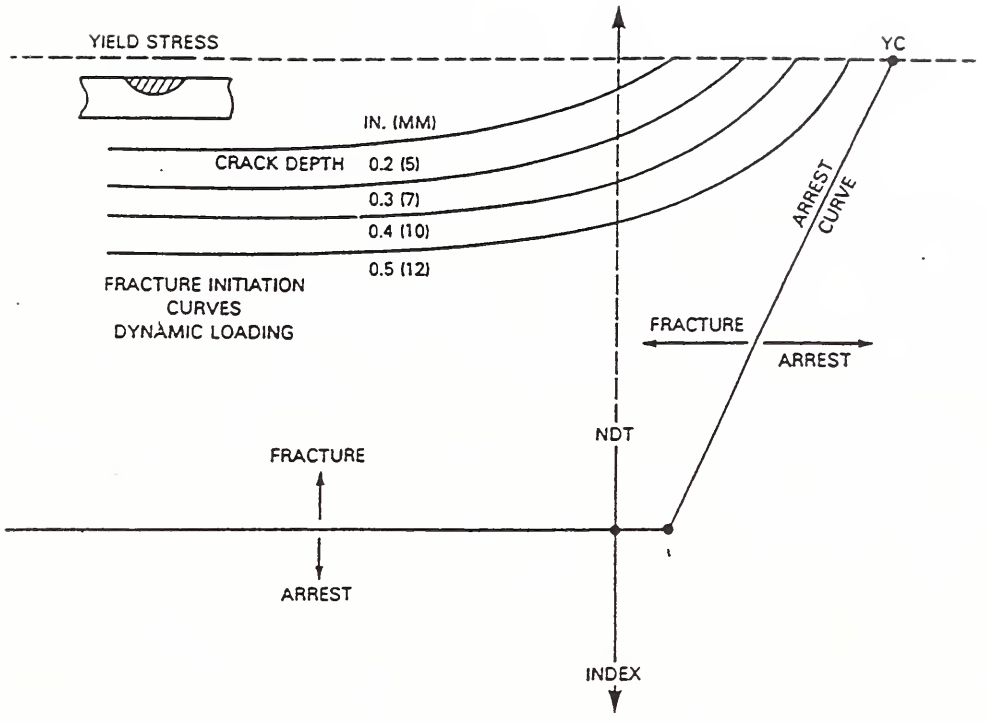

Figure 7-8. Slide Graph for Dynamic Loading.

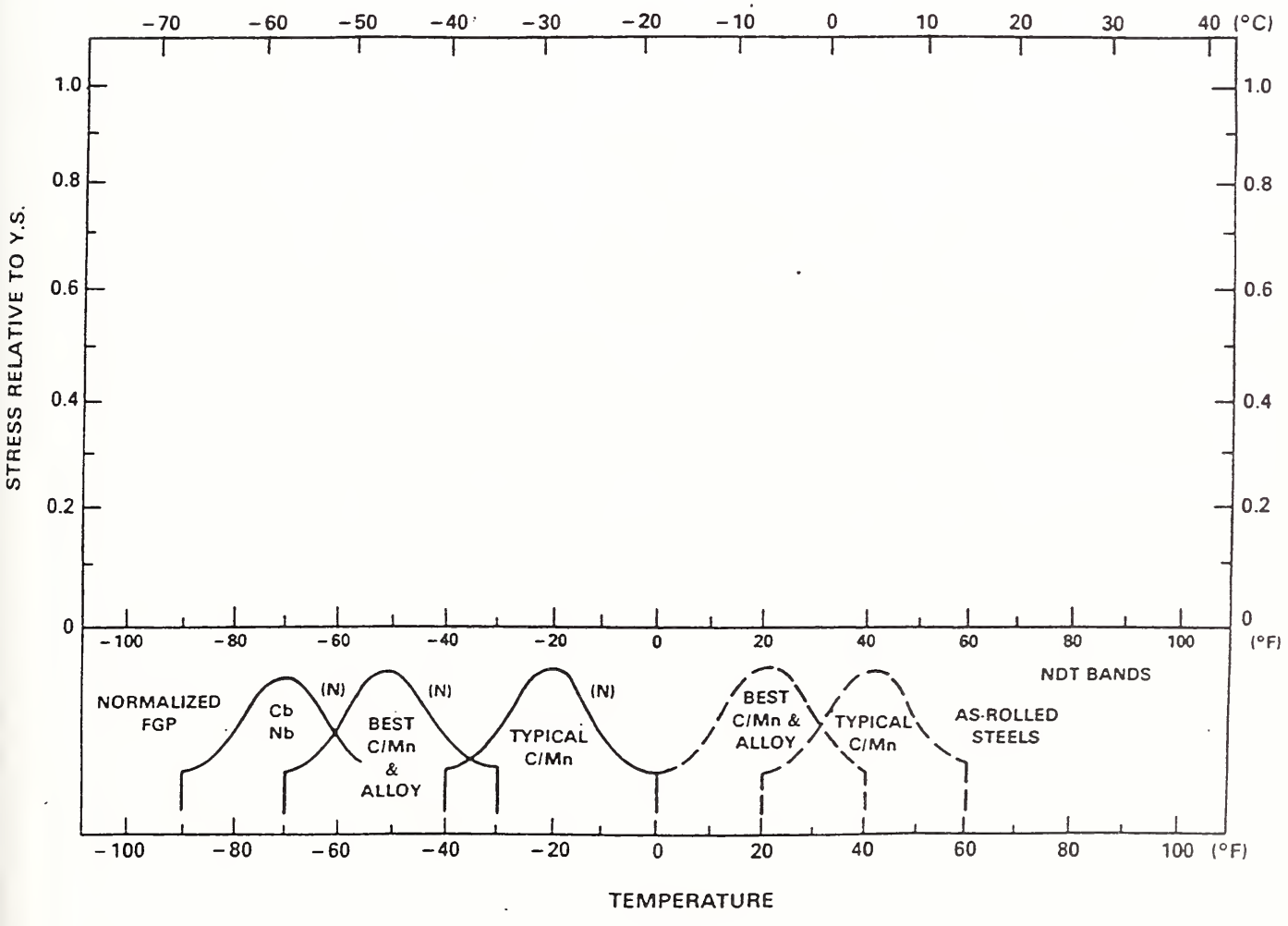

Figure 7-9. Stress-Temperature Diagram For Fracture Analysis of Railroad Tank Car Steels.

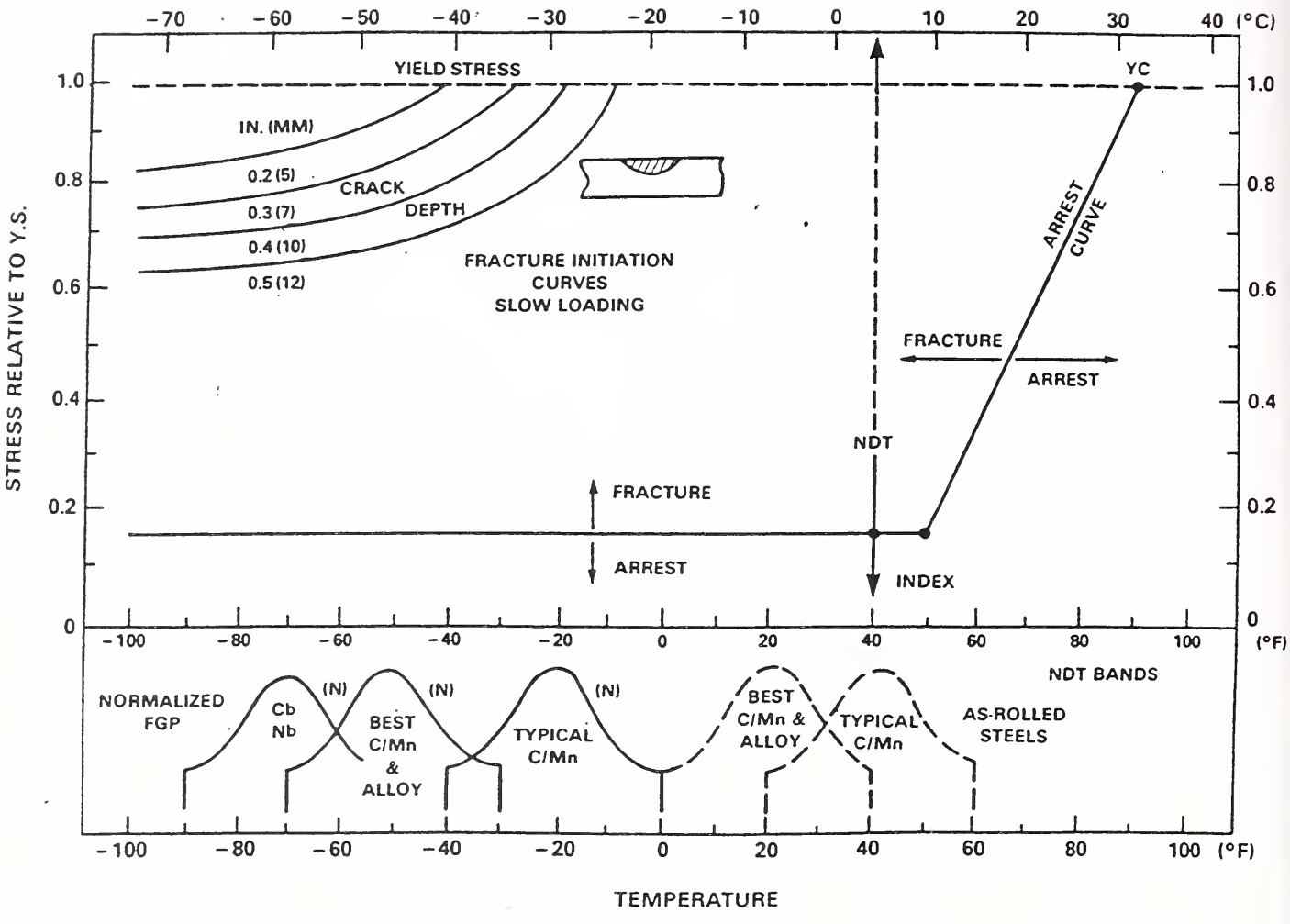

Figure 7-10. Complete Stress-Temperature Diagram For Fracture Analysis of Railroad Tank Car Steels.

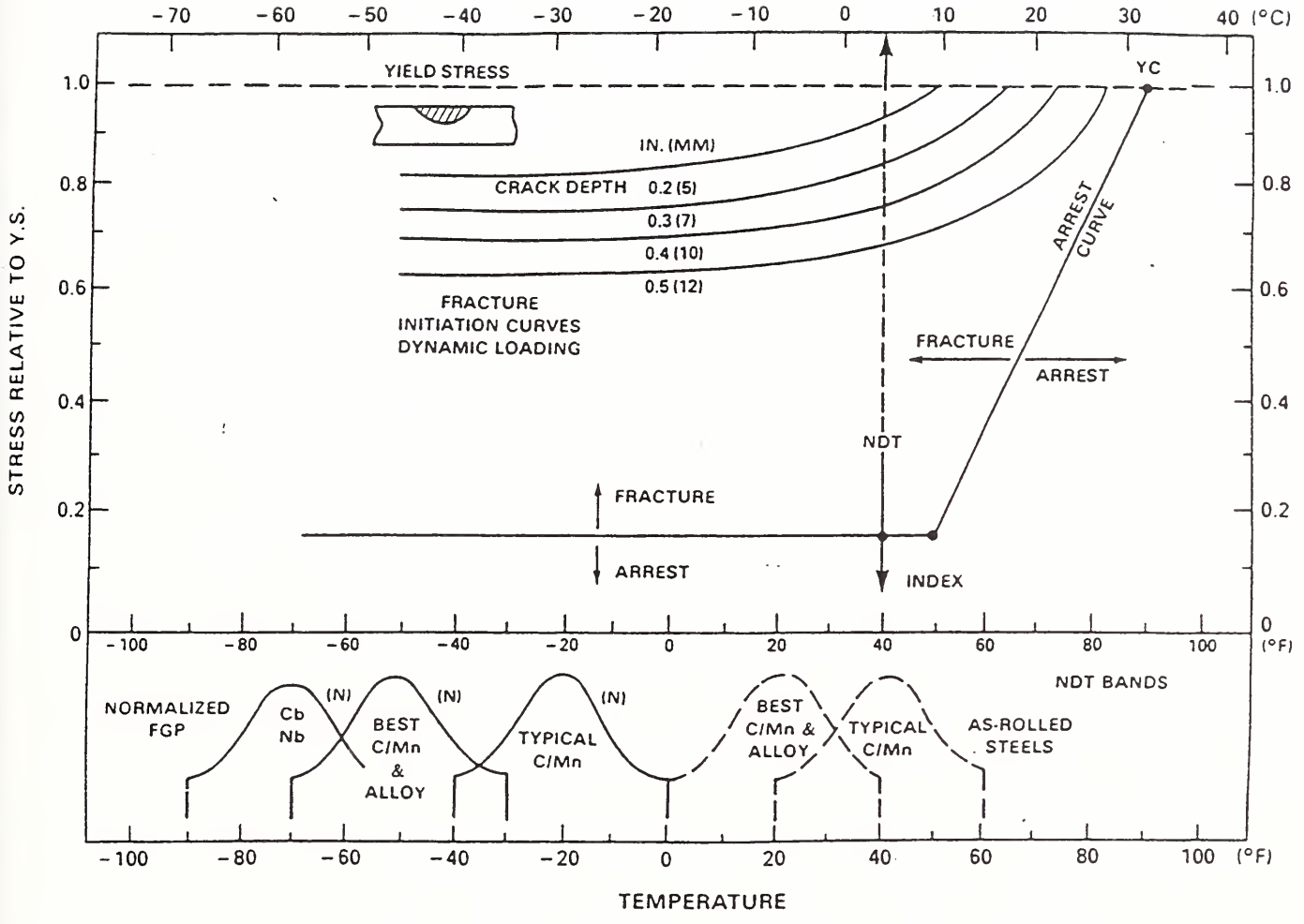

Figure 7-11. Slide Graph Analysis for Dynamic Loading.

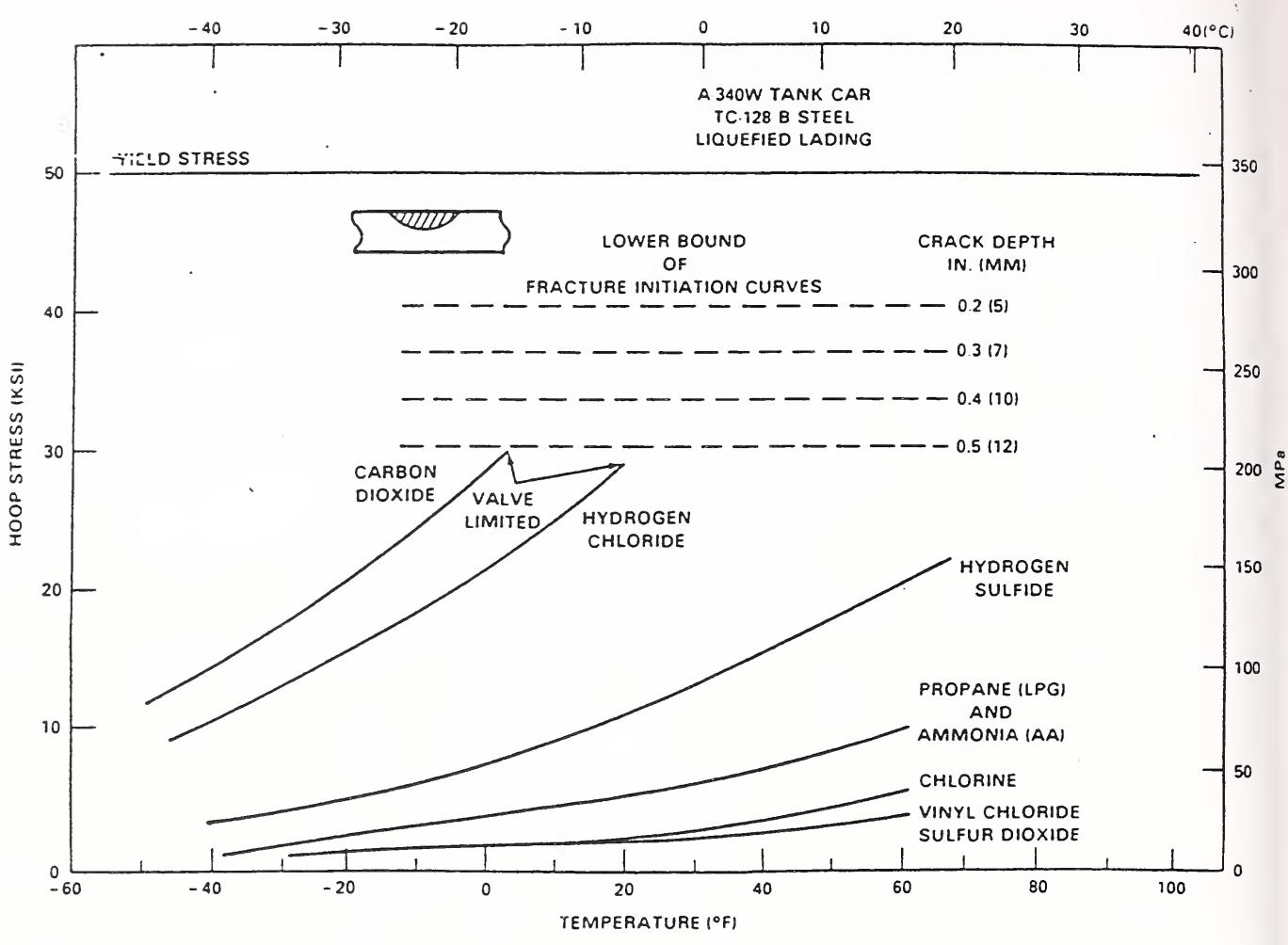

Figure 7-12. Fracture Initiation Assessment for Stresses due to Several Ladings.

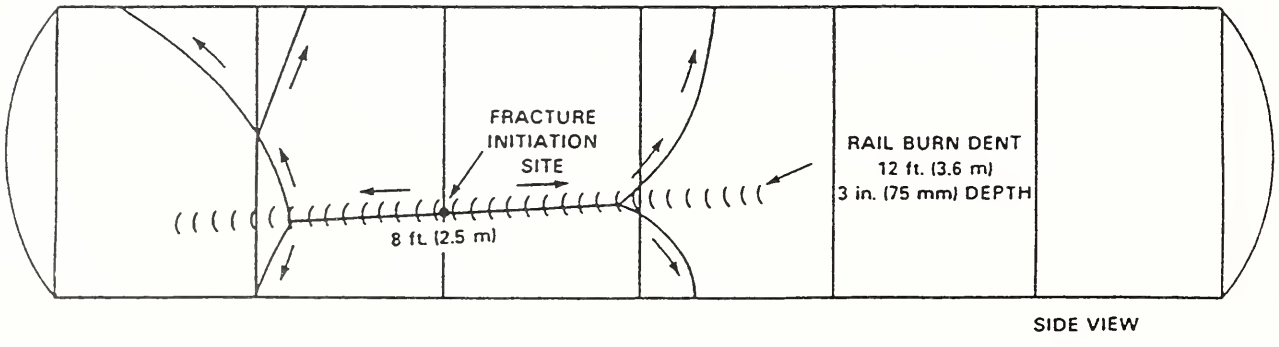

Figure 7-13. Long Rail-Burn Dent and Fracture Propagation Path.

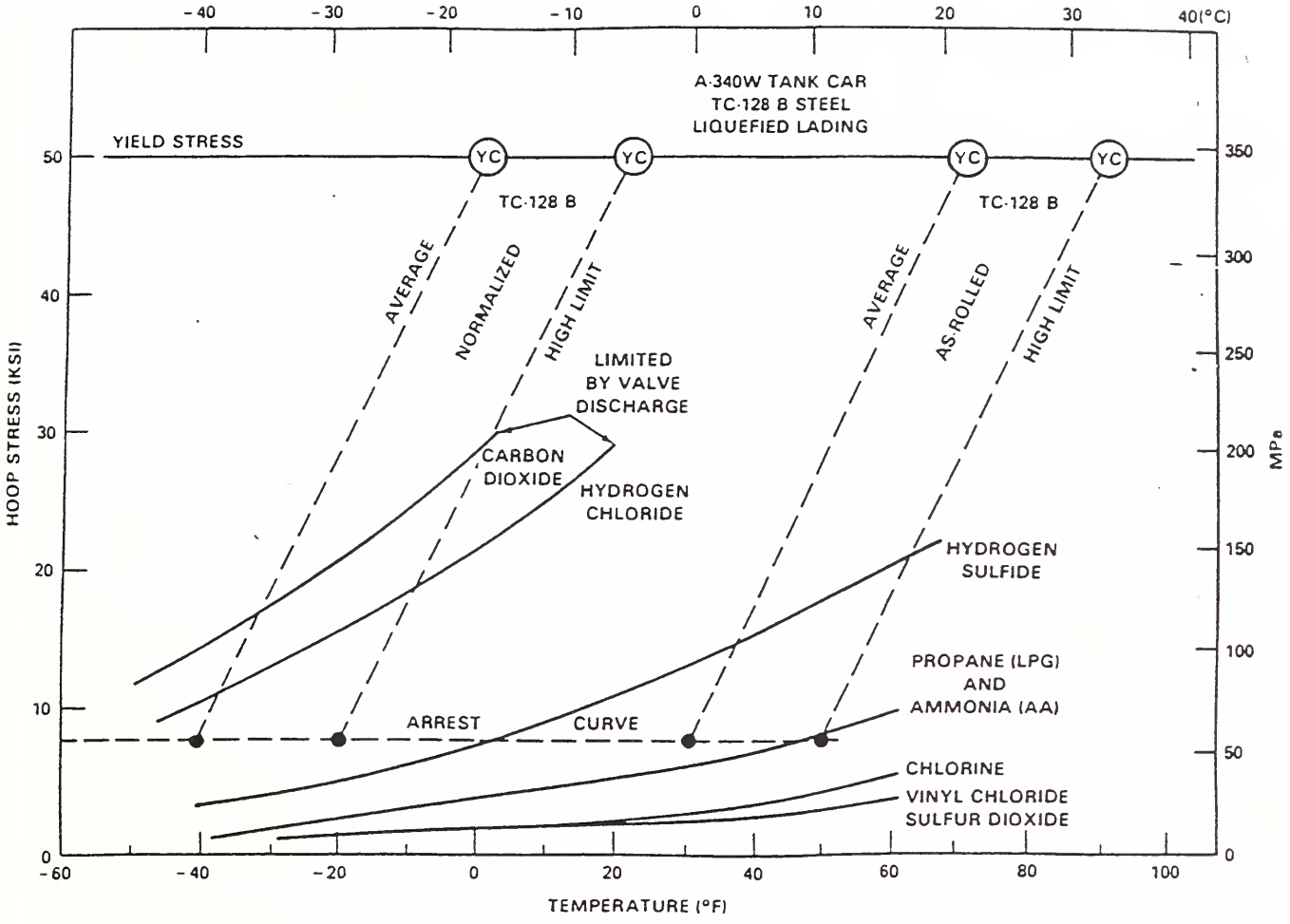

Figure 7-14. Fracture Arrest Assessment for Stresses due to Several Ladings.

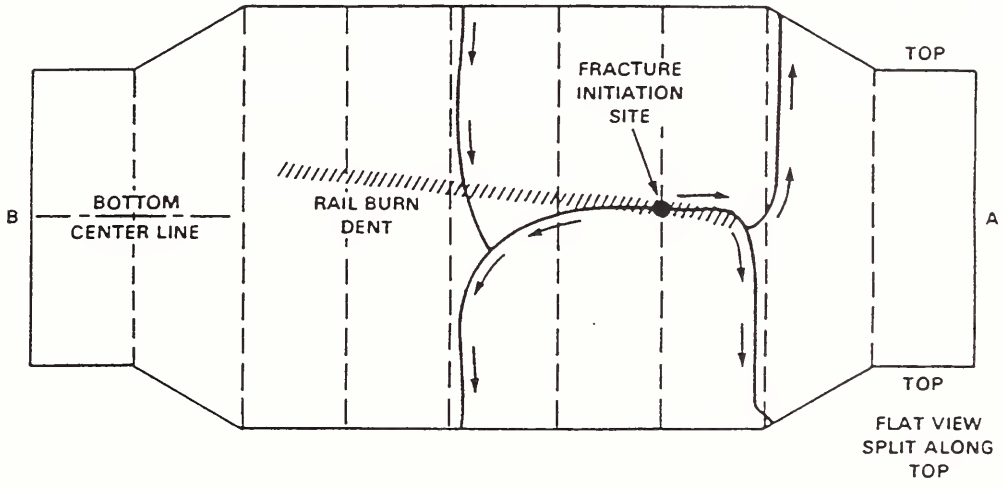

Figure 7-15. A Schematic of Fracture Path, Verdigris Tank Car Failure During Filling Operation.

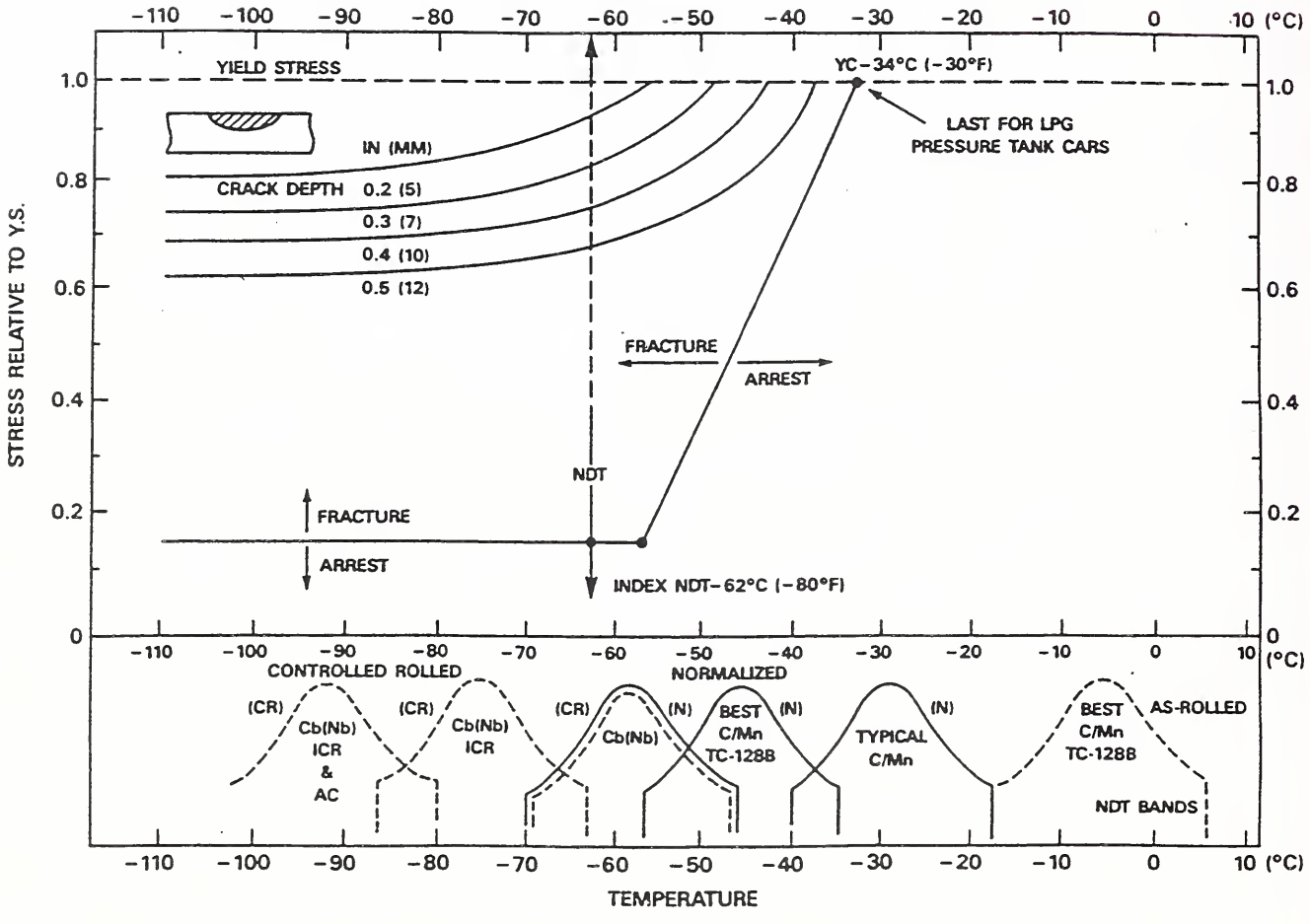

Figure 7-16. Assessment of Cb (Nb) Control-rolled Steels Using Slide Graph Diagram.

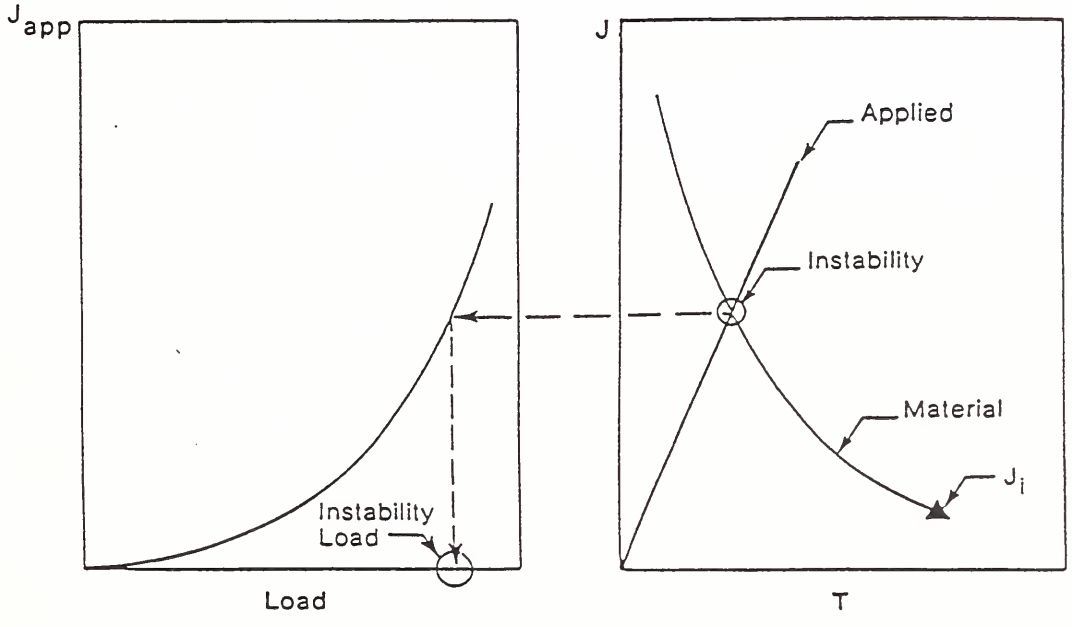

Figure 7-17. Illustration of the J-T Diagram.

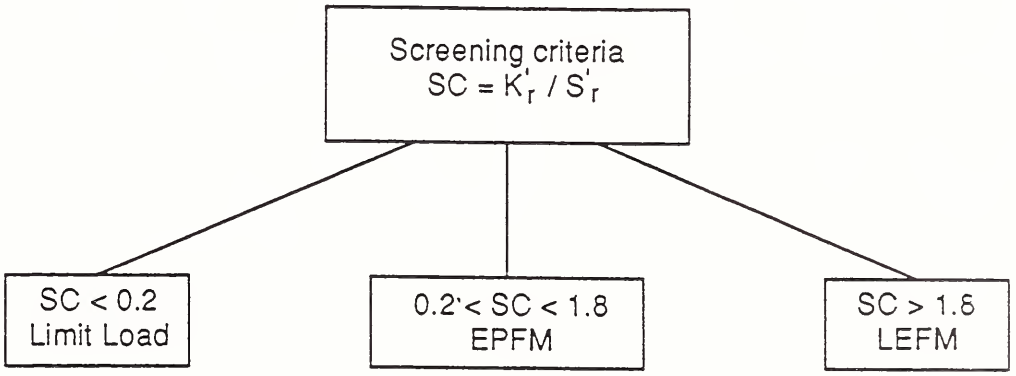

Figure 7-18. Screening Criteria for Carbon Steels used in LWR Piping.

Section 8

DISCUSSIONS AND CONCLUSIONS

This report reviewed the AAR, RPI-AAR, and NIST reports listed in References 1 through 13. The review covered accident analyses, materials properties determination and evaluation, and fracture mechanics analyses. The following paragraphs provide a discussion and conclusions under three broad categories.

(1) Accident Analyses

The investigations of railroad tank car accidents over the 16-year period (1965-1980) provided the following major conclusions [AAR-RPI reports 1, 3, 4, 5].

In general, material properties met the specification requirements. The as-rolled TC128 grade B material represented an improvement in cleanliness and strength with no loss in fracture properties when compared with the old steels. The analysis of current shell and head materials indicated that there was no fracture concern under normal operating conditions. Fracture propagation is possible only under abnormal conditions in an accident. However, accident records indicate that most cracks have arrested.

Only a small number (0.6%) of accidents resulted in brittle fracture. If all the tank cars had been fabricated from as-rolled TC-128B steel, the number of brittle fracture cases would have been reduced from 19 to 17 and the number of lading loss cases would not have changed. If all the tank cars had been built of normalized TC-128B steel, the number of brittle fracture cases would have been reduced from 19 to 5, and the number of lading loss cases would have decreased from 19 to 14.

Brittle fracture should not be expected for tank cars constructed of as-rolled TC128 grade B steel, except in (a) regions of abnormally high stresses, or (b) in situations where large areas of high stresses could temporarily result from an accident, such as a tank car impacting a massive object or structure.

The normalized TC128 grade B steel for shell will not provide improved performance at lower temperatures. No benefit is predicted for cases of full length brittle fracture, arrested brittle fractures, and ductile fracture.

Most tank car tanks ruptured in fire environments and involved ductile fracture. It is necessary to use quenched and tempered steels in order to assure that the fracture in dented regions will involve ductile rupture. Steels with much improved fracture properties are required to further reduce or eliminate brittle fracture cases. Even with these steels, the number of lading loss cases would have only decreased from 19 to 11. Therefore, the use of steels with improved fracture properties would have had a very small effect on the percentage of lading loss from all causes.

Both normalized and as-rolled TC128 grade B represent the equivalent of "best available" transition temperature characteristics for pearlitic steels. The TC128B steel is an optimum product for the service. Changes are not justified on the basis of fracture properties alone.

The brittle fracture initiation can be reduced to less than 0.1% or to near-zero rates by appropriate use of fracture-initiation-prevention procedures. Presently applied procedures for fracture initiation prevention provide the largest degree of reduction in brittle fracture rates. Modest improvements in design details for regions of welded attachments can provide the next largest degree of reduction in brittle fracture rates. These two remedial measures are expected to reduce brittle fracture experience to rates that are equivalent to, or better than, those attainable entirely by changing to normalized TC-128B steel. However, the use of normalized TC-128B steel does not eliminate the need for the improvements in welded attachments.

The most frequent reason for lading loss has been head penetration by couplers. The implementation of appropriate fracture-initiation-prevention procedures would have had a more significant effect on reducing lading loss than a change in steels. The procedures that accomplish the largest reduction in brittle fracture cases are presently applied by regulations, specific design and quality control practices, and design rules. These include the introduction of head shields, shelf couplers, thermal insulation, continuous underframe anchor design, local stress relief, and AAR guidelines for fatigue.

A small number of lading loss can be expected from exceptionally severe or unique accident conditions. It is not feasible to provide complete protection and it is not reasonable to assure a totally puncture-safe tank car.

The following analyses were not performed in Reports [3, 4, 5], which would have been useful in gaining a broader understanding of failures.

Leak-before-break analyses should have been performed to determine the potential for catastrophic fracture. In particular, calculations should have been performed to determine the critical length of a throughwall crack in longitudinal and circumferential directions. This information would have provided further insight into tank failures particularly the potential for development of end tubs. These analyses would have defined conditions under which an axial flaw would produce stable tear. The effect of the extent of railroad burn dent on potential for fracture was not quantified. Only a qualitative discussion was presented for ductile rupture cases. These cases should be analyzed using latest fracture mechanics method. As a minimum, analyses should be performed for relevant tank cars in accident to determine the predictability of stable ductile rupture (tear). This type of evaluation will identify any cases of potential ductile rupture under tank fire conditions.

The subject of crack initiation was handled from the causes perspective and measures were identified to minimize potential crack initiation. However, crack initiation is expected under accident conditions. Therefore, quantitative fracture mechanics analyses are needed to define the maximum allowable (undetected) flaw size that would not result into unstable fracture should it be subjected to accident conditions. This information would help in the development of pre-service and in-service inspection standards.

(2) **Materials Evaluation**

Test programs [6-10] conducted at NIST focused on tank car steel's mechanical and fracture toughness properties from room temperature to the lowest temperature the steel could possibly encounter while in use in North America.

Three major conclusions of these test programs [6-10] were: (1) the normalized material showed better impact properties at low test temperatures than the as-rolled AAR TC128 grade B steel, (2) the normalized and stress relieved (N+SR) steel showed more resistance to crack initiation and better crack arrest toughness than as-rolled or normalized AAR TC128 grade B steel, and (3) both the weld metal and the HAZ in N+SR steel were highly resistant to crack initiation and possessed the ability to arrest a propagating crack.

Experimental A 8XX Steel

The following conclusions were reached for the experimental A 8XX steel made using the inclusion shape control (ISC) practice.

The grain size of the A 8XX steel was not as fine as-expected in a normal control-rolled steel. The NDT temperature and Charpy V-notch test results [6] revealed that the new A 8XX grade B steel had lower impact properties at low test temperatures, and a higher NDT temperature than the inclusion shape control TC128 grade B steel. The primary reason for the difference in notch toughness properties was that the ferrite/pearlite grain size of the normalized and inclusion shape control AAR TC128 grade B steel was more uniform and finer than that of the control-rolled and ISC A 8XX steel.

The major conclusions of the retest program [7] were as follows. Retesting confirmed the Charpy V-notch impact, nil-ductility transition temperature, chemical, and inclusion analysis results previously reported in [6]. The normalized and inclusion shape controlled AAR TC128 grade B steel had a lower NDT temperature and better impact properties at low test temperatures than the new inclusion shape controlled A 8XX grade B steel.

The inclusion shape controlled AAR TC128 steel showed less scatter in fracture toughness value than the A 8XX steel. The fracture toughness of A 8XX steel was found to be much lower than that of the AAR TC128 grade B steel. The average K_{Ic} for the AAR TC128 grade B steel, in both L-T and T-L orientations, was 303 $MPa \cdot m^{1/2}$ (275 $Ksi \cdot in^{1/2}$), whereas for the A 8XX grade B steel the average was 75 $MPa \cdot m^{1/2}$ (68 $Ksi \cdot in^{1/2}$). Only at temperatures above -18°C (0°F), the A 8XX steel showed K_{Ic} values comparable to those measured for the AAR TC128 grade B steel.

The normalized and inclusion shape controlled AAR TC128 grade B steel revealed that it did not fail in an unstable manner even at a test temperature of -80°F. In contrast, the A 8XX steel showed unstable fracture behavior over the test temperature range of -80°F to +20°F.

The A 8XX steel was rejected by the industry because of its poor welding characteristics.

Tensile Strength and Stress Rupture Behavior

The following conclusions were reached for AAR M128-69-B tank car steel tested at accident temperatures representing the case where tank car is exposed to fire [2].

The rupture life of AAR M128-B steel was found to have strong dependance on both temperature and applied stress. There was a lack of sufficient elevated-temperature mechanical property data in the literature, which precluded the development of a design or trend curve for the variation of burst pressure with temperature for AAR M128-B steel. The development of the lower bound to the burst pressure-temperature curve is essential for evaluation of relief-valve design. It was suggested that modifications of tank car technology are necessary, which would either reduce the temperature dependence of the properties of the steel or reduce the maximum stresses and/or time at maximum stress experienced by the pressurized tank cars.

The following conclusions were derived from elevated temperature tests on normalized and stress relieved TC128 grade B steel [11]. Increased rate of loading produced a decrease in the difference between the ultimate tensile strength (UTS) and yield strength (YS), i.e., the YS increased while the UTS remained unchanged. At the low rate of loading, the difference between the UTS and YS was about 36 percent and at the higher rate of loading this difference was only 15 percent. Both UTS and YS decreased continuously with the increase in test temperature and time at temperature. The percent elongation was found to continuously increase with the increase in test temperature. The reduction-in-area was not as sensitive to temperature as the elongation. The yield-to-ultimate strength ratio (Y/T) was unaffected by test temperature or time at temperature. The Y/T ratio was 0.60 and 0.80 for crosshead speeds of 0.0127 and 0.127 cm/minute, respectively.

The rupture time could be increased by decreasing the 10-minute lifetime stress level. At 593°C, the rupture life would increase to three hours if the 10-minute lifetime stress were decreased by 27%. At higher temperatures a larger decrease in the stress is required to attain the same rupture life (43% reduction at 677°C). These results suggest that the stress-rupture time of this steel could be enhanced by reducing the time during which the tank car experiences the maximum internal pressure or by reducing the maximum internal pressure. This could be achieved by using additional relief valves, larger flow capacity relief valves, or lower opening-pressure relief valves.

Over the service temperature range, the UTS for the as-received normalized condition in the L-T orientation was greater than those for any other combination of orientation and stress relief. The lowest UTS was found for the normalized and stress relieved T-L specimens. The 0.2% offset yield strength (YS) in the L-T orientation for normalized, and the normalized and stress relieved steels was found to be greater than those in the T-L orientation. Further, the YS in the T-L orientation was essentially the same from -18°C (0°F) to room temperature. The reduction-in-area (RA) results indicated that the ductility in the T-L orientation is enhanced by stress relieving at 635°C (1175°F) for one hour.

The weld tests showed that the yield strength remained almost the same for the entire test temperatures. The reduction in area and elongation for all weld material were comparable to the base plate material. Vickers hardness measurements indicated that the weld metal, heat-affected zone, and

base metal were within allowable limits. No hard, brittle zones were found.

Crack Arrest Toughness

The major conclusions on the crack arrest toughness data for AAR TC128 grade B steel in the normalized, and normalized and stress relieved conditions were as follows:

Both the normalized, and normalized and stress relieved materials had crack arrest values that are characteristic of other ferrite/pearlite steels. The difference between the crack initiation toughness value and the crack arrest toughness value was found to be greater for the normalized and stress relieved material than for the normalized material. The normalized and stress relieved material did not show a continuously increasing toughness with temperature. Additional data would be needed to clearly establish the trend.

The following crack arrest fracture toughness behavior was found for SAW welded plates of normalized and stress relieved AAR TC128 grade B steel. It was not possible to initiate a crack in the all weld metal specimen. The heat-affected zone was found to have crack arrest toughness comparable to that for the base metal. This meant that the weld metal was very resistant to crack initiation and had a higher crack initiation toughness value than the base plate material. If a crack initiated in the base plate, it would not propagate in the weld metal. Both the weld metal and the HAZ steel were highly resistant to crack initiation and possessed the ability to arrest a propagating crack.

Skip Welds

The longitudinal residual stresses were largest close to the surface at positions close to the weld tip. The maximum value of longitudinal residual stress was found to be as high as or even higher than the yield strength of A515 grade 70 steel, 260 MPa (38 ksi). The residual stresses in conjunction with the primary loading stresses can produce localized high stresses typically exceeding the yield stress. The high combined stresses can lead to crack initiation and propagation.

The NIST study [13] speculated that the initial direction of crack propagation would be perpendicular to the weld direction. The crack may initiate anywhere along the weld bead region. However, with subsequent crack growth and the crack might enter a region where the transverse stress is high. This change could force the propagating crack to turn 90 degrees and continue propagating parallel to the weld direction through the region of high tensile transverse stress.

The NIST study involved welded plates that were free of lateral constraints on skip welds. It is expected that the lateral constraint typically experienced in tank cars can produce increased transverse stress levels. This aspect was not investigated in NIST study.

NIST tests conducted at -40°C at a loading rate of 3.97×10^{-6} m/s indicated that the fracture toughness for the "start" weld was higher than the "stop" weld. Values ranged from 81 to 130 $MPa \cdot m^{1/2}$ for the "start" weld specimens and 60 to 102 $MPa \cdot m^{1/2}$ for the "stop" weld specimens. The fracture toughness values for the heat affected zone specimens ranged from 58 to 109 $MPa \cdot m^{1/2}$. Impact toughness ranged from 5 to 8 Joules at -40°C. Both the fracture toughness and impact results

show that loading rates must be considered when evaluating the resistance to failure when using the skip weld method for attaching appurtenances to tank cars.

(3) Fracture Mechanics Evaluation

As a result of AAR-RPI analyses [4, 5] and discussions presented in Sections 7.4 through 7.8, the following observations and conclusions are made.

Brittle fracture of tank cars has never developed in normal service. Certain unusual conditions must be developed in order to initiate and propagate brittle fractures. A crack-like defect must be present or developed as a result of loading. An example of the latter type is a flaw introduced due to the rail-burn dent. For ladings involving low hoop stresses, brittle fracture can only propagate through regions of abnormally high elastic or plastic stresses. The normal stress levels for propane (LPG) and anhydrous ammonia are too low for catastrophic fracture. The tank cars with carbon dioxide and hydrogen chloride ladings should be given a higher priority as they produce highest hoop stresses of all lading cases.

The material properties vary between the L-T and T-L orientations. This applies to tensile strength, rupture stress, and fracture toughness data. The slide graph method does not discriminate such differences in properties in the evaluation of railroad tank cars. Additional discussion on the slide graph method is presented in Section 7.3.

In Reference [5], separate assumptions were made for fracture initiation and propagation analyses. It was suggested that local stress at the crack site should be used in the fracture initiation analysis, whereas through-thickness average stress should be used in fracture propagation analysis, see Table 7-1. The basis for this assumption was not indicated in Reference [5]. The use of local stresses may not be compatible with fracture mechanics solutions used.

The tank cars are subjected to a wide range of temperatures, from very cold temperatures in normal service at one extreme to as high a temperature as 680°C in the case of accident involving fire. Over this temperature range, the material's strength and toughness performance varies considerably. Consequently, the use of proper fracture mechanics method is essential to assuring structural integrity.

Fracture mechanics analysis procedures for the three broad categories of yielding, i.e., predominantly elastic, elastic-plastic and net-section yielding at the crack location, have not been established for railroad tank cars. The applicability regime for each fracture analysis method (K_I, J, net-section yielding criterion) can be established by a series of calculations covering a wide range of flaw size, loading cases, and material properties. A simple screening criterion or guideline should be developed to define the correct analysis method. It has been successfully developed and implemented for nuclear piping [Vol. 3 of Reference 25]. Latest fracture mechanics technology can be used to develop quick-look tables of the allowable flaw size for the type of lading, tank car steels, and for each potentially vulnerable location where fracture might initiate and propagate.

Two major categories can be identified for further analysis. The first includes all cases where the net-

section stress at flaw location exceeds 50% of yield stress, and the second category is for cases where potentially higher temperatures than those in normal service are involved. In the latter case, the normal applied stresses will produce sufficient yielding thus necessitating an elastic-plastic fracture analysis. The review of the reports revealed that such analyses have not been performed. The only analyses reported are based on stress-rupture considerations which do not account for performance degradation from a pre-existing flaw.

The critical flaw size results were reported only in NISTIR-5179 [12]. This report used the latest fracture mechanics method for the analysis of circumferential throughwall cracks in the tank car shell. Although desired, analyses for part-throughwall flaws were not conducted. It was assumed that the part-throughwall flaw after penetrating the tank shell remains stable, i.e., produces leak-before-break condition for the tank car. The validity of this assumption should be examined for critical locations of tank cars and for the whole range of service and accident temperatures.

The critical crack length for discharge pressure was approximately 30 to 50 times the tank car shell wall thickness. The analysis results showed that throughwall cracks up to four times the tank shell thickness can be tolerated at burst pressure. If a part-throughwall flaw upon penetrating the shell wall has a length less than four times the wall thickness, the resulting throughwall crack will be stable, otherwise unstable fracture will result from a part-throughwall flaw (i.e., no leak-before-break). The implications of this result should be investigated further. The effect of lowering the relief valve discharge setting should be investigated in terms of critical flaw size but this was not investigated. Service failure data indicated that the crack initially ran in the axial direction. Analyses have not been conducted to determine the critical crack size for axial cracks. It would be desirable to conduct such predictive analyses and compare the results against the service data.

Section 9

REFERENCES

1. Pellini, W.S., Eiber, R.J. and Olson, L.L., "Phase 03 Report on Fracture Properties of Tank Car Steels - Characterization and Analysis," August 20, 1975; Railroad Tank Car Safety Research and Test Project, AAR Technical Center, Report RA-03-4-32 (AAR R-192).

2. Early, J.G., "Ambient-and Elevated-Temperature Mechanical Properties of AAR M128-69-B Steel Plate Samples Taken from Fire Tested Insulated Tank Car RAX 202," NBSIR 75-725, May 1975.

3. Eiber, R.J. and Olson, L.L., "Final Phase 03 Report, Material Study on Steels Used in Current and Former Tank Cars Construction and From Cars Involved in Accidents," August 21, 1975; Railroad Tank Car Safety Research and Test Project, AAR Technical Center, Report RA-03-5-33 (AAR R-193).

4. Phillips, E.A. and Pellini, W.S., "Phase 03 Report on the Behavior of Pressure Tank Car Steels in Accidents," RPI-AAR Railroad Tank Car Safety Research and Test Project, Report No, RA-03-6-48 (Association of American Railroads Technical Center, Research Report No. R-553), Chicago, Illinois, June 20, 1983.

5. Pellini, W.S., "Guidelines for Fracture Mechanics Analysis of Pressure Tank Car Structural Integrity Factors," Final Draft, March 1984, AAR Technical Center.

6. Hicho, G.E. and Smith, J.H., "Mechanical Properties and Fracture Toughness of AAR TC 128 Grade B Steel and Micro-Alloyed Control-Rolled Steel, A 8XX Grade B, from -80F to +73F," NISTIR 90-4289, April 1990.

7. Hicho, G.E. and Smith, J.H., "Determination of the NDT Temperature and Charpy V-Notch Impact Properties of AARTCI28 Grade B Steel and A 8XX Grade B Steel," NISTIR 4300, April 1990.

8. Hicho, G.E., "Crack Arrest Fracture Toughness Measurements of Normalized and Inclusion Shape Controlled AAR TC 128 Grade B Steel, and Micro-Alloyed, Control-Rolled, and Inclusion Shape Controlled A 8XX Grade B Steel," NISTIR 4501, February 1991.

9. Hicho, G.E. and Harne, D.E., "Mechanical Properties and Fracture Toughness of AAR TC 128 Grade B Steel in the Normalized and Normalized and Stress Relieved Conditions," NISTIR 4660, September 1991.

10. Hicho, G.E. and Harne, D.E., "Weld and Heat Affected Zone Crack Arrest Fracture Toughness of AAR TC 128 Grade B Steel," NISTIR 4767, February 1992.

11. Hicho, G.E., "The Mechanical, Stress-Rupture, and Fracture Toughness Properties of Normalized and Stress Relieved AAR TC 128 Grade B Steel at Elevated Temperatures," NISTIR 5157, March 1993.

12. Hicho, G.E., Zahoor, A., Fields, R.J., and deWit, R., "Fracture Mechanics Evaluation of Railroad Tank Cars Containing Circumferential Cracks," NISTIR 5179, April 1993.

13. Hicho, G.E., Brand, P.C., and Prask, H.J., "Determination of the Residual Stresses Near the Ends of Skip Welds Using Neutron Diffraction and X-Ray Diffraction Procedures," NISTIR 5671, June 1995.

14. Eiber, R.J., Maxey, W.A. and Duffey, A.R., "Analysis of Fracture Behavior of Tank Cars in Accidents," RPI-AAR Tank Car Safety Project, Report No. RA-12-2-20 (Association of American Railroads Technical Center, Research Report No. R-143), Chicago, Illinois, September 1972.

15. Pellini, W,S., "Manual of Engineering Procedures for Fracture-Safe Design," Association of American Railroads Technical Center, Research Report No. R-451, Chicago, Illinois, November, 1980.

16. Pellini, W.S., "Guidelines for Fracture-Safe Design of Steel Structures," Association of American Railroads Technical Center, Research Report No. R-455, Chicago, Illinois, November 1980.

17. Pellini, W.S., "Guidelines for Fatigue-Reliable Design of Steel Structures," Association of American Railroads Technical Center, Research Report No. R-490, Chicago, Illinois, September 1981.

18. Pellini, W.S., "Guidelines for Fracture-Safe and Fatigue-Reliable Design of Steel Structures," The Welding Institute, Cambridge, CBI-6AL, England, 1983. Available from Micro Metallurgical Ltd., Thornhill, Ontario, L3T-3S9, Canada.

19. Pellini, W.S., "Feasibility Analysis for Tank Car Application of New Microalloyed and Controlled-Rolled Steels - Description of Fracture Properties and Comparisons with Steels in Present Use," Association of American Railroads Technical Center, Research Report No. 543, Chicago, Illinois, April 1983.

20. Pellini, W.S., "Analysis of Tank Car Failures Related to Rail Burn Dents," Association of American Railroads Technical Center, Research Report No. R-551, Chicago, Illinois, June 1983.

21. Pellini, W.S., "Slide-Graph Fracture Analysis System," Association of American Railroads Technical Center, Research Report No. R-542, Chicago, Illinois, June 1983.

22. Pellini, W.S., Armstrong R.A. and Stone, D.H., "Investigation of the Fabrication Quality of Tank Car GATX 26024, Involved in a Derailment at Inwood, Indiana," Association of American